

ACTA

UNIVERSITATIS OULUENSIS

Esa Kunnari

MULTIRATE MC-CDMA

*PERFORMANCE ANALYSIS IN STOCHASTICALLY
MODELED CORRELATED FADING CHANNELS,
WITH AN APPLICATION TO OFDM-UWB*

FACULTY OF TECHNOLOGY,
DEPARTMENT OF ELECTRICAL AND INFORMATION ENGINEERING,
UNIVERSITY OF OULU



ACTA UNIVERSITATIS OULUENSIS
C Technica 299

ESA KUNNARI

MULTIRATE MC-CDMA

Performance analysis in stochastically modeled
correlated fading channels, with an application
to OFDM-UWB

Academic dissertation to be presented, with the assent of
the Faculty of Technology of the University of Oulu, for
public defence in Raahensali (Auditorium L10), Linnanmaa,
on May 30th, 2008, at 12 noon

OULUN YLIOPISTO, OULU 2008

Copyright © 2008
Acta Univ. Oul. C 299, 2008

Supervised by
Professor Jari Linatti

Reviewed by
Professor Shinsuke Hara
Professor Lutz Lampe

ISBN 978-951-42-8808-1 (Paperback)
ISBN 978-951-42-8809-8 (PDF)
<http://herkules.oulu.fi/isbn9789514288098/>
ISSN 0355-3213 (Printed)
ISSN 1796-2226 (Online)
<http://herkules.oulu.fi/issn03553213/>

Cover design
Raimo Ahonen

OULU UNIVERSITY PRESS
OULU 2008

Kunnari, Esa, Multirate MC-CDMA. Performance analysis in stochastically modeled correlated fading channels, with an application to OFDM-UWB

Faculty of Technology, University of Oulu, P.O.Box 4000, FI-90014 University of Oulu, Finland, Department of Electrical and Information Engineering, University of Oulu, P.O.Box 4500, FI-90014 University of Oulu, Finland

Acta Univ. Oul. C 299, 2008

Oulu, Finland

Abstract

Multicarrier and multiple input–multiple output (MIMO) techniques have become popular in wireless communications over multipath fading channels in recent years. This thesis firstly considers the characterization and simulation of fading mobile radio channels for MIMO multicarrier systems. Secondly, the performance of spread-spectrum multicarrier (MC) code-division multiple-access (CDMA) with multirate transmission is analyzed. Thirdly, the analysis is applied to ultra-wideband (UWB) orthogonal frequency-division multiplexing (OFDM) systems enhanced with frequency-domain code-division multiplexing (CDM).

The response of a small-scale fading channel is derived as a function of time, transmit and receive antenna positions, and subcarrier frequency, which leads to a tapped delay-line model with time-, space-, and frequency-selective taps. The taps are modeled as a sum of a deterministic line-of-sight or dominant scattered path and a zero-mean Gaussian part composed of a number of unresolvable scattered paths and, therefore, are Rice fading. The Gaussian parts have the desired temporal and spatio-spectral correlations generated by time-correlation shaping filtering and a space-frequency correlation transformation, respectively. The simulator achieves a good accuracy while retaining a reasonable computational complexity.

The generic performance analysis of MC-CDMA includes both the multicode and variable spreading factor (VSF) multirate schemes that are inherent for CDMA and capable of providing efficient support for services of different required data rates. The analysis also takes into account the intersymbol interference caused by the multipath delay components exceeding a guard interval, which is commonly omitted in the literature by assuming the guard interval to be longer than the maximum delay spread. Results comparing and pointing out notable differences in the error rate performance of the two multirate schemes in conjunction with six different combining techniques are presented for a synchronous downlink and both a synchronous and asynchronous uplink.

The analysis of CDM-enhanced OFDM-UWB involves first a single piconet with different combinations of the VSF and multicode schemes. Frequency-domain spreading is found to improve the performance remarkably when a sufficient spreading factor and a suitable subcarrier combining method are used. Subsequently, CDMA of simultaneously operating piconets (SOPs) with either the VSF or multicode scheme is considered. While both multirate schemes result in a similar performance when the number of SOPs is large, notable differences arise when there are only a few SOPs.

Keywords: channel characteristics, fading simulation, multiband OFDM, multicarrier CDMA, multicode, variable spreading factor

Preface

The research for this doctoral thesis has been carried out at the Centre for Wireless Communications (CWC), University of Oulu, Oulu, Finland. The research on the modeling of small-scale fading channels, composing the first part of the thesis, was initiated in Advanced Wireless Communications Systems and Signal Processing (AWICS) project in 1999 and completed in the follow-up Future Radio Access (FUTURA) project. The research on the performance analysis of multirate multicarrier code-division multiple-access (MC-CDMA), composing the second part of this thesis, was also conducted in FUTURA project, starting from 2003 after my research odyssey among space-time coding and phase sweeping transmit diversity was over. The application of the conducted performance analysis of MC-CDMA to code-division multiplexed multiband orthogonal frequency-division multiplexing (MB-OFDM) ultra-wideband (UWB) systems, composing the third and the last part of this thesis, was carried out in Concepts and Algorithms for Multiband Ultra-wideband Communications (CAMU) project starting from 2005.

Firstly, I would like to acknowledge Professor Matti Latva-aho, who as a former director of CWC not only took me on as a Master's thesis researcher to CWC but also managed to convince me to continue towards a doctoral thesis. I would also like to acknowledge him for being my supervisor in the early stages of my post-graduate research and for proposing me the research topic of multirate MC-CDMA. I am most grateful to Professor Jari Linatti for his supervision during the major part of my research and the writing of this thesis. I would also like to express my gratefulness to him as a project manager of AWICS, FUTURA, and CAMU projects for providing me with the opportunity to work in these projects. Without his patient guidance and encouragement, this thesis would not have been completed. I am also indebted to him for suggesting to apply the conducted performance analysis of multirate MC-CDMA to UWB MB-OFDM.

I would like to express my gratitude to the reviewers of this thesis, Professor Shinsuke Hara, Osaka City University, Osaka, Japan, and Professor Lutz Lampe, University of British Columbia, Vancouver, Canada, for their supportive statements and insightful comments. These comments, together with those received from the anonymous reviewers of the original articles, have provided invaluable help in improving

the quality of the thesis. The steering feedback from Kari Horneman, Dr. Jorma Lilleberg, Esa Tiirola, and Dr. Juha Ylitalo as the representatives of the project partners is also highly acknowledged. I would also like to thank Samantha Eidenbach for the language revision of the thesis.

The financial support for my post-graduate studies and research from Infotech Oulu Graduate School is gratefully acknowledged. I would also like to extend my gratitude to the funding partners of the projects in which this thesis research was carried out, the Finnish Funding Agency for Technology and Innovation (Tekes), Nokia, the Finnish Defence Forces, and Elektrobit in AWICS and FUTURA projects, Instrumentointi in FUTURA project, and Academy of Finland in CAMU project. The personal grants from Nokia Foundation and HPY Research Foundation are also gratefully appreciated.

I would like to thank all the present and past colleagues, who have built up the unprejudiced working atmosphere at the CWC and Telecommunication Laboratory. The role of Professor Pentti Leppänen, the head of the laboratory, as the father figure of this dual unit is especially recognized. Lic. Tech. Ari Pouttu, the present director of the CWC, is acknowledged for his good humor and unreservedness and for providing flexible yet productive working conditions. The cheerful and always helpful administrative support personnel is credited with keeping things running smoothly and organizing recreational team-building activities. In particular, I would like to address my thanks to my office mates and regular lunch companions Dr. Giuseppe Abreu, Dr. Ing. Ulrico Celentano, Giuseppe Destino, Dr. Kari Hooli, Dr. Kimmo Kansanen, Juha Karjalainen, Jouko Leinonen, Dr. Pavel Loskot, Davide Macagnano, Markus Myllylä, Prof. Carlos Pomalaza-Ráez, Lic. Tech. Mariella Särestöniemi, Dr. Attaphongse Taparugssanagorn, Dr. Djordje Tujkovic, Dr. Antti Tölli, and Jari Ylioinas for the fruitful and refreshing discussions.

Lastly, I want to express my deepest gratitude to my mother Tellervo and father Seppo for their unconditional love and support. My older sister, Sari, and younger brother, Sampo, deserve my warmest thanks for their lifelong company and friendship. My thanks are also due to my family-in-law and other friends for providing occasional breaks away from the daily drudgery. I owe my loving thanks to my darling wife Maria for her love, understanding, companionship, and continuous efforts to put up with me, and to our three year old son, Joel, and one year old daughter, Helmi, for just being there and enriching our lives.

Oulu, May 13, 2008

Esa Kunnari

Abbreviations

$ \cdot $	absolute of the argument
$\lfloor \cdot \rfloor$	largest integer smaller than or equal to the argument
$[\cdot]_{\mathbf{i},:}$	submatrix of the argument with rows indexed in vector \mathbf{i}
$[\cdot]_{\mathbf{i},\mathbf{j}}$	submatrix of the argument with rows and columns indexed in vectors \mathbf{i} and \mathbf{j} , respectively
$(\cdot)^*$	complex conjugate of the argument
$(\cdot)'$	another value of the variable in the argument
$(\cdot)^H$	complex conjugate transpose of the argument
$(\cdot)^T$	transpose of the argument
$\hat{(\cdot)}$	estimate of the argument
$\angle(\cdot)$	phase of the argument
\otimes	Kronecker product
$\mathbf{0}_d$	zero vector of dimension d
$a(\cdot)$	spread function of channel
a_i	path coefficient of i th multipath component
a_j	coefficient of j th backward filter tap
a_{ki}	path coefficient of i th multipath component in k th resolvable path
\mathbf{a}_{fk}	vector of phase shifts over subcarriers for k th resolvable path
$\mathbf{a}_{p_r,k}$	vector of phase shifts over receive antennas for k th resolvable path
$\mathbf{a}_{p_t,k}$	vector of phase shifts over transmit antennas for k th resolvable path
A_h	amplitude of h th group
$\text{blockdiag}\{\cdot\}$	block diagonal matrix of the argument matrices
b_i	coefficient of i th forward filter tap
c	speed of light
$c_{0k}(\cdot)$	channel coefficient term for LOS or dominant scattered component in k th path
c_{hkl}	channel coefficient of l th subcarrier of k th user in h th group
$c_{hkl}^{[0,T_g]}$	channel coefficient term of delays from 0 to T_g for l th subcarrier of k th user in h th group

$c_{hkl}^{(T_g, T_s)_1}$	ICI coupling term of delays from T_g to T_s for l th subcarrier of k th user in h th group
$c_{hkl}^{(T_g, T_s)_2}$	channel coefficient term of delays from T_g to T_s for l th subcarrier of k th user in h th group
$c_{hkl}^{(T_g, T_s)_3}$	ISI coupling term of delays from T_g to T_s for l th subcarrier of k th user in h th group
$c_{hkl}^{[T_s, T_s+T_g]}$	asynchronicity induced intercode interference coupling term of delays from T_s to $T_s + T_g$ for l th subcarrier of k th user in h th group
$c_{hkl}^{(T_s+T_g, 2T_s)_1}$	asynchronicity induced ICI coupling term of delays from $T_s + T_g$ to $2T_s$ for l th subcarrier of k th user in h th group
$c_{hkl}^{(T_s+T_g, 2T_s)_2}$	asynchronicity induced intercode interference coupling term of delays from $T_s + T_g$ to $2T_s$ for l th subcarrier of k th user in h th group
$c_{hkl}^{(T_s+T_g, 2T_s)_3}$	asynchronicity induced ISI coupling term of delays from $T_s + T_g$ to $2T_s$ for l th subcarrier of k th user in h th group
$c_{hkn}^{(i)}$	channel coefficient of n th path of k th user in h th group at i th symbol
$c_k(\cdot)$	channel coefficient of k th resolvable path
$c_{sk}(\cdot)$	channel coefficient term for scattered components in k th path
$c_{sklmn}^{(i)}$	Gaussian component of channel coefficient between m th transmit and n th receive antenna on l th subcarrier in k th path at i th sample
$\mathbf{c}^{(i)}$	vector of channel coefficients at i th sample
$\mathbf{c}_0^{(i)}$	vector of deterministic components of channel coefficients at i th sample
$\mathbf{c}_{0k}^{(i)}$	vector of deterministic components of channel coefficients for k th path at i th sample
$\mathbf{c}_s^{(i)}$	vector of Gaussian components of channel coefficients at i th sample
$\mathbb{C}^{I \times J}$	set of I -by- J matrices of complex numbers
$\mathbf{C}_{hk}^{(i)}$	coupling matrix of k th user in h th group at i th symbol lag
$d_{hkqp}^{(i)}$	i th symbol of p th VSF stream of q th multicode stream of k th user in h th group
$\text{diag}(\cdot)$	diagonal matrix with the same main diagonal as the argument
\mathbf{d}	unit vector for direction
\mathbf{d}_i	unit vector for direction of i th multipath component
$\bar{\mathbf{d}}_k$	unit vector for mean direction of k th resolvable path
\mathbf{d}_r	unit vector for arrival direction
\mathbf{d}_{ri}	unit vector for arrival direction of i th multipath component

$\bar{\mathbf{d}}_{rk}$	unit vector for mean direction of arrival for k th resolvable path
\mathbf{d}_t	unit vector for departure direction
\mathbf{d}_{ti}	unit vector for departure direction of i th multipath component
$\bar{\mathbf{d}}_{rk}$	unit vector for mean direction of departure for k th resolvable path
$D_{hkqp}^{(i)}$	signal term of decision metric for p th VSF stream of q th multicode stream of k th user in h th group at i th symbol
D_r	dimension of receive array
D_t	dimension of transmit array
e	base of the natural logarithm
E_s	symbol energy
$E_x[f(x)]$	expectation of $f(x)$ over x
f	frequency
f_s	channel sampling frequency
g	chip index
G_h	spreading factor of h th rate group
G_{\max}	maximum power margin
G_{mean}	mean power margin
h	rate group index
$h(\cdot)$	impulse response
H	number of active rate groups
$H(z)$	transfer function in the z-transform domain
i	symbol interval index; multipath component index; forward filter tap index
I	number of filter taps
I_c	interpolation factor of cubic interpolation
I_f	interpolation factor of interpolation filter
$I_{hkqp}^{(i)}$	interference term of decision metric for p th VSF stream of q th multicode stream of k th user in h th group at i th symbol
$I_{hkqp}^{(i)}$ $h'k'q'p'g'$	interference from g' th chip of p' th VSF stream of q' th multicode stream of k' th user in h' th group to g th chip of p th VSF stream of q th multicode stream of k th user in h th group at i th symbol
\mathbf{I}	identity matrix
j	imaginary unit; backward filter tap index
$J_0(\cdot)$	zero-order Bessel function of the first kind

$J_{hkqp}^{(i)}$	ISI to g th chip of p th VSF stream of q th multicode stream of k th user in h th group at i th symbol
k	user index; resolvable path index
K	number of resolvable paths; Rice K -factor
K_h	number of users in h th group
K_k	Rice K -factor of k th resolvable path
l	subcarrier index
\mathbf{l}	vector of subcarrier indices
L	number of subcarriers
\mathbf{L}	lower triangular matrix
m	transmit antenna index
$\max(\cdot)$	maximum of the argument
$\min(\cdot)$	minimum of the argument
M	number of transmit antennas
n	multipath component index; receive antenna index
$n(t)$	noise
N	number of receive antennas
N_0	power spectral density of noise
$N_{hkqp}^{(i)}$	noise term of decision metric for p th VSF stream of q th multicode stream of k th user in h th group at i th symbol
$O_{hkqp}^{(i)}$ $h'k'q'p'g'$	ICI from g' th chip of p' th VSF stream of q' th multicode stream of k' th user in h' th group to g th chip of p th VSF stream of q th multicode stream of k th user in h th group at i th symbol
p	VSF stream index
$p(\cdot)$	probability density function; power spectrum of channel
$p_{hk}(\tau)$	delay power spectrum of k th user in h th group
$p_k(\cdot)$	power spectrum of channel for k th resolvable path
$p_s(t)$	symbol waveform
\mathbf{p}	vector for antenna position
\mathbf{p}_r	vector for receive antenna position
\mathbf{p}_t	vector for transmit antenna position
P_{AWGN}	error probability in AWGN channel
P_{fading}	error probability in fading channel
P_h	number of VSF streams in h th group
P_k	power of k th resolvable path

q	multicode stream index
Q_h	number of multicode streams in h th group
$r(\cdot)$	received lowpass signal
R	symbol rate
$R(\cdot)$	autocorrelation
$R_{0k}(\cdot)$	autocorrelation of channel coefficient term for LOS or dominant scattered component in k th path
$R_c(\Delta\omega_{ll'})$	spectral autocorrelation of channel
R_h	symbol rate of h th group
$R_s(\cdot)$	autocorrelation of channel coefficient term for scattered components
$R_{sk}(\cdot)$	autocorrelation of channel coefficient term for scattered components in k th path
\mathbf{R}_c	spectral covariance matrix of channel terms
\mathbf{R}_{chk}	spectral covariance matrix of channel terms for k th user in h th group
$\mathbf{R}_{chk}^{(a,b)c,d}$	spectral covariance matrix of $c_{hkl}^{(a,b)c}$ and $c_{hkl}^{(a,b)d}$, $l = 1, \dots, L$
\mathbf{R}_{Ihkqp}	interference covariance matrix for p th VSF stream of q th multicode stream of k th user in h th group
\mathbf{R}_{yhkp}	covariance matrix of received signal after OFDM demodulation for p th VSF stream of q th multicode stream of k th user in h th group
s_{hkqg}	g th chip of q th multicode stream of k th user in h th group
$s(t)$	transmitted baseband signal
$\text{sinc}(\cdot)$	sine cardinal function
\mathbf{s}_{hkq}	vector of chips for q th multicode stream of k th user in h th group
\mathbf{s}_{hkqp}	spreading sequence vector for p th VSF stream of q th multicode stream of k th user in h th group
S	number of channel samples
$S_{hkqpg}^{(i)}$	intercode interference from g' th chip of p' th VSF stream of q' th multicode stream of k' th user in h' th group to g th chip of p th VSF stream of q th multicode stream of k th user in h th group at i th symbol
\mathbf{S}_{hk}	spreading sequence matrix of k th user in h th group
t	time
T	sample interval
T_g	guard interval
T_o	observation interval
T_s	symbol interval; channel sample interval

T_u	useful symbol span
$u_{hk}(t)$	transmitted baseband signal of k th user in h th group
$U_{hkqp}^{(i)}$	decision metric for p th VSF stream of q th multicode stream of k th user in h th group at i th symbol
v	mobile speed
\mathbf{v}	mobile velocity vector
w_{hkqpg}	combining weight for g th chip of p th VSF stream of q th multicode stream of k th user in h th group
\mathbf{w}_{hkqp}	combining weight vector for p th VSF stream of q th multicode stream of k th user in h th group
W	bandwidth of baseband signal on a subcarrier
x_i	x-axis component of direction vector for i th multipath component
$y_{hkl}^{(i)}$	demodulator output for l th subcarrier of k th user in h th group at i th symbol
y_i	y-axis component of direction vector for i th multipath component
$y_j^{(i)}$	j th time correlation shaping filter output at i th sample
$\mathbf{y}^{(i)}$	vector of time correlation shaping filter outputs at i th sample
z	z-transform domain variable
z_i	z-axis component of direction vector for i th multipath component
α	envelope
α_k	envelope of channel coefficient for k th resolvable path
α_{rms}	root-mean-square value of envelope
β_k	phase of channel coefficient for k th resolvable path
γ_{hkqp}	instantaneous SINR of p th VSF stream of q th multicode stream of k th user in h th group
$\delta(\cdot)$	Dirac delta function
$\Delta(\cdot)$	finite difference in the argument
Δp	distance between two spatial positions
$\Delta \mathbf{p}_{rn}$	position vector difference from 1st to n th receive antenna
$\Delta \mathbf{p}_{tm}$	position vector difference from 1st to m th transmit antenna
$\Delta \omega_{ll'}$	spacing between subcarriers l and l'
θ	elevation
θ_i	elevation of i th multipath component
ϑ_k	phase shift of deterministic component over sample interval for k th path

λ_c	wavelength of center carrier
μ_k^2	power of channel coefficient term for LOS or dominant scattered component in k th path
ν_D	maximum Doppler frequency
ν_i	Doppler frequency of i th multipath component
ξ_k	random initial phase of k th resolvable path
$\rho_{klmn}^{kl'm'n'}$	spatiospectral correlation coefficient between $c_{sklmn}^{(i)}$ and $c_{skl'm'n'}^{(i)}$
σ_a	azimuth spread
σ_d	rms delay spread
σ_{dk}	rms delay spread for k th resolvable path
σ_k^2	average power of channel coefficient term for scattered components in k th path
σ_{ki}^2	normalized power of i th multipath component in k th resolvable path
σ_N^2	noise variance
Σ_{fk}	spectral covariance matrix of k th resolvable path
$\Sigma_{p_r,k}$	spatial covariance matrix of k th resolvable path for receiver
$\Sigma_{p_t,k}$	spatial covariance matrix of k th resolvable path for transmitter
$\Sigma_{p_t p_r f}$	diagonalization of spatiospectral covariance matrices of paths
$\Sigma_{p_t p_r f k}$	spatiospectral covariance matrix of k th resolvable path
$\Sigma_{p_t p_r k}$	spatial covariance matrix of k th resolvable path
τ	delay
τ_{hk}	delay of k th user in h th group
τ_{hkn}	delay of n th multipath component of k th user in h th group
$\bar{\tau}_k$	mean delay of k th resolvable path
τ_{ki}	delay of i th multipath component in k th resolvable path
τ_n	delay of n th multipath component
$\boldsymbol{\tau}_k$	set of delays in k th resolvable path
ϕ	azimuth
ϕ_i	azimuth of i th multipath component
$\bar{\phi}_k$	mean azimuth of k th resolvable path
$\bar{\phi}_r$	mean azimuth at receiver
$\bar{\phi}_t$	mean azimuth at transmitter
$\varphi_i(\cdot)$	phase of i th multipath component
$\varphi_{ki}(\cdot)$	phase of i th multipath component in k th resolvable path

ψ_k	angle between azimuth of velocity and mean azimuth of k th path
ω_l	angular frequency of l th subcarrier
2-D	two-dimensional
3-D	three-dimensional
3GPP	Third Generation Partnership Project
AD	analog to digital
AWGN	additive white Gaussian noise
BEP	bit-error probability
BER	bit-error rate
BPSK	binary phase-shift keying
cdf	cumulative distribution function
CDM	code-division multiplexing
CDMA	code-division multiple-access
COST	European Cooperation in the Field of Scientific and Technical Research
CW	continuous wave
CWC	Centre for Wireless Communications
DA	digital to analog
DC	direct current
DFT	discrete Fourier transform
DS	direct sequence
DSL	digital subscriber line
DVB	digital video broadcasting
EC	European Community
EGC	equal gain combining
FCC	Federal Communications Commission
FDM	frequency-division multiplexing
FDMA	frequency-division multiple-access
FFT	fast Fourier transform
FH	frequency hopping
FIR	finite impulse response
FLOP	floating point operation
GPS	Global Positioning System
GSM	Global System for Mobile Communications
HF	high frequency

HPY	Helsingin Puhelinyhdistys
I&D	integrate-and-dump
ICI	intercarrier interference
IFFT	inverse fast Fourier transform
IS-95	Interim Standard 95
IDFT	inverse discrete Fourier transform
IEE	Institution of Electrical Engineers
IEEE	Institute of Electrical and Electronics Engineers
IET	Institution of Engineering and Technology
iid	independent and identically distributed
IIR	infinite impulse response
ISI	intersymbol interference
LOS	line-of-sight
LTE	Long Term Evolution
MB	multiband
MC	multicarrier
MIMO	multiple input–multiple output
MMSE	minimum mean-square error
MMSECC	minimum mean-square error per carrier combining
MMSEUC	minimum mean-square error per user combining
MRC	maximal ratio combining
NLOS	non-line-of-sight
OC	optimum combining
OFDM	orthogonal frequency-division multiplexing
OFDMA	orthogonal frequency-division multiple-access
OQAM	offset quadrature amplitude modulation
ORC	orthogonality restoring combining
OVSF	orthogonal variable spreading factor
PAPR	peak-to-average power ratio
PC	personal computing
PIC	parallel interference cancellation
pdf	probability density function
QAM	quadrature amplitude modulation
QPSK	quadrature phase-shift keying
rms	root mean square

SINR	signal-to-interference-plus-noise ratio
SNR	signal-to-noise ratio
SOP	simultaneously operating piconet
SOS	sum of sinusoids
SS	spread spectrum
TDMA	time-division multiple-access
TH	time hopping
UMTS	Universal Mobile Telecommunications System
US	United States; uncorrelated scattering
UWB	ultra wideband
VSF	variable spreading factor
WLAN	wireless local area network
WMAN	wireless metropolitan area network
WPAN	wireless personal area network
XPR	cross-polarization power ratio

List of original articles

This thesis is based on the following original articles, which are referred to in the text by their Roman numerals:

- I Kunnari E & Iinatti J (2005) A Rice fading MIMO multicarrier channel model. Proc. IEEE International Symposium on Personal, Indoor and Mobile Radio Communications, Berlin, Germany, 1: 527–531.
- II Kunnari E & Iinatti J (2005) Analysis of multirate MC-CDMA over multipath channels with delay spread exceeding the guard interval. Proc. IEEE Global Telecommunications Conference, St. Louis, USA, 6: 3221–3225.
- III Kunnari E & Iinatti J (2006) Performance analysis of multirate MC-CDMA in Rayleigh-fading channels with delay power spectrum exceeding the guard interval. IEEE Journal on Selected Areas in Communications 24(3): 542–553.
- IV Kunnari E & Iinatti J (2007) Stochastic modelling of Rice fading channels with temporal, spatial and spectral correlation. IET Communications 1(2): 215–224.
- V Kunnari E & Iinatti J (2007) Performance analysis of OFDM based UWB systems with a frequency-domain CDMA for multiple SOPs. Proc. IEEE Vehicular Technology Conference, Dublin, Ireland, 2651–2655.
- VI Kunnari E & Iinatti J (2007) Performance analysis of OFDM based UWB systems enhanced with frequency-domain spreading. Proc. IEEE International Conference on Communications, Glasgow, UK, 4873–4878.

Contents

Abstract	
Preface	5
Abbreviations	7
List of original articles	17
Contents	19
1 Introduction	21
1.1 Background	21
1.2 Motivation and scope of the research	25
1.3 Outline of the thesis	26
2 Small-scale fading channels	29
2.1 Characteristics of small-scale fading	31
2.1.1 Envelope distribution	31
2.1.2 Delay dispersion and frequency selectivity	35
2.1.3 Doppler dispersion and time selectivity	37
2.1.4 Direction dispersion and space selectivity	39
2.1.5 Joint dispersion and selectivity	43
2.2 Simulation of small-scale fading	47
2.2.1 Geometric modeling	47
2.2.2 Stochastic modeling	49
3 Spread-spectrum communications	53
3.1 CDMA multiplexing	55
3.1.1 Walsh-Hadamard sequences	56
3.1.2 Maximum length sequences	57
3.1.3 Complementary sequences	58
3.2 Multicarrier transmission	59
3.2.1 OFDM modulation	59
3.2.2 Pulse shaped OFDM	61
3.3 Multicarrier CDMA	62
3.3.1 Time-domain spreading	63
3.3.2 Frequency-domain spreading	64

3.4	Multirate transmission in CDMA systems	68
3.4.1	Multicode	69
3.4.2	Variable spreading factor	70
3.4.3	Comparisons of multicode and VSF	71
3.5	Ultra-wideband communications	73
3.5.1	Impulse radio	75
3.5.2	Multiband OFDM	76
4	Summary of the original articles	81
4.1	Modeling of Rice fading MIMO multicarrier channels	81
4.1.1	Characterization of fading	81
4.1.2	Structure of a fading simulator	84
4.1.3	Performance of the simulator	88
4.2	Performance analysis of multirate MC-CDMA	90
4.2.1	System model	90
4.2.2	Performance analysis	94
4.2.3	Numerical results	95
4.3	OFDM-UWB systems enhanced with MC-CDMA	101
4.3.1	A single piconet	101
4.3.2	Multiple simultaneously operating piconets	103
5	Conclusion	105
5.1	Summary and discussion	105
5.2	Future work	107
	References	109
	Original articles	127

1 Introduction

The application of multicarrier and multiple input–multiple output (MIMO) techniques in a wide range of high data rate wireless communications over fading channels has become increasingly popular in recent years. In comparison with wideband single-carrier transmission, the key advantage of multicarrier transmission is the robustness against frequency-selective fading, narrowband interference and intersymbol interference (ISI). MIMO techniques employing multiple antennas at both the transmitter and receiver can provide either robustness to space-selective fading or improved capacity, or both. The research and development of these new multicarrier MIMO communication systems over wireless, mobile channels requires realistic, well-defined channel models. Furthermore, complying channel simulators are needed for reliable laboratory and computer simulations, reducing the need for more expensive and time consuming prototyping and field testing. As these new communication systems are expected to carry various multimedia services needing different data rates, they need multirate capable transmission schemes for efficient operation. Besides future cellular systems, the most favored emerging high-rate ultra-wideband (UWB) underlay systems rely on multicarrier transmission techniques providing favorable foundations for efficient multirate capable transmission schemes.

This thesis work was started with the modeling and simulation of fading mobile radio channels for multicarrier MIMO systems. Thereafter, the performance of a promising, multirate capable multicarrier and multiple-access technique was analyzed over fading channels. Finally, the application of the technique and its analysis to UWB systems was considered. These research topics are further introduced in Section 1.1, the motivation, scope, and novelty of the research are expressed in Section 1.2, and the contents of this thesis are briefly outlined in Section 1.3.

1.1 Background

A characteristic effect of a mobile radio channel is small-scale fading due to multipath propagation. Based on channel measurements and theoretical considerations, a large number of channel models have been presented in the past. The proposed models include, for example, those aimed for the simulation of MIMO single-carrier systems

in frequency-selective Rayleigh fading (Pedersen *et al.* 2000a, Xu *et al.* 2004, Xiao *et al.* 2004). Some other presented models are aimed, for example, for the modeling of either spatiotemporal correlation at a base station in frequency-nonselctive Rayleigh fading (Chen *et al.* 2000, Smith & Abhayapala 2003), spatiotemporal correlation in frequency-nonselctive Rice fading MIMO channels (Abdi & Kaveh 2002), or spatial correlation in outdoor MIMO channels (Gesbert *et al.* 2002). None of the above or other proposed models to the authors knowledge, however, address specifically frequency-selective, Rice fading multicarrier MIMO channels.

Fading can be simulated by using either ray tracing or a stochastic approach, or a combination of them. In stochastic modeling, fading has been given predefined characteristics, which have been derived for a limited number of broadly designated propagation environments based on measurements. In ray tracing, on the other hand, fading results from the imitated propagation in a particular environment. The three commonly used stochastic approaches to generate temporally correlated Rayleigh fading with the desired Doppler power spectrum are based either on the sum of sinusoids (SOS), inverse discrete Fourier transform (IDFT), or time correlation shaping filtering. The SOS technique is, in essence, a simple ray tracing setup. The method utilizing the IDFT performs, in fact, the shaping of the temporal correlation in the frequency domain by multiplying Gaussian noise with the square root of the desired Doppler power spectrum and then transforms the product into the time domain. This method is accurate for long sequences and high Doppler frequencies, but the computational load per channel coefficient increases with the length of the sequence. In time-domain time correlation shaping filtering, on the other hand, the accuracy of the process and the computational load per coefficient are independent of the sequence length. Moreover, coefficients can be generated as they are needed, whereas the IDFT method requires that they are all generated by a single IDFT operation. The ability to generate coefficients as they are needed is advantageous, for example, when the length of the sequence is not known in advance. In addition to perpetual temporal autocorrelation generated to Gaussian sequences by time correlation shaping filtering, crosscorrelation can be generated between the sequences by a block-wise linear matrix transformation. This transformation has been used in the existing fading simulators to generate either spatially or spectrally correlated fading sequences but not fading that would be both spatially and spectrally or jointly spatio-spectrally correlated.

Orthogonal frequency division multiplexing (OFDM) has become the most widely used multicarrier technique due to its spectral efficiency and computationally efficient

implementation by the discrete Fourier transform (DFT). OFDM is used nowadays for providing high data rate connections in, for example, digital subscriber line (DSL) modems, digital video broadcasting (DVB), and wireless local area network (WLAN) systems. In mobile radio communications, direct-sequence (DS) code-division multiple-access (CDMA) technique was adopted for the 3rd generation cellular systems due to its capability to provide higher flexibility, capacity and interference tolerance over the conventional time and frequency division access schemes. However, the ever-increasing data rates demanded also from the next generation mobile radio systems would result in impractically high chip rates if single-carrier DS-CDMA were used. The combination of OFDM and CDMA with frequency-domain spreading, generally referred to as multicarrier (MC) CDMA, enables a lower chip rate which is now equal to an OFDM symbol rate, and brings together the above mentioned advantages of OFDM and CDMA. Consequently, MC-CDMA has been widely considered to be a promising candidate for the multiplexing technique of the future high data rate mobile communications, especially for a downlink channel.

Two multirate transmission schemes that are particularly applicable for CDMA are the multicode scheme and the variable spreading factor (VSF) scheme. In the multicode scheme, the transmission rate of a user varies with the number of overlapping data streams that are assigned different spreading sequences of fixed length. In the VSF scheme, the rate varies with the number of nonoverlapping streams that are assigned the same spreading sequence whose length is inversely proportional to the rate. Therefore, the separation of multiple streams that provide a multiple of the basic rate is based in the multicode scheme on the same code-division principle as the separation of multiple users in a CDMA system. In contrast, the VSF scheme is based on time division in the case of a DS-CDMA system, and on frequency division in the case of a MC-CDMA system. In the 3rd generation DS-CDMA-based cellular systems, the multirate transmission is realized with the time-division-based VSF multirate scheme. One reason for this is that the VSF scheme does not give rise to the peak-to-average power ratio (PAPR) of a signal, which results in savings due to less stringent requirements for the dynamic range and linearity of handset power amplifiers and A/D and D/A converters. In MC-CDMA, on the other hand, PAPR is already substantial by the nature of OFDM and, consequently, several techniques for PAPR reduction have been proposed. Therefore, the increase in PAPR due to the multicode scheme does not bring previously nonexistent problems into an MC-CDMA system.

Besides the well-established OFDM and CDMA technologies for WLAN and cellular applications, respectively, and the recent proposals of their combinations, UWB radio transmission has gained increasing interest lately. UWB can provide high, multimedia-capable data rates with a very low power spectral density. The potential robustness against narrowband interference and frequency-selective fading further increases the attractiveness of UWB communications. These features make UWB transmission applicable for radio devices that coexist with other radio services in the same operational frequencies. UWB communications have gained great interest since the Federal Communications Commission (FCC) of the United States (US) allocated the 3.1-10.6 GHz band, which is overlapping with other radio systems, for unlicensed UWB communication devices in 2002. The UWB spectrum is considered to be used for a wide range of wireless personal area network (WPAN) communications, including wireless connectivity in personal computing, consumer electronics, and mobile applications. The two most favored approaches for UWB communications are carrierless impulse radio and multiband (MB) OFDM, the latter of which has been the choice for the first UWB standard (Ecma International 2005) due to the efficiency and maturity of OFDM technology.

In MB-OFDM, the UWB spectrum is divided into several subbands, each of which is carrying an OFDM signal. Frequency-hopping, interleaving, dual-carrier modulation, and frequency-domain spreading in the form of transmitting the same information on two subcarriers within the same OFDM symbol, are used to obtain diversity against frequency-selective fading and interference. To further improve the performance, more extensive frequency-domain spreading by spreading sequences, that is, the use of frequency-domain code-division multiplexing (CDM), has been proposed and simulated by Gerakoulis & Salmi (2002), Park *et al.* (2004), Ramachandran *et al.* (2004). In MB-OFDM, frequency-hopping provides, besides diversity, a way to achieve separation between simultaneously operating piconets (SOPs). However, collisions between frequency-hopping sequences and the number of destructively interfered symbols increase with the number of SOPs. As an alternative way to separate SOPs, a frequency-domain CDMA, being equivalent to MC-CDMA, may be used. The performance of this approach has been simulated by Popescu & Yaddanapudi (2006), Gong *et al.* (2006).

1.2 Motivation and scope of the research

In this thesis, firstly a stochastic model for small-scale fading with a Rice distributed envelope and temporal, spatial, and spectral correlation is proposed. The model stands out from the earlier proposed tapped-delay-line models with temporal and spatial correlation in that it includes also the explicit modeling of spectral correlation. That is, the fading processes of different subcarriers can be generated with desired, exact frequency-domain correlation values instead of settling for the unknown correlation that is hidden in a specific power delay profile and discovered only via the Fourier transform. This can be advantageous, for example, in the performance evaluation of multicarrier transmission schemes relying on certain level of frequency diversity. The model presents a fading channel in a generic form based on a channel spread function that is the joint spread in Doppler frequency, direction at both a transmitter and receiver, and delay. In the special case where the channel spread is separable in the aforementioned factors, the model unifies the well-known independent characteristics of fading in time, space, at both a mobile and base station, and frequency. Based on the model, a small-scale fading simulator, which utilizes time correlation shaping filtering and a space-frequency correlation transformation, is introduced. The simulator has been proven to achieve high accuracy while maintaining reasonable computational complexity and, therefore, can be efficiently used in the simulation of MIMO multicarrier systems. The simulator was initiated in the author's Master Thesis (Kunnari 2000) and an early version of it was used in obtaining the results of a number of articles including those authored or co-authored by this writer but not included in this thesis (Kunnari & Tujkovic 2001a,b, Kunnari 2002, Mucchi *et al.* 2002). Subsequently, the simulator was completed with theoretical background, improvements, and extensions including the options for Rice and spectrally correlated fading. Before the introduction in the international articles included in this thesis, the completed simulator was presented in a national forum (Kunnari 2003a,b). The extension of the simulator to the modeling of spectral correlation was utilized throughout the performance evaluations that were conducted in this thesis work and are outlined below.

Next, the error rate performance of the multicode and VSF multirate schemes are analyzed and compared in a MC-CDMA system over multipath Rayleigh fading channels. In the conducted performance evaluation, the proposed small-scale fading channel model and the attendant fading simulator are utilized to the appropriate extent. Both a synchronous downlink and uplink, as well as an asynchronous uplink are

considered. In most of the earlier published results on the subject, it has been claimed that these two multirate schemes achieve very similar performance. However, it is shown here that remarkable differences exist in the performance of the schemes. Moreover, the generality of the analysis enables straightforward incorporation of different combining schemes, of which six are reviewed and their performance with the multirate schemes are compared. Furthermore, in the earlier studies on the performance analysis of OFDM-based MC-CDMA, presented for example by Gui & Ng (1999), Linnartz (2001), Li & Latva-aho (2002), Shi & Latva-aho (2002b,a), the channel is assumed to be frequency selective, which supposes a substantial multipath delay spread, but the spread is assumed to be shorter than or truncated to the length of a guard interval for simplicity. Consequently, no guard interval or ISI is taken into account in those studies. In the analysis presented herein, the delay spread can extend over the guard interval, which is also modeled. Therefore, the deteriorating effect of ISI is also observed.

Lastly, the performance analysis of MC-CDMA is applied to OFDM-based UWB systems enhanced with frequency-domain CDM, for which, to the author's knowledge, only simulation results existed in the literature so far. The analysis is first applied to the case of a single piconet operated with a continuum of schemes from a plain nonspread OFDM scheme to a maximally spread multicode scheme via medium-spread combinations of the VSF and multicode transmissions. Subsequently, the analysis addresses frequency-domain CDMA that is used for the accommodation of multiple SOPs. In this case, a continuum of schemes from a plain nonspread single-SOP OFDM scheme to a maximally spread multi-SOP multicode scheme via medium-spread VSF transmissions are considered.

1.3 Outline of the thesis

The rest of this thesis is organized as follows. Chapters 2 and 3 present a review of literature, giving an overview of the past findings and the present status in the research fields related and relevant to the topics of this thesis. The former of the two chapters reviews the literature on small-scale fading mobile radio channels, and the latter reviews the literature on spread-spectrum communication techniques over those channels, having an emphasis on MC-CDMA and MB-OFDM. Although the review is extensive, it is by no means exhaustive, but it brings out the novelty of the contributions of this thesis. Chapter 4 summarizes the original articles forming the basis of this thesis. The summary groups together Articles I and IV on the modeling of small-scale, Rice fading channels

for the simulation of MIMO multicarrier system in Section 4.1, Articles II and III on the performance analysis of multirate MC-CDMA in Section 4.2, and Articles V and VI on the application of the analysis to OFDM-based UWB systems enhanced with frequency-domain CDM in Section 4.3. Finally, Chapter 5 concludes the thesis by summarizing it and discussing not only its results but also shortcomings that need further research in the future.

2 Small-scale fading channels

One of the earliest, if not the first, published study on land mobile radio channels is the one by Young & Lacy (1950). It reports on an investigation in New York City where pulses of a 450 “*megacycle*” carrier were transmitted from the top of a building and received at a mobile unit on the street level. The received “*echo*” pattern of the pulses was displayed on an oscilloscope from which it was recorded with a “*moving picture*” camera. These measurements were part of a program to study the possibilities of multichannel mobile radio systems occupying a relatively wide band. The obtained rudimentary results on the probabilities and strengths of multipath components at different delay intervals were applied for determining the maximum bandwidth of such systems. Since the advent of the research on wideband mobile radio channels, the terminology, measurement data recording, and the knowledge have evolved as channel characteristics effecting on ever advancing mobile radio technologies have been explored.

Young (1952) continued the early reporting on the characteristics of mobile radio channels by presenting results of a series of experiments comparing the transmission performance of carrier frequencies from 150 to 3700 MHz in urban and suburban areas. Along with frequency, Egli (1957) studied the effects of antenna height, polarization, and distance on the radio wave propagation in both fixed and mobile radio transmissions.

A review of work done on the characterization of time-variant channels in the late 1950s and early 1960s was given by Kailath (1963). Perhaps the most cited paper of those days is by Bello (1963), which introduced the concept of time-frequency duality in the context of system functions of channels modeled by time-varying linear filters. According to the paper, there is a duality between the uncorrelated scattering (US) and the wide-sense stationary (WSS) channels, delay dispersion and frequency selectivity, and Doppler dispersion and time selectivity. These studies, although motivated mainly by long-range radio links and radar, became part of the theoretical foundation for the later appearing characterizations of mobile radio channels.

The attenuation of a received signal propagated through a mobile radio channel can be generally decomposed into a path loss, large-scale fading, and small-scale fading. The path loss is defined as the mean attenuation of a signal, and it increases with distance and frequency. Moreover, the type of propagation environment and antenna heights determine an additional path loss over the free-space loss, so that the loss is higher

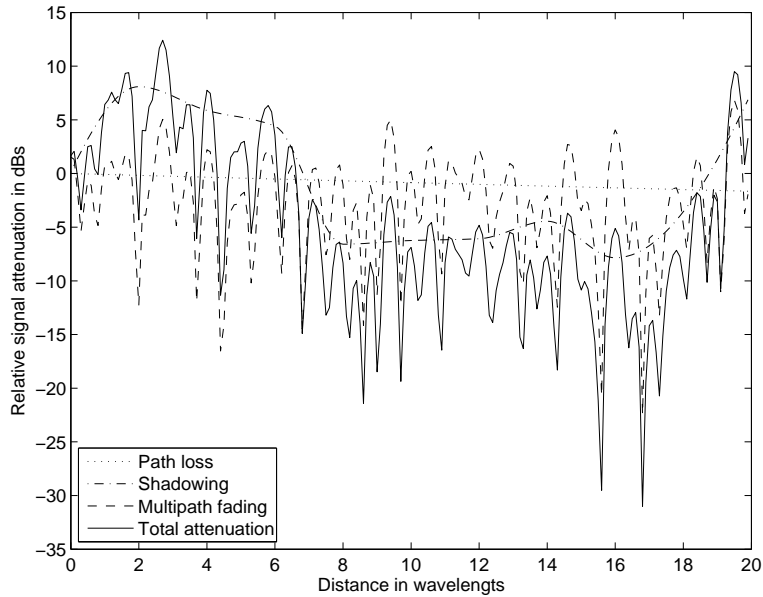


Fig. 1. The relative attenuation of received signal versus distance.

in hilly and urban areas and with low-rise antennas than in flat and rural areas and with high-rise antennas. Large-scale fading, which is also referred to as shadowing, is the variation of the mean path loss over distances that are in the range of the size of obstructions in the signal path. Large-scale fading has been found to be log-normally distributed and the deviation depends on the propagation environment and distance. Small-scale fading, which is also referred to as short-term or multipath fading, refers to the fluctuation of the signal level within transitions as short as half of a wavelength. The decomposition of total signal attenuation into a path loss, shadowing, and multipath fading and their relationship to distance is illustrated in Fig. 1. In this thesis, only the small-scale fading is considered. Literature on the characterization and computer simulation of small-scale fading is reviewed in Sections 2.1 and 2.2, respectively. More information on the average path loss, large-scale fading, and mobile radio channels in general is provided, for example, in the introductory magazine article by Sklar (1997), in the extensive journal publication edited by Bertoni (1988), in the book by Parsons (1992), and in the final reports of the European Cooperation in the Field of Scientific and Technical Research (COST) actions 207, 231, 259, and 273, edited by Failli (1989), Damosso & Correia (1999), Correia (2001), and Correia (2006), respectively.

2.1 Characteristics of small-scale fading

In mobile radio systems, the antenna of a portable unit is typically low and in the vicinity of various man-made and natural structures. The radio waves reflected and scattered by the surrounding structures add up together with a wave that has traveled along a possible line-of-sight (LOS) path to form a multipath signal at a receiver. Depending on the relative phases of the multipath signal components, which vary due to the differences in the respective path lengths, reflection coefficients, and Doppler shifts, the interaction of the components varies from constructive to destructive. This results in frequent deep fades of the composite signal over small shifts in time, location, and carrier frequency if a magnitude of none of the multipath components is vastly superior to the others. The existence of small-scale fading and its origin were known already at the dawn of the research on mobile radio channels (Young & Lacy 1950). The models proposed thereafter for the envelope distribution of small-scale faded signals are reviewed in Section 2.1.1, and the findings on the dispersion of multipath components over propagation delay, Doppler frequency, and direction of incidence, and the respective properties of the selectivity of small-scale fading in frequency, time, and space are reviewed in Sections 2.1.2, 2.1.3, and 2.1.4. Section 2.1.5 focuses on joint dispersions and the corresponding selectivities.

2.1.1 Envelope distribution

It is a generally approved approximation that the multiplicative complex path coefficients of scattered multipath components in physical multipath channels are mutually uncorrelated. This assumption of US (Bello 1963) is supported by the facts that the paths are normally much longer than the considered wavelengths and the lengths of the paths and scatterers along them vary greatly. While in the probability theory the independence of variables ensures their uncorrelatedness, the uncorrelatedness of variables does not necessarily imply their independence unless the variables are jointly Gaussian. However, based on the above mentioned facts that support the US assumption, it is generally considered to be irrefutable that the phases of scattered multipath components are independent and uniformly distributed over $[0, 2\pi)$ (Turin *et al.* 1972, Bertoni 1988). Consequently, the phase of a composite signal obtained by adding up the scattered components is also uniformly distributed over $[0, 2\pi)$ (Rice 1944, 1945). While there has been a consensus on the uniform phase distribution of the composite, small-scale

fading signal, its envelope has inspired several distribution models that are reviewed in the following section.

Rayleigh distribution

Typical propagation environments of mobile radio systems are rich in scattering structures and, therefore, also the number of scattered multipath components is large. If the magnitudes of the multipath components are somewhat similar so that there is no LOS or any scattered path dominant over the others, the envelope of the composite multipath signal has been found to follow the Rayleigh distribution, originally introduced by Rayleigh (1880) for the resultant of a large number of unit vectors of an arbitrary phase. In the case of mobile radio channels, this observation was done already by Young (1952) and in numerous other papers thereafter.

Besides Lord Rayleigh's original postulation, a Rayleigh-distributed random variable results from the square root of a sum of two uncorrelated jointly Gaussian zero-mean random variables with equal variances, that is, from the envelope of a zero-mean complex-valued circularly symmetric Gaussian random variable. The latter is widely used to model the channel coefficient of a multipath signal based on the central limit theorem and the US assumption. Strictly speaking, the classical central limit theorem (Proakis 1995) requires that the path coefficients of the multipath components would have to be independent and identically distributed (iid) in order to yield a multipath channel coefficient that approaches a Gaussian variable as the number of multipath components increases. However, variants of the theorem exist, including Lyapunov, Lindeberg, and m -dependent central limit theorems that have less stringent requirements for the component variables.

Much of the popularity of the zero-mean complex Gaussian model for a multipath channel coefficient, which leads to Rayleigh fading, can be explained by its mathematical tractability. With respect to Rice fading reviewed in the next section, Rayleigh fading also gives a sort of upper limit for the severity of small-scale fading as no LOS component is assumed.

Rice distribution

When an unobstructed LOS between a transmitter and receiver exists, the multipath signal component that has traveled along the LOS path is normally much stronger than

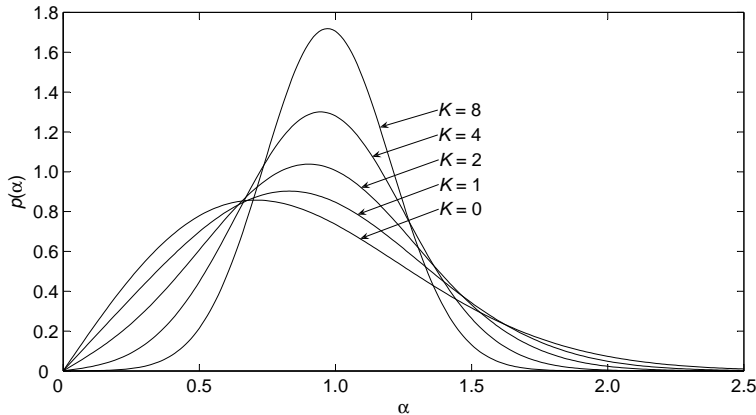


Fig. 2. The pdf of Rice distribution for different Rice K -factors.

the scattered components. Alternatively, in a non-LOS (NLOS) situation, there may be a scattered multipath component that is significantly stronger than the others. If the scattered components, other than the dominant scattered component in the NLOS case, can be modeled as a zero-mean complex circularly symmetric Gaussian variable as in the case of Rayleigh fading, it results, based on the principle of superposition, that the overall multipath signal is now composed of a constant-magnitude part due to the LOS or dominant scattered path and a Gaussian part due to the other scattered paths. This composition is analogous to a single sinusoidal wave interfered by additive Gaussian noise. Therefore, the envelope of this signal fades according to a distribution that was introduced by Rice (1948) and called either as Rice, Ricean, or Rician distribution after the discoverer thereafter.

The ratio of the power of the constant component over the mean power of the Gaussian component is called the Rice K -factor. The smaller the K -factor, the more severe and closer to the Rayleigh-type the fading is. The probability density function (pdf) of Rice distribution for different Rice K -factors is illustrated in Fig. 2. Measurement based values for the Rice K -factor in different type of propagation environments are given, for example, by Bultitude & Bedal (1989) and Glazunov *et al.* (1999).

Nakagami distribution

Another distribution for the envelope of a fading signal was proposed by Nakagami (1960), who named it originally as the m -distribution. Thereafter, it became also known

as the Nakagami- m distribution or simply as the Nakagami distribution. The parameter m , called the shape factor, can take all real values $m \geq 1/2$. For integer values of m , the Nakagami distribution can be interpreted as a generalization of the Rayleigh distribution, m being the number of iid Rayleigh-distributed variables, the sum of which is distributed according to a Nakagami m -distribution. For $m < 1$, the tails of the distribution, especially the one for the small values of a variable, are larger than with the Rayleigh distribution, and gradually increase as m decreases, until at $m = 1/2$ the distribution is the one-sided Gaussian distribution. Therefore, distributions with $m < 1$ can potentially describe fading phenomena that are more severe than Rayleigh fading. When $m > 1$, the distribution is more peaked than the Rayleigh distribution and, therefore, can model fading that is less severe than Rayleigh fading.

The Nakagami distribution was originally derived to fit empirical short-term fluctuations of short wave ionospheric radio links better than the Rice distribution, but thereafter has been reported to be better suited for the small-scale fading also in mobile radio channels (Suzuki 1977, Aulin 1981). The Nakagami distribution has also gained popularity in system performance analysis due to its better mathematical tractability in comparison with the Rice distribution. However, there is no widely accepted theory for a physical phenomenon in radio channels that would be behind the Nakagami distribution of fading. Moreover, it is criticized that in papers where empirical distributions are claimed to be closer to the Nakagami than Rice distribution, the criteria for the goodness-of-fit emphasize the fit on the envelope values around the mean with large probabilities rather than on the much less probable small values that are the most fundamental for a system performance (Stein 1987). A justification for the criticism can be found in the paper by Aulin (1981), where the Nakagami distribution is found to give the best fit to the empirical data based on the goodness-of-fit test, although the illustrations show that the Rice distribution yields the best match at low signal envelopes.

Other distributions

Other distributions that have been proposed for the envelope distribution of a small-scale fading signal, but which are less frequently referred to, include the Weibull distribution (Weibull 1951), which is more often used in the field of reliability and life data analysis, but also in conjunction with fading (Shepherd 1977), and the Hoyt distribution (Hoyt 1947), also known as the Nakagami- q distribution, which is typically observed on scintillating ionospheric radio links (Nakagami 1960).

Abdi *et al.* (2000b) presented a generic pdf in the form of a definite integral, with an infinite expansion for the sum of vectors with uniformly distributed angles and arbitrary dependent lengths in order to model the envelope distribution of multipath fading, among other applications. A spherically invariant random process, which can be represented by a Gaussian process multiplied by an independent positive random variable, has also been proposed for the modeling of multipath fading with great flexibility (Abdi *et al.* 2000a). Generalized distributions that include a number of aforementioned distributions as special cases have also been derived (Yacoub *et al.* 2005, Yacoub 2007).

Although the log-normal distribution is generally considered to describe large-scale fading statistics, it has also been proposed for the modeling of small-scale fluctuations based on experimental results (Turin *et al.* 1972). The proposed distributions also include those aiming at describing the effects of both the large- and small-scale fading (Suzuki 1977, Coulson *et al.* 1998a,b) and the effects of multiple sequential scattering along propagation paths (Andersen & Kovacs 2002, Salo *et al.* 2006).

2.1.2 Delay dispersion and frequency selectivity

In the seminal paper on mobile radio channels by Young & Lacy (1950), the dispersion of a received multipath signal in delay was the main interest because of the resulting ISI of wideband signals. In the paper, results of a statistical analysis on the probability of occurrence of paths of two classes of strengths within different delay ranges was presented. These very same measurement based results were one of the few that were publicly available for a reference when a rudimentary prediction model for the probability of occurrence of a path in a given range of delays and strengths was derived by Schmid (1970) two decades later. Turin *et al.* (1972) proposed a more refined statistical multipath channel model that was drawn on a model for multipath propagation in ionospheric radio links and revised based on recent propagation experiments in urban environments. The proposed model presents the channel as a linear filter, commonly referred to as a tapped delay line. The filter taps were modeled to have delays with a modified Poisson distribution, correlated large-scale and independent small-scale fading magnitudes with a log-normal distribution, and phases with a uniform distribution over $[0, 2\pi)$. This model has served as a reference in innumerable papers considering further refinements or modifications to the tapped delay-line based models of a mobile radio channel, including those by Suzuki (1977), Hashemi (1979), and Turkmani *et al.* (1991)

for outdoor environments and by Saleh & Valenzuela (1987), Rappaport *et al.* (1991), and Ganesh & Pahlavan (1991) for indoor environments.

The taps of the delay line represent so-called resolvable paths, each of which is composed of unresolvable multipath components that arrive within a resolvable delay interval. It is widely accepted that the taps experience practically uncorrelated small-scale fading, which is supported by the US assumption and experimental measurements (Turkmani *et al.* 1991). An exception to this rule may be, however, the last taps of LOS indoor environments, between which Kivinen *et al.* (2001) have found more noteworthy correlation values. These findings were explained by the fact that the US assumption may not be valid for the last taps, since they are composed mainly of multipath components that have gone through multiple backward-and-forward reflections between the ends of a corridor or hall. The envelope of the small-scale fading of the taps is most often modeled as Rayleigh distributed. The phases of complex tap gains are modeled, without an exception, as uncorrelated and uniformly distributed over $[0, 2\pi)$. If large-scale fading is modeled, it is usually assumed that it is log-normally distributed and correlated between the taps. The average powers of the taps are determined based on a power delay profile, reviewed in the following.

A power delay profile, also referred to as a delay power spectrum, represents the distribution of average received power in delay. The delay power spectrum is dictated by the scattering environment and, consequently, its exact shape varies from site to site. However, when averaged over several sites of the same type of propagation environment, the delay power spectrum can be approximated as a decaying exponential function $\sigma_d^{-1} e^{-\tau/\sigma_d}$, where τ is the delay and σ_d is the root-mean-square (rms) delay spread that is equivalent to the standard deviation of the delay and determines the slope of the decay (Gans 1972). Noting that the propagation delay is directly proportional to the covered distance, the above approximation is consistent with the exponential increase of an average path loss with distance, which is common to all prediction models for the median transmission loss (Bertoni 1988). That is, a multipath component's average power decreases exponentially with its traveled distance that is directly proportional to its travel time. Hansen (2003) has also presented analytical calculations yielding to an exponentially decaying delay power spectrum in a single room environment. It follows from the exponentially decaying delay power spectrum that the spectral correlation function, which can be obtained as the Fourier transform of the delay power spectrum, is the well-known Fourier transform pair of the exponential function, $(1 + j2\pi\Delta f\sigma_d)^{-1}$, where Δf is the difference in the frequency.

While the delay power spectrum with a single exponentially decaying function is an appropriate model for homogeneous propagation environments, reflections from distant hillsides or large buildings in addition to local scatters may result in a spectrum with more than one distinct clusters of arrivals. This tendency of clustering, observed for the initial arrivals in an urban environment already by Turin *et al.* (1972), was taken into account in the reference models of the final report of COST 207 action. This report proposes delay power spectra that have, in addition to the first exponentially decaying function, another attenuated and delayed function for so-called bad urban and hilly environments, while a spectrum with a single function was proposed for typical, nonhilly urban and rural environments (Failli 1989). Experimental measurements confirm that the majority of the urban propagation environments can be classified as having one or two delay clusters (Pedersen *et al.* 2000b, Toeltsch *et al.* 2002). For indoor propagation, the clustering of arrivals was introduced in the often referred to statistical model by Saleh & Valenzuela (1987). They observed that in addition to the always present first arriving cluster of waves propagated mostly over open spaces and through a few walls, one-half of the measured rooms showed evidence of one additional cluster due to reflections from, for example, metalized walls and doors.

2.1.3 Doppler dispersion and time selectivity

Ossanna (1964) was the first to propose a statistical model for the frequency power spectrum of multipath fading, later known as the Doppler power spectrum. In the derived two-dimensional (2-D) geometrical propagation model, there are only two interfering paths between the mobile unit and the base station. One is a direct LOS path and the other is a path reflected from a side of a house, the orientation of which with respect to the mobile is random. The obtained theoretical Doppler power spectra were found to be in fairly good agreement with those measured on suburban streets. Soon thereafter, Gilbert (1965) considered more generic multipath propagation models that can have a larger number of paths and, therefore, are more applicable to urban environments with rich scattering. A feature common to Gilbert's models is the isotropic distribution of scatterers around the mobile, spaced either evenly or randomly. Gilbert's approach was to first derive the spatial correlation from which he then derived the temporal correlation and, subsequently, the Doppler power spectrum. The isotropic scatterer distribution around a mobile was supported by the test reports of Stidham (1966), who had found

that the pointing direction of a highly directional mobile antenna has only a small effect on the signal level in NLOS situations.

Drawing on Gilbert's work, Clarke (1968) considered a scattering model in which the scatterers were assumed to be uniformly distributed around the mobile. It was further assumed that the scattered waves are planar, of equal magnitude, and have uniformly distributed random phases. Based on the model, the temporal correlation function and the corresponding Doppler power spectrum, which are a Fourier transform pair, were derived, respectively, as $J_0(2\pi v_D \Delta t)$ and $[\pi v_D \sqrt{1 - (v/v_D)^2}]^{-1}$, $|v| \leq v_D$, where $J_0(\cdot)$ is the zero-order Bessel function of the first kind, Δt is the difference in observation time, and v is the Doppler frequency and v_D its maximum. The Doppler frequency is given by $v = (\mathbf{v} \cdot \mathbf{d})/\lambda_c$, where \mathbf{v} is the velocity vector of the mobile, \mathbf{d} is the unit direction vector of a scattered path, and λ_c is the carrier wavelength. It follows that the maximum Doppler frequency is $v_D = v/\lambda_c$, where v is the mobile speed. The above spectrum is the most commonly applied Doppler power spectrum and often referred to as the classical Jakes' spectrum after Jakes (1974), who introduced a laboratory device for the simulation of Rayleigh fading with this particular spectrum.

In most propagation environments, the arrival directions of multipath components are concentrated on small elevation angles close to the horizontal plane (Lee & Brandt 1973, Kalliola *et al.* 2002). Consequently, the horizontal direction dispersion is typically dominant over the vertical one, which supports the two-dimensionality of the Clarke's scattering model discussed above. However, more general and accurate three-dimensional (3-D) scattering models, which include both the azimuth and elevation of arrival, have also been considered in conjunction with Doppler dispersion (Aulin 1979, Parsons & Turkmani 1991, Vatalaro & Forcella 1997, Clarke & Khoo 1997, Qu & Yeap 1999, Narasimhan & Cox 1999). In the special case of an isotropic distribution of scatterers in three dimensions, the temporal correlation function is obtained as $\text{sinc}(2v_D \Delta t)$, where $\text{sinc}(\cdot)$ is the sine cardinal function. The corresponding Doppler power spectrum is simply $(2v_D)^{-1}$, $|v| \leq v_D$, which is often referred to as the flat spectrum due to its uniformity (Clarke & Khoo 1997, Qu & Yeap 1999). The channel measurements by Zhao *et al.* (2003) demonstrate that the flat Doppler spectrum can be found especially in NLOS indoor environments, where strong scattering takes place from the ceiling and the floor besides the walls. Moreover, some resolvable paths were reported to have flat spectra also in NLOS outdoor environments where the base station antenna stands above the nearby rooftops. In the latter case, the vertical direction dispersion is increased by the waves propagating down at streets by diffraction from the

roof edges in the direction of the base station and by reflection from the high walls across the streets (Kuchar *et al.* 2000, Laurila *et al.* 2002, Kalliola *et al.* 2003).

The isotropic distribution of scatterers around a mobile serves well as both a mathematically tractable theoretical model and an empirical average over a random route and orientation of a mobile in varied environments. However, instantaneous scatterer distributions and the resulting Doppler power spectra along the route of a mobile are composed of clusters that vary with different scattering objects dominating at different locations, which was demonstrated already by the measurements of Cox (1971, 1972). In urban environments, the direction of arrival of multipath components with large excess delays have been found to be concentrated in the direction of street canyons that act as waveguides (Fuhl *et al.* 1997, Kuchar *et al.* 2000, Laurila *et al.* 2002). For these instances, rectangular (Kuchar *et al.* 2000) and parabolic (Chen & Dubey 2005) scatterer distributions have been proposed. Also the von Mises distribution, which may be thought of as the circular version of the Gaussian one, has been proposed as a mathematically convenient approximation for nonisotropic scatterer distributions at a mobile site (Abdi *et al.* 2002). Regardless of the actual shape of a Doppler power spectrum, a practical measure of the time selectivity of fading, the so-called channel coherence time is, however, dictated solely by the inverse of the Doppler spread, which is the range of values of ν over which the spectrum is essentially nonzero (Proakis 1995).

2.1.4 Direction dispersion and space selectivity

The dispersion in the direction of departure or arrival of multipath components with respect to transmitting and receiving antenna elements determines the space selectivity of a small-scale fading channel. In general, the direction dispersions diverge greatly at the different ends of a radio link in the case of a base station and a mobile unit due to their dissimilar operation surroundings.

Models characterizing the direction dispersion at a mobile unit were already considered in conjunction with the Doppler dispersion in the previous section, as the latter is fundamentally dependent on the former. Especially in the case of an isotropic distribution of scatterers around a mobile, which is a popular assumption discussed above, the temporal correlation and the spatial correlation at the mobile end can be related via a time-distance transformation (Gilbert 1965, Clarke 1968, Gans 1972, Parsons & Turkmani 1991). According to the transformation, a spatial difference Δp is

interpreted as a distance covered by a mobile whose speed is v during a time difference Δt , that is, $\Delta p = v\Delta t$. Then it follows that the substitution of $\Delta t = \Delta p/v$ into the temporal correlation functions given for the isotropic 2- and 3-D scattering in the section above leads to the respective spatial correlation functions $J_0(2\pi\Delta p/\lambda_c)$ and $\text{sinc}(2\Delta p/\lambda_c)$ for the mobile end. Since the direction dispersion is typically large at a mobile, it results in spatial correlation that decreases rapidly with the spacing $\Delta p/\lambda_c$. Consequently, most of the spatial diversity advantage can be obtained at a mobile with an antenna spacing as small as a quarter of a wavelength, as was found already by Rustako (1967).

At the elevated base station antennas in outdoor environments, the direction dispersion of multipath components is typically much smaller than that at a mobile, around which most of the scatterers are concentrated. Consequently, the spatial correlation is significantly higher at the base station than at a mobile. The pioneering measurements by Lee (1971) suggested that the horizontal spacing between two vertically polarized base station antennas locating well above nearby objects needs to be tens of wavelengths in order to make sure that the correlation levels are small enough to achieve most of the diversity advantage. Furthermore, the correlation in the endfire case, in which the mobile is in line with the base station antennas, was found to be much higher than in the broadside case in which the direction of a mobile is perpendicular to a line joining the antennas. The first theoretical derivation of the spatial correlation at the base station was presented by Gans (1972). In his rudimentary model, a mobile unit that was surrounded by a ring of scatterers was considered fixed while the base station was moving. The correlation at the base station was then related to that at the mobile.

Lee (1973) presented further experimental results and compared those with theoretical ones that were derived by assuming an azimuthal direction power spectrum in the form of a cosine function raised to a power of n , where n controls the spread of the spectrum. As Lee pointed out, his results provide a sort of upper bound on the spatial correlation and, therefore, are most applicable to rural environments with high-rise antennas. For more urban environments also with local scattering around the base station, Rhee & Zysman (1974) showed that an antenna separation of less than ten wavelengths in the horizontal plane is enough for obtaining sufficient diversity in the case of vertical polarization. Furthermore, they found that in obtaining a smaller correlation, horizontal antenna spacing is preferable to the vertical one, and vertical polarization to the horizontal one.

The next milestone paper on the spatial correlation at two base station antennas that are separated both horizontally and vertically was the one by Adachi *et al.* (1986).

Besides experimental results emphasizing the applicability of vertically spaced antennas, they presented an illustrative theoretical analysis that was further developed from the analysis presented by Lee (1973). To compute numerical results, the direction power spectra in both the azimuthal and elevation plane were assumed to be Gaussian. Turkmani & Parsons (1991) reported on another theoretical study of the spatial correlation at a base station based on a 3-D scattering model developed in an accompanying paper by Parsons & Turkmani (1991). In this model, the scatterers lie on a cylinder surrounding a mobile and their distribution is isotropic in azimuth and of the form of a cosine function in elevation. It was concluded that although the vertical separation of base station antennas has the advantage of producing a response which is independent of the direction of the mobile, the horizontal separation yields similar correlations with much smaller spacings. In addition to the above mentioned models for the direction dispersion at a base station, also the uniform distribution of azimuth over a given range of angles has been assumed for mathematical convenience (Salz & Winters 1994).

More recent channel measurements indicate that the Laplacian distribution, which is also known as the double exponential distribution, models the azimuth power spectrum at a base station better than the earlier proposed distributions in both rural and urban environments (Pedersen *et al.* 1997, 1998, 2000b). A generalized double exponential distribution, with different slopes on the opposite sides of the peak, has been found to give the best fit also for the elevation power spectrum in most propagation environments (Kalliola *et al.* 2002). A thorough theoretical treatment of direction dispersion and space selectivity in radio channels was given by Fleury (2000), who also extended Bello's seminal channel characterization to include spatial properties. Teal *et al.* (2002) presented closed-form solutions for the spatial correlation with the direction power spectrum following a variety of distributions, including many of the above mentioned ones. Closed-form expressions have also been derived for the correlation between the elements of uniform linear, circular, and rectangular arrays, and the elements of arrayed electromagnetic vector sensors in a 3-D channel with uniform azimuth and elevation power spectra (Yong & Thompson 2005).

The clustering of multipath components is apparent also in the direction or arrival, which was demonstrated first for indoor channels by Lo & Litva (1992). Thereafter, the azimuth power spectrum within clusters in indoor channels has been found to be approximately Laplacian distributed, and the mean azimuth of the clusters either uniformly (Spencer *et al.* 2000) or Gaussian distributed (Chong *et al.* 2003). In outdoor channels, the azimuth power spectra within the multiple clusters appearing in so-called

bad urban environments were also found to follow the Laplacian distribution (Pedersen *et al.* 2000b). The directional clustering in both the azimuthal and elevation planes in an urban outdoor environment was illustrated by Toeltsch *et al.* (2002). A few significant directional clusters at both the base station and mobile, in addition to diffused and smaller components distributed all around the mobile, were reported by Pajusco (2003).

Polarization dispersion and selectivity

Spatial dispersion of a received signal occurs not only in the direction of arrival but also in the direction of polarization. Dispersion in polarization is mainly due to the varying amounts of cross-polarization coupling induced by different scatterers and reflectors along the route of multipath components. Moreover, the random orientation of a handheld mobile unit gives rise to the polarization mismatch between the base station and mobile. Polarization dispersion in mobile radio channels was reported already by Lee & Yeh (1972) in their proposition of a two-branch polarization diversity system with one vertically and one horizontally polarized antenna at both the base station and mobile. They found that the cross-polarization power ratio (XPR) of a 900 MHz signal varied from 4 to 9 dB at few different streets in a suburban environment, regardless of the original polarization.

Kozono *et al.* (1984) presented an analysis of a $\pm 45^\circ$ polarization diversity reception at a base station while having vertical polarization at a mobile. For comparison, results of measurements carried out in an urban environment at 900 MHz were also presented. They concluded that the power correlation of small-scale fading at the elements of a $\pm 45^\circ$ polarization diversity antenna was lower than 0.6 and that the power level decrease in comparison with vertical polarization was lower than 2.5 dB, provided that the angular offset between the main beam direction of the antenna and the direction of the mobile were less than 45° . Cox *et al.* (1986) found that at 816 MHz the XPR is 3.5 dB in a suburban environment, 2.5 dB in indoor-to-outdoor transmission, and even greater in indoor environments. Furthermore, they concluded that the measurements did not show evidence of consistent nonuniformity in the azimuthal distribution of cross-polarized signal components except for a few residential locations.

Vaughan (1990) presented measurements of 463 MHz signals that were received from two co-located base station antennas, one with vertical and the other with horizontal polarization, after transmitting from a mobile with vertical polarization. The results showed that the envelopes of the orthogonally polarized signals are uncorrelated and

Rayleigh-like and the XPR is 7 and 12 dB in urban and suburban areas, respectively. Eggers *et al.* (1993) concluded, based on their research of compound space and polarization diversity systems, that the joint space-polarization correlation is a product of the marginal correlations in space and polarization. This suggests that the direction of polarization is independent of the direction of arrival.

Kalliola *et al.* (2002) found that the XPR was 11 dB in urban microcells, regardless of the base station antenna height. The same was found to be true also in outdoor-to-indoor transmission, whereas in indoor picocells and urban and highway macrocells the XPR was 7 dB. Somewhat consistently, Toeltsch *et al.* (2002) obtained an XPR of 8 dB in an urban environment. They also noticed that clusters with long delays and reflections from high elevations generally have higher XPRs. The dependence of XPR on distance and the delay profile was modeled by Shafi *et al.* (2006).

2.1.5 Joint dispersion and selectivity

Most of the early papers on dispersive multipath channels consider either only one of the dispersions in delay, Doppler, and direction, or respectively, one of the selectivities in frequency, time, and space, or treat them separately. The separability of delay, Doppler, and direction dispersions, however, does not hold true in general, but requires special conditions to be fulfilled. In the following, literature considering the various joint dispersions and selectivities, the conditions enabling their separation into independent marginal factors, and the effect of that separation on channel characteristics is reviewed.

One of the early papers on joint dispersions in mobile radio channels is the one by Cox (1972) on delay-Doppler characteristics in a suburban environment. The reported measurement results on the joint delay-Doppler dispersion are, however, merely snapshots of the Doppler power spectrum at different delays which indicate that the involved scatterer clusters are changing with delay. Braun & Dersch (1991) presented 3-D snapshots of typical measured delay-Doppler power spectra in urban, suburban, and rural environments.

Liberti & Rappaport (1996) derived a joint distribution for the azimuth and delay of arrival based on a geometric single-scattering propagation model where the transmitter and receiver are in the focal points of concentric ellipses that bound regions of scatterers giving rise to multipath components of consecutive delays. Nørklit & Andersen (1998) considered a somewhat similar geometric model but took a 3-D ellipsoidal approach in order to take into account the difference in the antenna heights of a base station

and a mobile. Ertel & Reed (1999) derived the joint pdf of the azimuth and delay at both the base station and mobile for both the elliptic and circular models, the latter of which assumes a uniform distribution of scatterers within a given radius around the mobile. The space-frequency correlation at high elevated base station antennas in an urban environment was derived by Kalkan & Clarke (1997). However, their derivation assumed that the angle and delay of arrivals are independent, which resulted in separable spatial and spectral correlations. The independency of the angle and delay of arrivals was also assumed by Spencer *et al.* (2000), who based their assumption on limited measurement data in indoor channels. Chong *et al.* (2003) came to the same conclusions for NLOS indoor channels, but in the case of LOS some dependency between the angle and delay was found. The separability of the azimuth and delay power spectra was proposed also by Pedersen *et al.* (2000b) based on measurements in typical urban outdoor environments. They, however, found that the rms azimuth and delay spreads were correlated. The clustering of multipath components jointly in angle and delay has been observed in both indoor (Spencer *et al.* 2000, Chong *et al.* 2003) and outdoor (Pedersen *et al.* 2000b, Toeltsch *et al.* 2002) channels.

The joint correlation in space and time in mobile radio systems was analyzed already by Lee (1969), who applied it in conjunction with multiantenna predetection diversity combining and a directional antenna array. Later on, he further applied it in the derivation of the level crossing rate for the aforementioned diversity combining (Lee 1970). Motivated by the recent introduction of the space-time coded modulation, the joint correlation in space and time received interest again at the turn of the millennium. As a result, a space-time correlation function at a base station was derived by Chen *et al.* (2000) based on the isotropic distribution of scatterers on a ring around a mobile. Their results were generalized for nonisotropic scatterer distributions by Smith & Abhayapala (2003).

MIMO channels

Spatial multiplexing techniques, which deploy multiple antennas at both the transmitter and receiver in order to create parallel subchannels, have been introduced over the past decade. The capacity enhancements enabled by these techniques have led to great interest in so-called multiple input–multiple output (MIMO) radio channels. The available capacity of MIMO channels is heavily affected by the spatial correlation of those channels. Shiu *et al.* (2000) derived an approximative joint spatial correlation

at both the transmitter and receiver based on the two common assumptions that there is a ring of scatterers around a mobile and the angle spread seen at a base station is small. They showed that the number of subchannels, their gains and, therefore, the capacity of a MIMO system decreases as the spatial correlation increases. Reduction in the number of subchannels may occur although the spatial correlations would be close to zero. Channels with this phenomenon may be generalized as having scattering at both ends and a spatially restricted reradiating source in between. Therefore, these type of channels have been described as having either a "keyhole" (Chizhik *et al.* 2002) or a "pinhole" (Gesbert *et al.* 2002). Multiple scattering has been observed also by Steinbauer *et al.* (2001), who illustrated joint departure and arrival angles and delays of multipath components detected in microcell environments.

In its simplest form, the joint spatial correlation has been derived as a product of the spatial correlations between the transmit antennas and between the receive antennas (Kermoal *et al.* 2002). This derivation was done under the condition that the correlation at the receiver is independent of that at the transmitter, and vice versa. Under this condition, the spatial correlation matrix for a MIMO channel can be expressed simply as the Kronecker product of the spatial correlation matrices for the transmitter and receiver ends. Hence, this MIMO channel model is known as the Kronecker model. The suitability of the Kronecker MIMO channel model was investigated by McNamara *et al.* (2002), who found it to give a good fit in NLOS channels but found it more mismatched under LOS conditions. Özcelik *et al.* (2003) showed based on measurement in indoor NLOS channels, that the Kronecker model creates artifact paths in the joint direction power spectrum of departure and arrival. This leads to the systematic underestimation of channel capacity which increases with correlation up to 27%. On the other hand, Chizhik *et al.* (2003) concluded from measurements in Manhattan, New York that the Kronecker model gives a median capacity error of only 3%, except in a tunnel that is akin to a "keyhole". Furthermore, Yu *et al.* (2004) observed that the Kronecker structure of the joint spatial correlation can be extended to each tap of a delay line model for frequency-selective NLOS indoor channels. Shafi *et al.* (2006) presented a MIMO channel model as a scaled sum of 2- and 3-D components, which include also cross-polarized components. The joint spatial correlation was then expressed as a scaled sum of the separate Kronecker models of the components.

A totally different approach to statistical MIMO channel modeling with joint spatial characterization was taken by Sayeed (2002), who proposed a virtual channel representation that corresponds to a fixed coordinate transformation via spatial basis

functions. His work, together with the Kronecker model, inspired Weichselberger *et al.* (2006) to propose a MIMO channel model in which the joint spatial correlation is modeled by describing the average coupling between the eigenmodes of the two channel ends. Recently, Czink *et al.* (2007) presented measurement results for the joint direction of arrival and departure dispersion of multipath clusters in indoor MIMO channels.

A joint space-time correlation function for Rice fading MIMO channels was presented by Abdi & Kaveh (2002) based on a ring of scatterers around a mobile. The distribution of azimuth within the narrow spread seen at a base station was determined by that seen at the mobile where it followed the von Mises distribution. Another joint space-time correlation model for Rayleigh fading MIMO channels was presented by Byers & Takawira (2004), who considered so-called two-ring model in which both the transmitter and receiver are surrounded by rings of scatterers. However, they assumed that the angle of arrival is independent of that of departure, which led to separable spatial correlations for the two ends of the channel.

The channel characterization in this thesis considers the dispersions of the multipath components in delay, Doppler, and direction. The resolvable paths are characterized as a superposition of a deterministic and a Gaussian component, which results in a Rice fading envelope. The deterministic component represents the LOS or a dominant scattered multipath component, whereas the Gaussian component represents the sum of the other unresolvable scattered components within that resolvable path. The Gaussian components are then characterized based on the joint power spectrum of the channel in delay, Doppler, and direction at both the transmitter and receiver. For the construction of the presented fading simulator, however, the Doppler power spectrum is assumed to be separable. In the absence of candidate functions for the remaining joint power spectrum in delay and direction, no expressions for the corresponding joint spatio-spectral correlation is given. However, the joint spatio-spectral correlation can be modeled in the simulator if known, and if not, the product of the desired spectral and spatial correlations can be used instead if the power spectrum of the channel can be assumed to be separable in delay and direction. Similarly, spatial correlation at both the transmitter and receiver can be modeled either jointly or separately depending on whether the joint direction power spectrum is inseparable or separable, respectively.

2.2 Simulation of small-scale fading

The need for cost-effective and repeatable experimental evaluations of radio techniques has led to the development of simulators for multipath fading radio channels. Since the first published research on the simulation of multipath fading (Bray *et al.* 1947), several simulation methods have been proposed, among which the usage of acoustic, ultrasonic pressure waves of radio frequencies in a liquid is the most physical one (Chapin & Roberts 1966). Another method, which reproduces the channel characteristics very accurately, is the playback of measured and recorded channel fluctuations. Goldberg *et al.* (1965) introduced this method for the simulation of high frequency (HF) ionospheric links. Thereafter, the method was also applied to very high frequency (VHF) land mobile radio links (Bussgang *et al.* 1976). This method, however, does not provide the variability and versatility of the synthetic fading simulation. In the following, literature on the two main approaches to the synthetic generation of small-scale, Rayleigh or Rice fading is reviewed. The first, more intuitive approach based on a geometric model of a channel and simple ray tracing is considered in Section 2.2.1, and the second, stochastic approach in Section 2.2.2. In this thesis, a simple geometric-based approach is applied for the modeling of the deterministic part of the Rice fading channel coefficients, whereas a stochastic approach is used to generate the Gaussian part of the coefficients.

2.2.1 Geometric modeling

The most straightforward approach to the simulation of small-scale fading is to imitate the multipath propagation in a geometric model of a channel by using ray tracing. In contrast to computationally very intensive ray tracing techniques used in site-specific field strength prediction in wireless network planning (Toscano *et al.* 2003), ray tracing and the underlying geometric channel models used in the simulation of fading are often highly simplified for generality and low computational complexity.

Clarke's geometric model with a ring of uniformly distributed scatterers around a mobile was the basis for a simple geometric ray tracing based fading simulator introduced briefly by Aranguren & Langseth (1973). The analog simulator consisted of a series of nine low-frequency oscillators that were used to modulate a 30 MHz carrier. The frequencies of the oscillators corresponded with the Doppler frequencies experienced by the component waves arriving via nine scatterers. A more thorough description of this approach to fading simulation and a realization of a simulator were presented by

Jakes (1974), whose popularization of the simulation model was so successful that it became known as the Jakes' model. An implementation of the simulator by using a microprocessor instead of analog components has also been described (Casas & Leung 1990).

Geometric ray tracing based simulation models such as the Jakes' model can be also categorized as sum-of-sinusoids (SOS) models, which can be used to simulate pseudo-random narrowband Gaussian noise processes as shown already by Rice (1944, 1945). These sequences, although having a random appearance and stochastic features such as a random initial state, are essentially deterministic and periodic in nature, which may limit their usability for long simulation runs. Moreover, it is problematic to create multiple uncorrelated fading sequences with the original Jakes' simulator, a remedy for which was proposed by Dent *et al.* (1993) who modified the simulator to use orthogonal weighting functions for the oscillators. The complexity of this modification, however, increases faster than linearly with the number of sequences.

The statistical properties of SOS models and the computation of a proper set of parameters for the sinusoids were investigated by Pätzold *et al.* (1998). He has also studied the usage of table-lookup techniques to improve the computational efficiency of computer implementations of SOS models (Pätzold *et al.* 2000). Pop & Beaulieu (2001) pointed out that a reduction in the number of sinusoids in order to limit the complexity leads to the nonstationarity of the envelope autocorrelation of the generated fading sequence. They also proposed an improvement to the Jakes' simulator which was claimed to restore the stationarity by introducing random phase shifts in the low-frequency oscillators. However, Xiao *et al.* (2002) analyzed this improved Jakes' simulator and showed that although the envelope autocorrelation of the generated complex fading sequence asymptotically approaches the one obtained from Clarke's model, the autocorrelations and cross-correlations of the quadrature components, and the autocorrelation of the squared envelope do not. Subsequently, further improved models that achieve the desired second-order statistics and also enable the simulation of multiple uncorrelated Rayleigh fading waveforms have been proposed (Zheng & Xiao 2002, 2003). An extension to the simulation of Rice fading has also been presented (Xiao *et al.* 2006).

Variants of SOS based simulation models include the one presented by Fitting (1967) for the simulation of wideband troposcatter channels. This versatile simulator was able to produce multiple Rayleigh- and non-Rayleigh-type fading sequences with controllable mutual correlation. Another geometrically based variant for the simulation

of microcell channels was proposed by Liberti & Rappaport (1996) based on their elliptic single-scattering model. In their approach, multipath components were generated with random parameters from their analytically derived joint distribution for the azimuth and delay of arrival. Xiao *et al.* (2004) used an SOS model to generate multiple temporally correlated but mutually uncorrelated fading sequences in the simulation of MIMO channels, while a linear matrix transformation was used to generate spatial correlation between the sequences.

2.2.2 Stochastic modeling

Instead of obtaining simulated fading as a deterministic outcome of the summation of modeled multipath components in a particular geometric model, fading sequences can be generated directly by stochastic methods to meet desired, predefined characteristics. These characteristics can be drawn from a limited number of broadly designated environments based on measurements.

Time correlation shaping filtering

The most common stochastic approach to generate temporally correlated Rayleigh fading is to pass complex white Gaussian noise through a lowpass filter whose frequency response approximates the square root of the desired frequency power spectrum. In the simulation of small-scale fading in mobile radio channels, the desired spectrum is the Doppler spectrum. The first papers on this time correlation shaping filtering approach are by Krulee (1963) and Freudberg (1965). Schilling *et al.* (1967) reviewed briefly an analog implementation of this approach, and Arredondo *et al.* (1973) gave a more detailed design. An improved analog simulator using an acoustic wave delay line for the simulation of frequency-selective channels was presented by Caples *et al.* (1980). Another simulator implementing the filtering on a digital signal processor was described by Arnold & Bodtmann (1983). Verdin & Tozer (1993) presented a design of the shaping filter in which the filter was approximated by a windowed Bessel function and implemented by using multirate, finite impulse response (FIR) filtering in order to limit computational complexity. Kim *et al.* (1999) derived the FIR shaping filter coefficients from the IDFT of the classical Jakes' Doppler power spectrum. Stephenne & Champagne (2000) further reduced the computational requirements by using a lower order infinite response filter (IIR), the coefficients of which for the classical spectrum

were determined via a transfer function error minimization method. He also employed two-part interpolation in which classical low pass interpolation filtering is followed by computationally less intensive cubic interpolation. The correlation shaping filtering approach has also been used in commercial real-time hardware channel simulators (Kolu & Jämsä 2002). Time-correlation shaping IIR filtering was applied to the Gaussian part of the channel coefficients also in this thesis. In addition to providing the simulation with the classical Jakes' Doppler power spectrum, filter coefficients for the flat spectrum were also derived. Moreover, the two-part interpolation introduced by Stephenne & Champagne (2000) was further improved to reduce the computational complexity and to enable the simulation of faster fading.

A computationally efficient method to correlation shaping filtering is to carry out the filtering in the frequency domain by multiplying Gaussian noise with the square root of the desired Doppler power spectrum, and then to transform the product into the time domain by the IDFT. An algorithm for this method was proposed by Smith (1975) as a FORTRAN computer code, and the method has been used, for example, by Klingenbrunn & Mogensen (1999), and analyzed by Young & Beaulieu (2000). This method is accurate for long fading sequences, but its drawbacks are that the whole sequence has to be generated by a single IDFT operation and the computational load per sample increases with the length of the sequence. A variant of the correlation shaping filtering approach for computationally more efficient simulation of channels with a large number of densely spaced delay components or even a continuous delay power profile was proposed by Fechtel (1993). Crespo & Jiménez (1995) proposed another variant that uses a harmonic decomposition technique instead of filtering, which was claimed to, among other advantages, reduce computational complexity. However, neither of the above two variants has gained popularity. An autoregressive model, which is essentially an all-pole IIR filter, has also been applied to the generation of temporally correlated Rayleigh fading (Baddour & Beaulieu 2005).

Modeling of generic correlated variables

While the above mentioned stochastic simulation models were used for the generation of temporally correlated Rayleigh fading sequences, a linear memoryless matrix transformation can be used to obtain a generic set of correlated random variables (Morgan 1984). In this approach, a vector of uncorrelated variables is multiplied by the factorization of a desired covariance matrix to obtain a vector of variables with the

corresponding correlation statistics. This approach has been used for generating spatially correlated channel samples after factorizing the covariance matrix by the eigenvalue decomposition (Salz & Winters 1994, Kim *et al.* 1999, Stephenne & Champagne 2000), the matrix square root (Pedersen *et al.* 2000a), or the Cholesky decomposition (Kermoal *et al.* 2002). The Cholesky decomposition has also been used to generate spectral (Klingenbrunn & Mogensen 1999) and arbitrary (Beaulieu & Merani 2000) correlations between Rayleigh fading sequences. An advantage of the Cholesky decomposition is the triangular structure of its outcome which provides computational savings in comparison with, for example, the other above mentioned factorizations. In this thesis, the matrix transformation approach is used for generating spatio-spectral correlations between the Gaussian parts of the channel coefficients. Furthermore, an incomplete Cholesky decomposition is used instead of the complete one in order to further reduce the computational load and to improve the numerical stability of the decomposition.

A computationally simpler but physically untenable approach is to derive mutually correlated fading sequences from a single temporally correlated sequence by means of suitable mutual delays (Verschoor *et al.* 1988). Howard & Pahlavan (1992) generated spectrally correlated frequency-domain channel responses by using an autoregressive model, for which Hassan-Ali & Pahlavan (1997) determined poles corresponding to an indoor channel by using ray tracing software. Also correlation shaping filtering has been used for generating spectrally correlated frequency-domain samples of the channel transfer function (Witrisal *et al.* 1998). Baddour & Beaulieu (2004) proposed an interesting autoregressive model for the generation of multiple cross-correlated Rayleigh fading sequences that are jointly correlated in time and between sequences.

Other modeling approaches

Other stochastic approaches to the simulation of correlated fading include the one by Hashemi (1979), who considered the addition of phase variations into the channel impulse response model proposed by Turin *et al.* (1972). The purpose of this addition was to account also for the temporal and spatial correlation of fading, which were missing from the original model. While assuming the envelope to be quasi-static with time and distance, he modeled the phase increments by a Gaussian distributed random variable whose variance determined the temporal and spatial correlation. Further models for the phase variation in indoor channels were studied by Nikookar & Hashemi (2000).

Another model in which the envelope and phase are modeled separately is the spatial channel model proposed first with Nakagami-type small-scale fading (Zwick *et al.* 2000) and later as a more refined model with Rayleigh fading (Zwick *et al.* 2002). This model is a mixture of geometric and stochastic approaches and brings together different channel characterizations whose relations are not so obvious. A mixture of the two modeling approaches was also presented by Xu *et al.* (2004), who used the geometric wave superposition approach to model Rayleigh fading with joint space-time correlation at a mobile and the stochastic approach to model correlated fading at a base station.

Markov models have also been proposed for the modeling of Rayleigh fading sequences (Swarts & Ferreira 1993, Wang & Moayeri 1995).

3 Spread-spectrum communications

In the early years of radio communications, when spark gap transmitters were used to generate sequences of rapidly damping waves, transmissions had fairly wide spread spectra. This, however, was not intentional but merely a limitation of the technology being used. As the usable frequency spectrum got crowded and interference worsened, the evolved continuous wave narrowband transmission superseded the old spectrally wasteful technology with the help of legislation. The actual spread-spectrum communications, which transmit signals with a random appearance and a bandwidth much wider than that of the data being communicated, emerged during and after World War II for the needs of robust military communications. The development of the early systems and their origins and numerous other events from the history of spread-spectrum communications are covered by the reviews of Scholtz (1982, 1983) and Price (1983). In military communications, the signal characteristics of spread-spectrum systems provide resistance to jamming and a low probability of intercept, which are key attributes for systems operating in hostile environments. For civil and commercial applications that have followed much later, spread-spectrum communications provide spectral efficiency, flexible multi-access capability, resistance to intra- and intersystem interference, and high time resolution for multipath exploitation and accurate positioning.

Spread-spectrum communications can be realized by different approaches. From the perspective of the narrowband carrier wave technology, the most straightforward approach is to spread the data over multiple narrowband carriers that are transmitted either successively in a certain order or simultaneously. Both of these variants were invented already by Tesla (1903a,b), one of the main contributors to the development of radio with his work on tuned radio frequency circuits. Thereafter, the former of the above variants has become known as frequency-hopping spread-spectrum (FH-SS) which has found use especially in military communications but also in commercial systems such as GSM cellular and Bluetooth personal area networks. The latter variant is called multicarrier spread-spectrum (MC-SS) which has obtained increasing academic and commercial interest over the past 15 years. The second approach to spectrum spreading from the carrier wave perspective is to modulate the carrier with, in addition to the data, a pseudorandom sequence with a rate that is much higher than that of the data. This approach is known as direct-sequence spread-spectrum (DS-SS) which

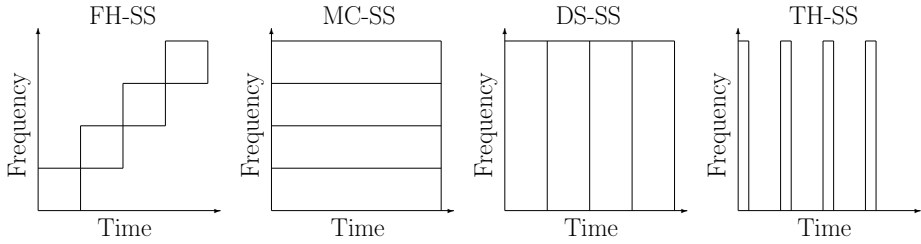


Fig. 3. Time and frequency allocation of different spread-spectrum approaches.

can be traced back to an invention by Kotowski & Dannehl (1940). They patented a device for masking voice signals with a pseudonoise signal produced by a rotating generator, a synchronous duplicate of which was used for unmasking the voice at a receiver. Although their invention did not encompass significant spectrum spreading but only data encryption, they are credited as the inventors of DS-SS by many. A tutorial on DS-SS, and also on FH-SS, was given by Pickholtz *et al.* (1982). A third approach to spread-spectrum communications is carrierless transmission of sequences of short impulses whose frequency spectrum extends over very wide bandwidth. This approach is reminiscent of the early radio communications with spark gap transmitters and also of the pulsed radio approaches for data modulation and multiplexing. While the above applications of impulse radio did not emphasize the spread-spectrum characteristics, the more recent ones do so and are therefore referred to as time-hopping spread-spectrum (TH-SS). Owing to its spread-spectrum nature and very wide bandwidth, impulse radio was one of the first approaches to be proposed for the arising ultra-wideband (UWB) communications. The allocation of the aforementioned spread-spectrum signaling approaches in frequency spectrum and time is illustrated in Fig. 3.

Two spread-spectrum related schemes, which are well proven for wireless communication over frequency-selective fading channels, are code-division multiple-access (CDMA) multiplexing and multicarrier transmission, literature on which is briefly reviewed in Sections 3.1 and 3.2, respectively. Their combination, multicarrier CDMA has gained interest over the past 15 years, and the main scientific contributions to the literature on it are reviewed in Section 3.3. The literature on the methods for carrying out multirate transmission in systems employing code-division multiplexing (CDM) is reviewed in Section 3.4. Finally, literature on the evolving UWB communications based on either impulse radio or multicarrier transmission is reviewed in Section 3.5.

3.1 CDMA multiplexing

CDMA (code-division multiple-access) and CDM (code-division multiplexing) are, respectively, multiple-access and multiplexing techniques in which multiple simultaneous transmissions occupy the same frequency band at the same time. While the term multiple-access most commonly refers to the multiplexing of transmissions from or to different sources, the more generic term multiplexing often refers to the case of a single source and destination. As the term code-division implies, the transmissions in CDMA are divided from each other by separable code sequences, in contrast to more conventional frequency-division multiple-access (FDMA) and time-division multiple-access (TDMA) methods where the transmissions are divided into disjoint frequency bands and time slots, respectively. This CDMA approach is sometimes called as direct-sequence (DS) CDMA to distinguish it from the somewhat misleadingly termed frequency-hopping (FH) CDMA and time-hopping (TH) CDMA, which are effectively FH-FDMA and TH-TDMA schemes, respectively.

CDMA stems from the DS-SS technique in which each data symbol to be transmitted is multiplied by a spreading code sequence before the modulation of the carrier wave. An early DS-SS system was the Rake system (Price & Green 1958), which gave its name to the type of receiver used that coherently combines the multipath signal components of resolvable delays. Although the system was introduced mainly for reliable communication over multipath channels, the authors already saw a promise that *"the Rake technique can be extended to the multiplexing of a considerable number of independent, wide-band transmissions into the same frequency band."* A few years thereafter, CDMA was considered as a candidate to a multiple-access scheme in which a number of earth stations communicate via a single satellite repeater (Schwartz *et al.* 1966). The first widespread employment of CDMA in satellite systems, however, was not in communications but in the multiplexing of navigation signals broadcasted from different satellites in the Global Positioning System (GPS). The first experimental satellite of GPS was launched already in 1978. Thereafter, CDMA has also been used in Globalstar, a commercial satellite mobile communication system that started operation in 2000.

In terrestrial cellular communications, CDMA was applied for the first time in Interim Standard 95 (IS-95) that is the air interface for a second generation, Qualcomm pioneered mobile radio system now known as cdmaOne. This system, commercially launched in Hong Kong and South Korea in late 1995 and early 1996, is now being

supplanted by a backward compatible third generation CDMA2000. A competing third generation air interface is called Wideband CDMA (W-CDMA), where the prefix wideband is justified by having a bandwidth of 5 MHz in comparison with the 1.25 MHz of IS-95. W-CDMA was originally developed by NTT DoCoMo for a Japanese, Freedom of Mobile Multimedia Access (FOMA) service which is the world's first third generation system launched in 2001. It was also adopted into UMTS, the third generation successor of GSM. Analysis of CDMA in cellular communications is presented, for example, by Pikholtz *et al.* (1991).

The spreading codes in CDMA systems are conventionally binary sequences, the bits of which, called chips, are usually converted to the alphabet $\{1, -1\}$ by mapping $0 \rightarrow 1$ and $1 \rightarrow -1$. Polyphase complex sequences, especially complex quaternary sequences in conjunction with quadrature phase-shift keying (QPSK) have also been considered (Xie & Rahardja 2005). The sets of spreading code sequences can be categorized as being either orthogonal or quasi-orthogonal, depending on whether the sequences within a set are fully or almost orthogonal to each other when being phase aligned. Orthogonal sequences are ideal for synchronous CDMA schemes such as downlink transmission over a frequency-nonselctive channel in which the multiplexed transmissions can be and remain synchronized in time to within a fraction of a chip. For asynchronous CDMA schemes in which the relative phases of the multiplexed sequences are arbitrary, and for transmissions over frequency-selective multipath channels in which the relative delays of the multipath components approach or exceed a chip interval, an ideal set of sequences would have zero periodic crosscorrelation functions and impulse-like periodic autocorrelation functions. Although such an ideal set seems to be impossible to construct (Welch 1974), quasi-orthogonal sequences with low crosscorrelations and autocorrelation sidelobes provide good approximations and are generally better suited to asynchronous schemes and frequency-selective channels than the fully orthogonal ones. There are also concepts of generalized orthogonality and generalized quasi-orthogonality that are targeted at sequence design for quasi-synchronous schemes (Fan 2004).

3.1.1 Walsh-Hadamard sequences

By far the most popular orthogonal sequences for spreading, among other applications, are the so-called Walsh-Hadamard sequences whose despreading can be efficiently implemented by the fast Walsh-Hadamard transform. The name arises from the parallel work of Walsh and Hadamard on orthogonal bases. Walsh popularized the orthogonal

functions, later carrying his name, that are composed of sequences of square pulses of positive and negative polarities and unit magnitude. The initial polarity of the functions is positive, and transitions between the polarities may occur only at fixed, unit time intervals. There are 2^n functions of length 2^n , n being a positive integer (Walsh 1923, Beauchamp 1975). Hadamard, on the other hand, gave his name to square matrices whose elements are plus or minus ones, and whose rows are mutually orthogonal. Despite their naming, Hadamard matrices were invented by Sylvester (1867). A necessary condition for a Hadamard matrix of order n to exist is that $n = 1, 2$, or a multiple of 4 (Geramita 1979). The 2^n Walsh functions of length 2^n give the rows of a $2^n \times 2^n$ Hadamard matrix arranged in an order that is known as sequency or m-sequence order. The order in Hadamard matrices constructed by the Kronecker product based recursive expansion is termed the natural, Sylvester or Hadamard order.

3.1.2 Maximum length sequences

Quasi-orthogonal sequences are most commonly periodic, pseudorandom binary sequences constructed from so-called maximum length sequences, usually abbreviated as m-sequences. An m-sequence, again, can be generated by using a linear feedback shift register of length n that cycles through all possible $2^n - 1$ states while producing a sequence of the maximal length of $2^n - 1$. While the m-sequences have excellent autocorrelation properties, their out-of-phase value being only $-1/(2^n - 1)$, there are pairs of m-sequences of the same length that have relatively high crosscorrelation peaks. Then, pairs of sequences that have a three valued crosscorrelation function whose maximal magnitude is smaller than that of the rest of the sequences are called preferred pairs. These pairs are used to generate sets of very popular quasi-orthogonal sequences called Gold sequences (Gold 1967). A set of $2^n + 1$ Gold sequences of length $2^n - 1$ is composed of a preferred pair of m-sequences, together with the element-wise multiplications of these two sequences in their different phases. The Gold sequences obtain a low crosscorrelation which is similar to that of the preferred pair used for the generation. This, however, comes at the expense of an increase in the out-of-phase autocorrelation which is now at the same level with the crosscorrelation.

A set of 2^n fully orthogonal Gold sequences of length 2^n can be constructed from a set of quasi-orthogonal Gold sequences by leaving out the other of the two preferred m-sequences and appending an additional plus one to the end of each sequence (Tachikawa 1992). It has been found that there is a permutational, one-to-one equivalence between

orthogonal Gold and Walsh-Hadamard sequences (Popović 1997). This finding is grounded on the equivalence found between matrices of m-sequences and Walsh-Hadamard matrices (Cohn & Lempel 1977). While orthogonal Gold sequences based on a preferred pair of m-sequences provide optimal periodic crosscorrelation, the same construct can be applied to any set of sequences generated by using any pair of m-sequences (Donelan & O'Farrel 1999). Moreover, any binary sequence of length n with an out-of-phase autocorrelation of $-1/n$ can be used to generate a matrix of $n + 1$ orthogonal sequences by first cyclically shifting the sequence and then placing a leading row and column of ones (Gerakoulis & Ghassemzadeh 2000). Understandably, these sequences have disastrous periodic crosscorrelation properties. Gerakoulis & Ghassemzadeh (2000) presented some other methods for the construction of orthogonal spreading codes, including complex and polyphase sequences.

3.1.3 Complementary sequences

Although there are no binary sequences having an impulse-like periodic autocorrelation function free of sidelobes, it is possible to construct pairs of sequences whose autocorrelation functions sum up to zero at all nonzero shifts when added coherently. These sequence pairs are usually termed as complementary sequences, as Golay (1961) did when deriving them, but they have also been called Golay sequences after their inventor. Tseng & Liu (1972) generalized the concept of complementary sequences to sets of more than two sequences. They also defined mutually orthogonal complementary sets as a collection of complementary sets of sequences in which the sum of the coherently added cross-correlation functions of the corresponding sequences from any two sets is zero at every shift.

Golay conceived the complementary sequences originally in connection with infrared multislit spectrometry, but thereafter they have been applied in ultrasound, acoustic, and radar measurements, and lately their polyphase variant was applied in a complementary code keying modulation scheme in IEEE 802.11b wireless local area network (WLAN) standard. The use of complementary sequences as spreading codes has also been considered, for example, by Weng & Guangguo (1987), Suehiro & Hatori (1988), and Chen *et al.* (2001), and their efficiency in that purpose was analyzed by Farkas & Turcsany (2004).

3.2 Multicarrier transmission

The delay dispersion of a received signal experienced in multipath channels causes ISI and frequency distortion, which restricts the usable bandwidth for a carrier wave transmission if no means to cope with the dispersion is employed. In order to increase the data carrying capacity without exceeding the tolerable ISI and frequency distortion levels, the data can be multiplexed and modulated into a number of narrowband subcarriers of different frequencies. This multicarrier transmission approach is referred to as frequency-division multiplexing (FDM). In conventional FDM, the frequency bands of subcarriers are strictly limited and separated by empty guard bands in order to prevent interference between them. Moreover, each subcarrier is modulated and bandpass demodulated separately, which both require a lot of filtering. In modern FDM, on the contrary, the bands of adjacent subcarriers partly overlap while the orthogonality between the carried signals is still maintained. The latter has become known as orthogonal FDM (OFDM), which is superior in spectral efficiency in comparison with the former. Moreover, the modulation and demodulation in modern OFDM are done jointly for multiple subcarriers by using computationally efficient digital signal processing implementations of fast Fourier transform (FFT) and its inverse (IFFT), respectively. For this reason, OFDM is also called multicarrier modulation, an overview of which is given by Bingham (1990) and in the following section.

3.2.1 OFDM modulation

An early implementation of OFDM took place already in the 1950s in the Kineplex system for long range HF data transmission (Doelz *et al.* 1957). Although the system had separate modulators and matched filter demodulators of an analog construction for all subcarriers, it resembled the modern OFDM in that it used an equidistant subcarrier spacing equal to the inverse of the integration interval of the demodulator. Moreover, it already employed a guard interval between successive integration intervals to provide tolerance for multipath propagation. Following this first public appearance of OFDM, theoretical considerations of sinusoidal functions as orthogonal signals were conducted by Harmuth (1960) and Franco & Lachs (1961). Thereafter, Bello (1965) presented an analysis of OFDM over time- and frequency-selective fading channels, with a special focus on an early version of another OFDM system named Kathryn. Zimmerman & Kirsch (1967) described a later version of the Kathryn system that, similarly to the

modern OFDM systems, already utilized Fourier transform in the modulation and demodulation. However, the transform was carried out at the time by means of analog signal processing. Still another OFDM based HF data modem, Andeft, was presented and analyzed by Porter (1968). A digital implementation of an OFDM modem that was named Tadim and that used the discrete Fourier transform (DFT) was presented by Powers & Zimmerman (1968). Weinstein & Ebert (1971) conducted a theoretical investigation of a DFT-based OFDM system that has been widely referred to in the literature. They also proposed a time windowing function to obtain gradual, rather than abrupt, transitions between successive sinusoidal symbol waveforms. The time windowing suppresses the sidelobes of a sinc-function shaped subcarrier spectrum that follows from the time truncation of sinusoidal waveforms.

In recent years, OFDM has become increasingly popular as implementational advances have paved the way for a number of OFDM systems for both wired and wireless broadband communication. To date, the wired OFDM systems include digital subscriber line (DSL) technologies such as asymmetric DSL (ADSL) and very high speed DSL (VDSL) internet access over telephone wires, and power line communication modems for home networking and internet access over power wires. The version of OFDM that is used in wired systems is often referred to as discrete multitone (DMT). It differs from the conventional bandpass OFDM of wireless systems mainly in that it operates in the baseband and uses rate adaptive bit loading on each subcarrier or tone. Among the most widely spread wireless OFDM systems are the WLAN equipment supporting, most notably certain IEEE 802.11 standards, several digital broadcasting systems such as the digital audio broadcasting (DAB), also known as Eureka 147, and the terrestrial digital video broadcasting (DVB-T). Other wireless applications of OFDM that are loaded with high expectations are the wireless metropolitan area network (WMAN) and long range fixed and mobile access targeted systems such as WiMAX (Worldwide Interoperability for Microwave Access) and FLASH-OFDM (Fast Low-latency Access with Seamless Handoff OFDM). These two systems aim at competing not only with each other but also with the third generation cellular mobile systems which are also evolving towards OFDM according to the Long Term Evolution (LTE) of the 3GPP (Third Generation Partnership Project).

The modulation formats most commonly used in OFDM systems are the different orders of square quadrature amplitude modulation (QAM). Although the rectangular forms of QAM have sub-optimal spacings of the constellation points for a given energy, they are favored because of their straightforward modulation and demodulation as two

separate pulse amplitude modulation constellations on quadrature carriers. By utilizing this feature, Cho & Yoon (2002) derived the bit error probability (BEP) of an arbitrary rectangular QAM with Gray coded bit mapping in an additive white Gaussian noise (AWGN) channel. High order QAM requires highly linear power amplifiers already by itself, but when used in an OFDM system that has a large number of subcarriers and therefore a large peak-to-average power ratio (PAPR) on its own, the requirements get much more stringent. The linearity over a wide range of input levels, however, makes an amplifier costly and very power-inefficient. Therefore, several techniques for reducing the PAPR of OFDM signals have been introduced (Nee & Prasad 2000, Han 2005, Nguyen & Lampe 2006, 2007). Besides high PAPR, another drawback of OFDM is its susceptibility to intercarrier interference due to channel time variations within an OFDM symbol (Schniter 2004, Wang *et al.* 2006, 2007).

3.2.2 Pulse shaped OFDM

The advantage of the rectangular pulse used in the conventional OFDM is that it allows the additional guard interval, a cyclic prefix, to compensate for the delay dispersion of a channel. However, the redundant cyclic prefix decreases the spectral efficiency. Moreover, the widely spread spectral sidelobes of rectangular pulses on sinusoidal carriers are exposed to narrowband interferers. Furthermore, they may be cut off in bandlimited channels, which in turn results in intercarrier interference. The latter motivated Chang (1966) to design bandlimited orthogonal signals for OFDM. He came up with pulse shape filtering in which the frequency response is strictly bandlimited and has the familiar cosine roll-off from the center frequency of a subcarrier to those of the adjacent subcarriers. The performance of the proposed approach was studied by Chang & Gibby (1968). Saltzberg (1967) analyzed an OFDM scheme that used bandlimited pulse shape filtering and offset quadrature amplitude modulation (OQAM) in which the symbol transitions on the quadrature carriers are staggered or offset in time by half the symbol period. Hirosaki (1980) proposed a per-carrier equalizer for the OQAM-based OFDM scheme in order to eliminate remaining intersymbol and intercarrier interference. Thereafter, he provided a computationally more efficient implementation of the scheme based on the DFT (Hirosaki 1981).

The improvement in the frequency-domain localization of the signals with cosine roll-off filtering comes at the expense of time-domain delocalization which requires long filters and is prone to intercarrier interference in highly time-selective channels. The

time-frequency dual of cosine roll-off filtering is a scheme using strictly time-limited pulses of the same half-sinusoidal shape. With these pulses, the 4-ary OQAM, offset QPSK, is equivalent to quadrature minimum-shift keying type of continuous phase modulation (Le Floch *et al.* 1995). The frequency response with the half-sinusoidal pulse has again sidelobes which, however, decrease faster than with the rectangular pulse. Construction of wavelet-based pulses that would optimally compromise between the contradictory time- and frequency-domain localization properties has also been considered (Haas & Belfiore 1994, Le Floch *et al.* 1995, Vahlin & Holte 1996).

A pulse shaped OFDM system is essentially a filter bank based transmultiplexer, which was originally developed to convert a set of telephone channels from time-division multiplexing (TDM) to FDM and vice versa (Bellanger & Daguet 1974). A theoretical treatment of filter banks was given by Vetterli (1987), and designs of filter bank based transmultiplexers for pulse shaped OFDM systems have been presented, for example, by Viholainen *et al.* (1998) and Siohan *et al.* (2002). The drawback of the pulse shapes, other than the rectangular one, is that instead of a simple guard interval, they require more complex time-domain equalization in delay dispersive channels (Hirotsuki 1980, Wiegand & Fliege 1996, Renfors *et al.* 1999, Viholainen *et al.* 1999, Ihalainen *et al.* 2007). This has biased the pulse shape selection in favor of the rectangular one since the spectral sidelobes of the rectangular pulse can also be dampened by using relatively low complex OFDM symbol windowing together with overlapping roll-off intervals. The roll-off intervals, however, further decrease the spectral efficiency. The usage of rectangular pulses with zero padding in place of the cyclic prefix has also been considered (Muquet *et al.* 2002).

3.3 Multicarrier CDMA

The bright outlook for both the CDMA- and OFDM-based commercial communication systems in the beginning of 1990s brought about the idea of combining these two techniques and their advantageous features into a single scheme. This scheme would unify the orthogonal frequency multiplexing of OFDM, providing frequency diversity, ISI-free transmission and less stringent requirements for timing synchronization, and the orthogonal or quasi-orthogonal code multiplexing of CDMA, offering flexible multiuser and -rate capabilities. The code multiplexing can be done in this combination, which is generally referred to as multicarrier CDMA or OFDM-CDMA, by using spreading codes in either the time- or frequency-domain. The different multicarrier CDMA proposals

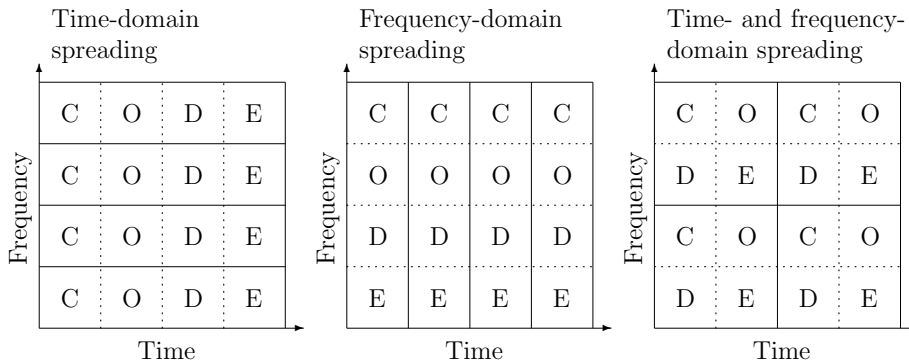


Fig. 4. Different approaches to using spreading codes in multicarrier CDMA.

found in the literature and falling into the two categories of either time- or frequency-domain spreading are reviewed in Sections 3.3.1 and 3.3.2, respectively. In addition, hybrid schemes with both time- and frequency-domain spreading have been proposed (Matsumoto *et al.* 2002, Atarashi *et al.* 2002, You & Hong 2003, Zhou *et al.* 2005, Zhang *et al.* 2005b). The use of spreading codes in the above mentioned three different approaches to multicarrier CDMA is illustrated in Fig. 4. As an alternative to CDMA, multiple access in OFDM can also be arranged by TDMA, or more straightforwardly by FDMA, with the latter of which the combination is also known as orthogonal FDMA (OFDMA).

3.3.1 Time-domain spreading

The first descriptions of multicarrier CDMA systems with time-domain spreading can be found in the coincident, independent proposals by DaSilva & Sousa (1993, 1994), Kondo & Milstein (1993, 1996), and Vandendorpe (1993, 1995). While all the three proposed schemes use the same user-specific spreading code for all subcarriers, the ones by DaSilva & Sousa and Kondo & Milstein carry out the spreading before multicarrier modulation in which the subcarrier spacing is equal to the inverse of a chip interval, whereas the one by Vandendorpe does the spreading after the modulation in which the subcarrier spacing is equal to the inverse of a data symbol interval. Consequently, the subcarrier spectrum in the first two of the above mentioned schemes fulfills the orthogonality condition by having nulls at the center frequencies of adjacent subcarriers. In the third scheme, however, the spectral nulls of a subcarrier are spread apart and,

depending on the spreading factor, over a number of neighboring subcarriers which results in intercarrier interference. Therefore, interest in multicarrier CDMA with time-domain spreading, also known as multicarrier DS-CDMA (MC-DS-CDMA), has concentrated mainly on the approach of the first two schemes that maintain the frequency orthogonality by transmitting only one chip per an OFDM symbol.

The performance of a MC-DS-CDMA scheme over an asynchronous, frequency-selective Rayleigh fading uplink channel was analyzed by Sourour & Nakagawa (1996), who confirmed that the scheme can outperform the conventional single-carrier CDMA with a Rake receiver. Iltis (1997) proposed using a decorrelating detector in a quasi-synchronous MC-DS-CDMA scheme in order to completely reject the residual intercarrier interference. Rowitch & Milstein (1999a,b) analyzed a MC-DS-CDMA scheme with convolutional and repetition coding across a number of subcarriers in an asynchronous uplink channel with or without narrowband interference. Tseng & Bell (2000) investigated the use of complementary spreading sequences for the reduction of multiple-access interference in asynchronous systems. Each user had a distinct set of sequences, from which a different sequence was assigned to each subcarrier. Expectedly, they found that their complementary spreading scheme was vulnerable to frequency-selective fading. However, they anticipated that their scheme would outperform the conventional single-sequence spreading in a Rice fading channel with a strong LOS component. The performance analysis of a MC-DS-CDMA system by using the characteristic function method was presented by Smida *et al.* (2001). MC-DS-CDMA with its time-domain spreading has been often considered to be more appropriate for asynchronous uplink channels than its frequency-domain counterpart (Suwa *et al.* 2002). This is due to the deterioration of the orthogonality between frequency-domain spreading codes as users experience differently frequency-selective channels.

3.3.2 Frequency-domain spreading

At the same time as the proposals of time-domain spread multicarrier CDMA were made, frequency-domain schemes in which the chips of a spread data symbol are assigned across the subcarriers were also proposed independently by Yee *et al.* (1993), Fazel & Papke (1993), and Chouly *et al.* (1993). These schemes with frequency-domain spreading have become known simply as multicarrier CDMA (MC-CDMA), as a differentiation from MC-DS-CDMA with time-domain spreading. Lately, this combination of OFDM and CDMA, with orthogonal frequency-domain spreading

sequences, has also been referred to as orthogonal frequency- and code-division multiplexing (OFCDM). MC-CDMA schemes that provide only modest frequency-domain spreading to obtain diversity in combination with an OFDMA multiple-access technique have also been proposed (Kaiser & Fazel 1997, Wang & Giannakis 2000, Giannakis *et al.* 2000, Wang & Giannakis 2001).

An advantage of frequency-domain spreading in comparison with time-domain spreading is the inherent frequency diversity in frequency-selective channels, which on the other hand can also be disadvantageous as the orthogonality between spreading codes deteriorates. The balance between these contradictory consequences, however, can be shifted in favor of frequency diversity in a downlink channel when a suitable method is used to gather the received symbol energy from the subcarriers. Therefore, MC-CDMA has been usually considered to perform better than MC-DS-CDMA or single-carrier DS-CDMA in a synchronous downlink channel (Hara & Prasad 1997, Abeta *et al.* 2000).

Subcarrier combining

In MC-CDMA, the receive operation that gathers the symbol energy from across a number of subcarriers has a twofold task. Firstly, it should despread the symbol so that the interference between overlapping spreading codes is avoided, and secondly, combine the channel responses of the subcarriers in such a way that the best is made of the available frequency diversity. These objectives of the joint despreading and diversity combining, however, are conflicting. Consequently, various proposed subcarrier combining schemes have differences in their ability to compromise between the interference avoidance and diversity maximization.

In their proposal of frequency-domain spread MC-CDMA, Yee *et al.* (1993) used either maximal ratio combining (MRC), which is well known to maximize the signal-to-noise ratio (SNR) in an AWGN channel, or equal gain combining (EGC), which can be viewed just as a phase equalization, to combine the subcarriers. They found that MRC performs better than EGC in a noise-limited channel, while it is the opposite in an interference-limited channel. Fazel (1993) noted from his simulations that orthogonality restoring combining (ORC), which equalizes the subcarrier channels by inverse channel gains, outperforms EGC at high SNR because ORC does not have an error floor due to the intercode interference. At low SNR, however, it is the opposite as ORC enhances noise at faded subcarriers. His simulations also showed that multi-user maximum-

likelihood detection or iterative interference cancellation provides better performance at the expense of increased complexity. Chouly *et al.* (1993) considered, in addition to ORC, two subcarrier combining schemes that are based on the minimum mean-square error (MMSE) criterion. The first applies the MMSE criterion per carrier, that is, to the output of an OFDM demodulator before despreading and combining, whereas the other applies the criterion per user, that is, to the output of the despreading and combining operation. The simulation results showed that MMSE per carrier combining (MMSECC) improves the performance over that of ORC, and that further improvement is obtained with MMSE per user combining (MMSEUC). A so-called controlled equalization, which limits the noise enhancement of ORC by discarding the subcarriers whose signal levels are below a certain threshold, has also been proposed (Yee & Linnartz 1993, 1994a). This scheme has also been referred to as threshold ORC (Müller *et al.* 1995). Subcarrier combining based on the MMSE criteria and Wiener filtering (Yee & Linnartz 1994b) and multi-user decorrelating detection (Bar-Ness *et al.* 1994) have also been considered.

While the above reviewed articles concentrated on synchronous downlink channels with independently faded subcarriers, Gui & Ng (1999) analyzed the performance of MC-CDMA over asynchronous uplink channels with correlated subcarriers when either MRC or EGC is used. They concluded, against the common understanding, that MC-CDMA performs better than single- or multicarrier DS-CDMA. Moreover, they claimed that MRC performs better than EGC. Hara & Prasad (1999) considered the design of an MC-CDMA system, namely, the determination of the number of subcarriers and the length of the guard interval that minimize the bit-error rate (BER) under given Doppler and delay spread of a channel. Moreover, their comparative simulation results for single-carrier DS-CDMA and MC-CDMA with ORC, EGC, MRC, or MMSECC illustrated that the MMSECC-based MC-CDMA is a promising scheme for a downlink, whereas in an uplink it is inferior to DS-CDMA. Lok *et al.* (1999) proposed a blind adaptive algorithm for the optimum combining (OC) of subcarriers in both synchronous and asynchronous systems. OC maximizes the signal-to-noise-plus-interference ratio (SINR) of the output (Winters 1984). The MMSE criterion based combining has been further considered in conjunction with parallel interference cancellation (PIC) (Héland *et al.* 2000), with both delay and Doppler spreads in a synchronous downlink (Linnartz 2001), with so-called partial sampling aimed at interference suppression in asynchronous systems (Zong *et al.* 2001), with decision-directed, least mean square (LMS) and recursive least square (RLS) based adaptive detection schemes (Kalofonos *et al.* 2003),

with an adaptive, cross-coupled decision feedback scheme (Liu *et al.* 2004), with PIC and low-density parity-check (LDPC) codes (Duan *et al.* 2005), and with combined pre- and post-equalization and PIC (Cosovic *et al.* 2005). Besides PIC, also the use of successive interference cancellation (SIC) for suppressing multiple-access interference in MC-CDMA has been proposed (Andrews & Meng 2004). Cacciapuoti *et al.* (2007) considered both MMSE and zero-forcing based per user combining in MC-CDMA downlink employing either a cyclic prefix or zero padding.

A number of other performance analyses of MC-CDMA with various subcarrier combining schemes have been presented based, for example, on EGC, an asynchronous uplink, and an approximation of the sum of several Nakagami- m variables (Li & Latva-aho 2002), on MRC, a downlink, an error floor and a characteristic function and residue calculation method (Shi & Latva-aho 2002b) or an exact error rate and a moment generating function method (Shi & Latva-aho 2002a), on EGC and MRC, synchronous and asynchronous systems, and Monte Carlo integration (Shi & Latva-aho 2003a), and on MRC and the characteristic function method and the Gaussian approximation for the interference (Li & Latva-aho 2005). Mourad *et al.* (2004) investigated the intra-cell interference statistics for different levels of channel correlation and how they can be mapped to the system-level performance evaluation of an MC-CDMA system with MRC, EGC, or MMSECC. In this thesis, it is confirmed that besides the more complex MMSEUC and OC methods, also the simpler MMSECC gives good performance in a downlink, even in a fully loaded system. In an uplink, however, only MMSEUC and OC can provide reasonably good, nearly equal performance.

Spreading codes

The spreading sequences employed in MC-CDMA should, in addition to being mutually orthogonal, also provide a low PAPR in order to limit the required linearity range of the power amplifiers used. Popović (1999) introduced a spectral cross-correlation function between the spreading sequences and used it together with the dynamic range and the crest factor, which equals the square root of PAPR, to evaluate the performance of Walsh-Hadamard, Gold, orthogonal Gold, and polyphase Zadoff-Chu sequences in MC-CDMA. He came to the conclusion that Zadoff-Chu sequences are the optimal choice for asynchronous systems. Choi *et al.* (1999) compared Walsh-Hadamard, orthogonal Gold, and polyphase Zadoff-Chu and Frank codes, and found that Zadoff-Chu sequences show the best BER performance over independently faded subcarriers,

while Walsh-Hadamard sequences exhibit the best crest factor distribution in a fully loaded synchronous downlink.

Taking into account also the intercarrier interference in an asynchronous uplink, Shi & Latva-aho (2003b) showed that at high SNR, orthogonal Gold sequences provide better BER performance than Walsh-Hadamard, Gold, and Zadoff-Chu sequences when the system load is high, while Zadoff-Chu sequences perform the best when the load is low. At low SNR, however, Walsh-Hadamard sequences outperform the others slightly. Gu *et al.* (2005) compared the BER performance of Walsh-Hadamard, Gold, orthogonal Gold, and that of the 4-phase Family A sequences and unified complex Hadamard transform (UCHT) sequences over a synchronous uplink. They found that Walsh-Hadamard and UCHT sequences perform the best and are followed by similarly performing Gold and orthogonal Gold sequences, while 4-phase Family A sequences perform the worst. In this thesis, it is briefly illustrated that orthogonal Gold sequences result in slightly better performance than Walsh-Hadamard sequences, especially in an uplink at low system loads.

Complex spreading sequences that are based on linearly increasing phase offsets over subcarriers, therefore referred to as carrier interferometry codes, have also been proposed (Natarajan *et al.* 2004, Akhavan-Bahabdi & Shiva 2005). These codes are claimed to double the system capacity by doubling the number of available spreading sequences. Cacciapuoti *et al.* (2007) also remarked that, if appropriate complex spreading sequences are used, zero-forcing multiuser detectors can be designed even for overloaded downlink MC-CDMA transmission. The use of complementary spreading sequence pairs resulting in PAPR reduction in comparison with the single-sequence schemes has also been considered (Nobilet *et al.* 2001, Choi *et al.* 2002, Choi & Hanzo 2003, Zhang *et al.* 2005a).

3.4 Multirate transmission in CDMA systems

The capability of multiple data transmission rates provides significant advantages in multi-user mobile radio systems. The data rate can be traded for the improved robustness of transmission, or it can be adapted to time-varying channel conditions in order to meet the set error rate criteria. In particular, the rate can be imposed based on the type of requested service and the available capacity in the system at a given moment. In a general case with a fixed channel symbol rate, the data rate can be adjusted by, for example, the type and order of modulation, the rate of channel error coding, and the

time and frequency share of a channel. While the two latter rate adjustment methods are congenial with time- and frequency-division multiplexing, respectively, there are two multirate transmission schemes applicable particularly to CDM. These two schemes are the multicode scheme and the variable spreading factor (VSF) scheme which are reviewed, respectively, in Sections 3.4.1 and 3.4.2. The literature on their comparisons is reviewed in Section 3.4.3.

3.4.1 Multicode

The transmission rate of a user in the multicode multirate scheme is determined by the number of assigned spreading sequences drawn from a set of preferably orthogonal sequences of fixed and equal lengths. The assigned sequences multiplex a number of data streams overlapping in time and frequency and, therefore, provide a multiple of the basic rate of a single-stream transmission. Consequently, the separation of multiple streams in the multicode scheme is based on the same code-division principle as the separation of multiple users. The basic principle of multicode transmission is illustrated in Fig. 5.

Probably the first use of the multicode multirate scheme in single-carrier CDMA was the prototype system described by Doi *et al.* (1994). This dual-rate system was designed to transmit low rate voice signals with a single spreading sequence and high rate data signals with six sequences. Since the multicode transmission increases the PAPR, Zhu *et al.* (2005) proposed a multirate multicode method in which the multilevel sum of multiple orthogonal Gold sequences of a user is limited to a binary sequence by simply taking the sign of the sum.

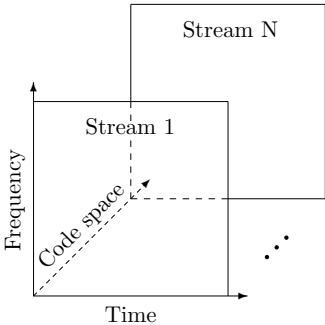


Fig. 5. Principle of the multicode scheme.

Among the first treatments of multirate multicode transmission in MC-CDMA systems with frequency-domain spreading were the ones by Tan & Bar-Ness (2002) and Fu & Mark (2003), where the performances in a synchronous downlink and asynchronous uplink, respectively, were considered. Tan & Bar-Ness (2002) concluded that the interference between the multiple codes of each user can be reduced or even eliminated by properly selecting the codes from a set of orthogonal Walsh-Hadamard sequences. Fu & Mark (2003) came to the conclusion that the system performance improves when the number of codes per user and the spreading factor increase proportionally.

3.4.2 Variable spreading factor

In the VSF multirate scheme, the transmission rate of a user is determined by the length of the assigned spreading sequence, the rate being inversely proportional to the sequence length. The data bits are spread by the same user specific sequence and transmitted sequentially. Therefore, the multiplexing of multiple data streams in the VSF scheme is based on the time-division principle in the time-domain spread single- and multicarrier DS-SS, whereas in MC-CDMA with frequency-domain spreading, it is based on frequency division. These two approaches are illustrated in Fig. 6.

One of the first uses of the VSF multirate scheme was in an experimental, DS-SS based third generation mobile radio system concept described by Baier *et al.* (1994). Thereafter, Adachi *et al.* (1997) proposed a tree-structured construction of orthogonal spreading codes of different lengths to be used with the VSF scheme. This construction of orthogonal variable spreading factor (OVSF) sequences was subsequently adopted for the third generation W-CDMA mobile radio air interface.

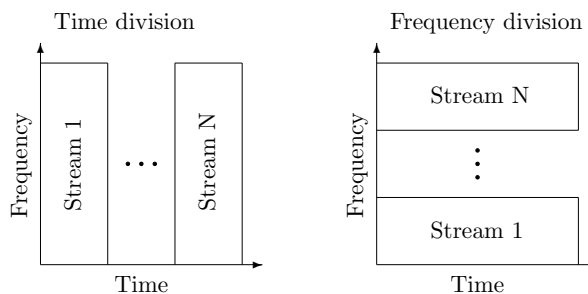


Fig. 6. Time- and frequency-division principles in the VSF scheme.

In conjunction with MC-CDMA, among the first treatments of the VSF multirate scheme are those by Tan & Bar-Ness (2002) and Lestable *et al.* (2002). Tan & Bar-Ness (2002) stated that the interference between the users of different rates can be eliminated by a proper selection of the spreading codes in which the shorter code is orthogonal to the coinciding sub-blocks of the longer codes, that is, by OVFSF codes. Lestable *et al.* (2002) used OVFSF codes with and without random interleaving of the chips on the subcarriers. They restated the fact that the downside of the obtained increase in frequency diversity is the aggravated multiple-access interference and concluded that a compromise between the diversity and interference has to be made.

3.4.3 Comparisons of multicode and VSF

The multicode and VSF multirate schemes have some basic differences regarding their composition. Perhaps the main reason for favoring the VSF scheme over the multicode scheme in the third generation DS-SS-based mobile radio systems is that the VSF scheme does not give rise to the PAPR. This results in savings especially in uplink transmission due to the less stringent requirements for the dynamic range and linearity of DA converters and power amplifiers of handset devices. In MC-SS, on the other hand, the PAPR is already substantial by the nature of OFDM and, therefore, the increase in the PAPR caused by the multicode scheme does not introduce new problems. Another significant implementational advantage of the VSF scheme is that it does not need multiple concurrent spreading and despreading operations per user as the multicode scheme does. A minor advantage of the VSF scheme is also its shorter detection delay for high rate users.

In terms of processing gain and, therefore, noise and interference rejection, the VSF scheme provides less protection for high rate users than it does for low rate users, while the multirate scheme treats users of different rates equally. The reduction of processing gain with data rate in the VSF scheme, of course, may be compensated by increasing the transmit power. This, however, will increase the near-far problem. In the VSF scheme over a quasi-static fading channel, the interference from high to low rate users also varies with the high-rate symbols within a low-rate symbol and, vice versa, the interference from low to high rate users is correlated among the high-rate symbols within a low-rate symbol. This should be taken into account in the detection process in order to obtain the best possible performance. When applied in MC-SS with frequency-domain spreading, the multicode scheme provides frequency diversity

equally to all rates, whereas the VSF scheme provides it more to widely spread low rate transmissions. On the other hand, the deterioration of the orthogonality also worsens with frequency diversity.

Comparisons in single-carrier DS-CDMA

When considering the multicode and VSF multirate schemes for a DS-CDMA air interface, McTiffin *et al.* (1994) saw that it is preferable to use the multicode scheme in a downlink and the VSF scheme in an uplink. Their reasoning was that while multicode transmission more readily permits the use of orthogonal codes in a downlink, orthogonality in an uplink can not be achieved. Moreover, the multicode scheme increases the PAPR of a transmitted signal, which is more problematic to the transmitter of a mobile device than that of a base station due to battery power limitations. Ottosson & Svensson (1995) compared the error rate performance of the multicode and VSF schemes in an asynchronous DS-CDMA system and concluded that the schemes give almost the same performance. Johansson (1999) repeated the comparison in conjunction with multistage successive interference cancellation and showed that the two multirate schemes converge to similar performance, although the multicode scheme performs better for the first few stages.

Mitra (1999) compared the performance of the multicode and VSF schemes when maximum-likelihood-based detection was used. She came to the conclusion that the VSF scheme can provide better performance for high rate users, while for low rate users the performance of the two schemes is comparable. Biglieri *et al.* (2000) used results from the asymptotic analysis of a synchronous DS-CDMA system with random spreading and showed that the multicode and VSF schemes have an equivalent system capacity when single-user matched filter detection is used. When, however, MMSE-based linear detection is used, the multicode scheme dominates the VSF scheme unless the latter detects also the high-rate users by using the whole low-rate symbol interval as an observation interval. Guo & Letaief (2001) made similar conclusions with matched filter and MMSE detection and found them to hold also with PIC. Fan *et al.* (2003) evaluated the BER performance of the multicode and VSF schemes using the true interference distributions instead of the Gaussian approximation. They concluded that while there are differences in the performance of the two multirate schemes, depending on the distribution of multiple-access and multipath interference, they are likely to be insignificant for practical cellular systems most of the time.

Comparisons in multicarrier CDMA

Since most of the above comparisons between the multicode and VSF schemes in conventional single-carrier DS-SS-CDMA came to the twofold conclusions that the two schemes are performing either somewhat equally well or the multicode scheme performs noticeably better, it could be expected that one of the above conclusions would be drawn for multicarrier DS-SS-CDMA which is also using time-domain spreading. Lim & Lee (2001) came to the latter conclusion after considering the two schemes in an asynchronous MC-SS-CDMA system with and without SIC.

In frequency-domain spread MC-SS-CDMA, however, the contradictory outcomes of frequency-selective fading, which are diversity and orthogonality deterioration, may alter the preference of one of the two multirate schemes over the other. However, in comparisons of the multicode and VSF schemes in MC-SS-CDMA with MMSE-based subcarrier combining (Tan & Bar-Ness 2002), space-time block coding and EGC (Hu & Chew 2004), and a semiblind MMSE-based detection with multiple receive antennas and a hybrid serial/parallel interference cancellation (Li & Latva-aho 2006), it has been concluded that the two multirate schemes obtain very similar performances. Li & Latva-aho (2006) found the above to hold true when subcarrier interleaving was used with the VSF scheme, whereas without interleaving, the performance of the VSF scheme was worse. In distinction from the above referred studies, it is shown in this thesis that, of the two multirate schemes in MC-SS-CDMA, the multicode one can provide significantly better error rate performance especially for high rate users.

3.5 Ultra-wideband communications

Since the power spectral density of a spread-spectrum signal is inversely proportional to its bandwidth, a signal with very wide bandwidth results in very low power spectral density. Moreover, the robustness of spread-spectrum communication against narrow-band interference and frequency-selective fading increases with the bandwidth. The above two facts enable very wideband spread-spectrum systems to coexist in the same operational frequencies with other, pre-existing narrower-band radio services so that the interference to and from the pre-existing services stay below tolerable levels. Owing to their very wide bandwidth, these underlay spread-spectrum communication systems are referred to as being ultra-wideband (UWB).

The first regulations on UWB devices, categorizing them to either imaging, vehicular radar, or communication and measurement systems, were given by the FCC of the US in February 2002. These regulations allocated the 3.1–10.6 GHz band, which is overlapping with other radio systems, for unlicensed UWB communication devices. According to the regulations, the -10 dB bandwidth of a UWB transmission in the given band must be at least 500 MHz. The emitted in-band power spectral density must not exceed -41.3 dBm/MHz, averaged over a 1 ms time interval. This in-band emission limit equals that of unintentional radiators, while out-of-band limits for UWB communication systems go as low as -75.3 dBm/MHz in the 960–1610 MHz band within which, for example, GPS operates. The regulations for UWB communications within the European Community (EC), decided in February 2007, are even stricter. They allow the maximum -41.3 dBm/MHz density to be used in the future only in the 6.0–8.5 GHz band in the absence of appropriate techniques for mitigating the emitted interference. As the above regulations, as well as those either already decided on or likely to follow in the other parts of the world, allow extremely low emission levels, UWB communications can provide the highest data rates only in short-range WPAN usage, including wireless connectivity in personal computing, consumer electronics, and mobile applications. However, the rate can be traded for the range by increasing redundancy in the form of either simple repetition or advanced channel coding.

A number of spread-spectrum approaches can be used to generate signals that are appropriate for UWB communications and conform to the given regulations. The two main approaches are the carrierless, impulse radio falling into TH-SS, and the multicarrier, multiband OFDM (MB-OFDM) falling into MC-SS. The impulse radio approach is briefly reviewed in Section 3.5.1, and the MB-OFDM approach and the proposed extensions of it towards MC-CDMA are reviewed in Section 3.5.2. Besides the above two approaches that have gained the widest support in UWB standardization, DS-SS with a suitable chip waveform has been applied to UWB communications (Foerster 2002). The use of MC-DS-CDMA for UWB communications has also been studied (Wang & Milstein 2004). Yang & Giannakis (2006) presented a theoretical framework for a flexible UWB scheme that can be configured as either a CDMA, FDMA, or TDMA system. In addition, fast frequency chirps, which are generated by quickly sweeping the frequency oscillator of a transmitter and which have been successfully used for radar and imaging applications, have also been proposed for UWB systems (Doi *et al.* 2003, Dowla & Nekoogar 2003). The latest proposal is a so-called frequency modulation (FM) UWB in which the carrier is first frequency-shift keying

(FSK) modulated by data and then by a sinusoidal signal in order to spread the spectrum (Gerrits *et al.* 2005). The coexistence of TH-SS and DS-SS based UWB systems with GPS, cellular systems, and WLANs has been considered, for example, by Hämäläinen (2006), and the effect of MB-OFDM interference on narrowband systems was analyzed by Nasri *et al.* (2007).

3.5.1 Impulse radio

The first use of impulse radio dates back to the early years of radio with spark gap transmitters. Radio communications, however, soon developed towards the more easily manageable continuous wave (CW) technology. In the same era, Hülsmeier (1906) patented a “*telemobiloscope*” for the detection and collision avoidance of ships. The device was composed of a spark gap transmitter and a separate receiver that rang a bell when a reflection from, for example, a ship was received. While this pre-radar device used the pulsed radio transmission of its era, the development of CW technology also attracted radar experiments towards CW transmission. This led up to the first CW interference radars being able to detect only the presence of an object. The additional need for ranging information motivated the research on a pulse radar that enabled a straightforward measurement of the time-of-flight of reflected waves. The simultaneous progress in producing high-power short-wavelength radio waves by a magnetron brought up pulse radars with an improved range and accuracy and a smaller size in mid 1930s. Thereafter, in the beginning of 1940s, pulsed radio found use in military, hyperbolic navigation systems in which a navigator determines its position based on the relative arrival times of pulses that are transmitted synchronously from widely separated stations in known positions (Pierce 1946).

The idea of utilizing pulsed radio also in communications followed soon after their successful use in radar and navigation systems. The first systems, which were microwave relays for military communications, used pulse position modulation for encoding voice signals while time-division multiplexing was used for accommodating multiple voice channels (Lacy 1947). White (1950) considered the use of distinct pulse patterns to multiplex asynchronously several sources over the same frequency band at the same time. An experimental system based on a similar approach was described by Pierce & Hopper (1952), who found the system to work satisfactorily.

While the above communication applications of the pulsed radio shared some basic principles with modern impulse radio system, they were not proposed as spread-spectrum

and even less as UWB systems. Two decades later, Ross (1973) patented a pulsed radio system that used sub-nanosecond impulses with an extremely wide spectrum to be used as an underlay system in frequency bands already allotted to other services. This invention is often referred to as the ancestor of the modern UWB impulse radio communications. The history and development of UWB communications was covered in more detail by Barrett (2001).

The potential of pulse modulation and multiplexing in TH-SS communication systems was illustrated again in 1990s by Scholtz (1993). Later on, Win & Scholtz (2000) further outlined the attractive features and the design issues of UWB TH-SS impulse radio for multiple-access communications. Eventually, in March 2007, impulse radio operating in frequencies allocated for UWB communications was approved as an optional air interface to IEEE 802.15.4a standard on low rate WPANs. The aim of this amendment is to provide not only higher and scalable data rates, lower power and cost, and longer ranges, but also high precision range measurement capability. These features are expected to be beneficial especially for the applications of wireless sensor networks.

3.5.2 Multiband OFDM

After the failure of IEEE 802.15.3a standardization to select a UWB physical layer technology for high rate WPANs from the two remaining proposals, one being multiband OFDM (MB-OFDM) and the other direct sequence UWB (DS-UWB), the WiMedia alliance behind the MB-OFDM proposal proceeded with Ecma International standards organization. Subsequently, in December 2005, Ecma International, formerly known as European Computer Manufacturers Association (ECMA), released the first UWB standard, Ecma-368. Thereafter, this standard has also been accepted by European Telecommunications Standards Institute (ETSI) and International Standards Organization (ISO). The MB-OFDM technology has been selected as a high-rate option for the next generation Bluetooth WPANs and also for Certified Wireless USB, one of the competing technologies for the wireless replacement of Universal Serial Bus (USB) cable interface. Another competitor for the latter application is Cable-Free USB, which has been developed by Freescale, a founding member of the rival alliance behind the DS-UWB effort.

The design of an MB-OFDM system complying with the MB-OFDM proposal of the WiMedia alliance was described by Batra *et al.* (2004), and further technical insight into the medium access control (MAC) protocol of the system was provided by

Hiertz *et al.* (2005). The strength of the MB-OFDM approach is its mature, field proven OFDM technology. From the perspective of implementation, hardware components for the UWB applications of OFDM are readily available which enables a short time-to-market. Performance-wise, OFDM with a guard interval is more efficient than DS-SS in capturing the energy of delay-dispersed multipath signals. Moreover, the spectral flexibility of OFDM, which is further enhanced by using multiple bands in MB-OFDM, makes it possible to tailor the system to the specific regulations worldwide and to adapt to different interference environments.

According to ECMA-368 standard on MB-OFDM (Ecma International 2005), the 3.168–10.560 GHz frequency range within the 3.1-10.6 GHz UWB spectrum is divided into 14 bands, each of which is 528 MHz wide and allotted to an OFDM modulated carrier. The reason for choosing the bandwidth of 528 MHz is twofold. While the bandwidth is enough to exceed the minimum required bandwidth of 500 MHz and to meet the designed data rates, it allows for an implementation with a low signal processing speed and power consumption and leads to a simple frequency plan and synthesize circuit (Batra *et al.* 2004). The 14 bands form five band groups, the first four of which, starting from the lower edge of the spectrum, consist of three bands while the fifth is made up of the remaining two bands. Although only the first band group is mandatory, the spectral mask within the EC favors the third group. Within each of the first four band groups, there are seven logical channels for multiple simultaneously operating piconets (SOPs). Channels 5–7 use only a single band, while channels 1–4 employ frequency-hopping through the three bands of a group so that the bands for the channels are reassigned after each OFDM symbol according to unique hopping patterns. The two bands of the fifth band group accommodate only two single band channels. Therefore, the number of logical channels or supported SOPs is 30 altogether.

The OFDM symbols within each of the 528 MHz band of ECMA-368 standard are composed by using a 128-point IFFT. Of the 128 points, the one representing the DC component is set to zero in order to avoid difficulties in carrier feedthrough and DA and AD converter offsets. The next 122 midmost points are used as actual subcarriers, and the rest of the points at the edges of the spectrum are set to zero to avoid interference between the bands. Of the 122 subcarriers, 100 are used to carry data, 12 are dedicated as pilot subcarriers, and 10 are guard subcarriers of which five are on both edges of the band. The guard subcarriers carry a copy of the content of the nearest five data subcarriers if not exploited for other purposes. As the subcarrier spacing becomes 4.125

MHz, the integration period for IFFT and FFT is 242.42 ns. Then, together with the 70.08 ns guard interval, the total OFDM symbol interval becomes 312.5 ns.

There are eight supported data rates in ECMA-368 standard, ranging from 53.3 to 480 Mb/s and depending on a channel code rate and whether the time- and frequency-domain spreading schemes are used. Convolutional channel coding of rate $1/3$ is used, and additional coding rates up to $3/4$ are obtained by puncturing. The coded bits are block interleaved first across six consecutive OFDM symbols and secondly across data subcarriers within an OFDM symbol. Thirdly, cyclic shifting of the bits over a block of data subcarriers is performed between successive OFDM symbols. The modulation on subcarriers is QPSK for data rates of 200 Mb/s and lower, while higher rates use dual carrier modulation with square 16-QAM constellations in order to obtain frequency diversity without decreasing the data rate. Above, time-domain spreading refers to transmitting the same data on two consecutive OFDM symbols, whereas frequency-domain spreading refers to that on two subcarriers within the same symbol.

Enhancements of the OFDM-based UWB system concept, in particular to ECMA-368 standard, are already investigated in order to improve the performance of the future systems. The proposed enhancements include, for example, higher order modulations, wider bands, advanced channel coding, enhanced acquisition and synchronization, adaptive bit loading, and MIMO techniques (Snow *et al.* 2007, Berens *et al.* 2007), as well as more fundamental extensions to the system concept such as the inclusion of frequency-domain CDM which is reviewed in the following section.

Enhanced frequency-domain spreading

In an MB-OFDM system complying with the ECMA-368 standard, frequency diversity against frequency-selective fading and interference is utilized by four different methods. These methods are the interleaving of channel coded bits across subcarriers and OFDM symbols, frequency-hopping among three adjacent bands, frequency-domain spreading in the form of transmitting the same information on two subcarriers within the same OFDM symbol, and dual carrier modulation. However, 14 out of 30 logical channels do not use frequency-hopping, and three medium rates out of eight supported data rates in total do not use either frequency-domain spreading or dual carrier modulation. Therefore, 17.5% of the possible combinations of a logical channel and a data rate utilize frequency diversity only via channel coding and interleaving. Also the highest data rates

with high rate coding provide very little redundancy for this purpose and, despite their dual carrier modulation, may not achieve enough diversity for sufficient performance.

In order to enhance the obtained frequency diversity and, along with it, the performance, more extensive frequency-domain spreading by making use of spreading sequences has been proposed for OFDM-based UWB communication systems. These extensions shift the systems towards UWB MC-CDMA. Gerakoulis & Salmi (2002) was one of the first to propose an OFDM system with frequency-domain CDM for providing frequency diversity without sacrificing the data rate. The subcarrier combining scheme of their receiver performed only despreading without weighting, which is equivalent to EGC. It was shown by simulations that the impact of both the narrowband and multipath interference is worse on an ordinary OFDM than on one with spreading. Park *et al.* (2004) compared the error rate performance of DS-SS, MB-OFDM, and MC-CDMA for UWB communications based on simulations, and found MC-CDMA with EGC to outperform the other approaches. Ramachandran *et al.* (2004) proposed the use of frequency-domain spreading sequences within the frequency bands of MB-OFDM and showed that the spreading improves the performance greatly when MMSECC is used for subcarrier combining. Similar results were also obtained with EGC by Peng *et al.* (2006). Panday & Natarajan (2007) compared the performance of MB-OFDM with different frequency-domain spreading sequences and concluded that all the considered sequences give similar performance with QPSK modulation, whereas with binary phase-shift keying (BPSK), differences arise. Stephan *et al.* (2007) proposed a combination of MC-CDMA and OFDMA in which a block of subcarriers is assigned to each SOP adaptively based on channel conditions. While the above studies were based on simulations, analytical results illustrating the performance enhancements obtained by frequency-domain CDM are presented in this thesis.

In the ECMA-368 standard, the separation of multiple SOPs on different logical channels within the frequency bands of a band group is based on either the frequency-hopping or frequency-division principle, depending on a band group and a logical channel. Since there are four frequency-hopping channels in addition to three fixed-band channels sharing the three bands in each of the first four band groups, collisions between SOPs are inevitable and gradually increase when the number of SOPs within a band group exceeds three. The frequency-domain spreading by spreading sequences, which was considered above as a method to provide frequency diversity, has also been proposed as an alternative, code-division approach for accommodating multiple SOPs in OFDM-based UWB systems. This approach, which is an application of the

MC-CDMA technique, was simulated by Popescu & Yaddanapudi (2006) with different spreading sequences, of which the Walsh-Hadamard sequences were found to give the best performance. Gong *et al.* (2006) demonstrated by simulation that MC-CDMA with orthogonal spreading codes can effectively mitigate the co-channel interference in environments with multiple SOPs. Again, the above results for the application of MC-CDMA in OFDM-based UWB systems were drawn from simulations. In this thesis, on the other hand, analytical results are provided.

4 Summary of the original articles

This chapter summarizes the research results obtained during this thesis work and published in the appended original articles. The modeling of Rice fading channels for the simulation of MIMO multicarrier system, which was considered in Articles I and IV, is summarized in Section 4.1. The performance analysis of multirate MC-CDMA, which was conducted by utilizing the above channel modeling methods and presented in Articles II and III, is reviewed in Section 4.2. The application of the analysis to OFDM-based UWB systems enhanced with frequency-domain CDM, introduced in Articles V and VI, is summarized in Section 4.3.

4.1 Modeling of Rice fading MIMO multicarrier channels

The characterization of a Rice fading channel with temporal, spatial, and spectral correlation, and a complying stochastic fading simulator, which were constructed in the beginning of this thesis work, were first introduced in international forums in Article I. A subsequent publication in Article IV was complemented by the review of the separable temporal, spatial, and spectral correlation functions of fading and by additional results on the performance of the presented simulator. The notation of symbols was revised for Article IV, with which the symbols in this thesis comply. Following the sectioning in the original articles, the summary is subdivided into the characterization of fading in Section 4.1.1, the introduction of the fading simulator in Section 4.1.2, and an overview of the simulator performance in Section 4.1.3.

4.1.1 *Characterization of fading*

The modeled channel is composed of a transmit and a receive antenna array, and a propagation environment composed of scatterers and a possible LOS path. Either the transmitter or the receiver is mobile. For simplicity, the Doppler shift is assumed to affect only the center carrier of a multicarrier system within an observation interval. Similarly, the array dimensions are assumed to be small enough so that the phase shifts across the arrays can be determined based solely on the center carrier. For the latter to hold, $D_t + D_r \ll c/(\max f - \min f)$, where D_t and D_r are the transmit and receive

array dimensions, respectively, c is the speed of light, and f is a subcarrier frequency. For example, for relatively narrowband OFDM systems such as the mobile versions of WiMAX and FLASH-OFDM with a minimum bandwidth of 1.25 MHz, the above condition is generously $D_t + D_r \ll 240$ m, whereas for UWB MB-OFDM with the bandwidth of 528 MHz, it reduces to $D_t + D_r \ll 0.6$ m.

The time domain representation of a lowpass received signal on a subcarrier can be expressed as the sum of all multipath components, that is, as

$$r(t, \mathbf{p}_t, \mathbf{p}_r, f) = \sum_i a_i e^{j\varphi_i(t, \mathbf{p}_t, \mathbf{p}_r, f)} s(t - \tau_i), \quad (1)$$

where t is time, \mathbf{p}_t and \mathbf{p}_r are the vectors determining the transmit and receive antenna positions, respectively, f is the subcarrier frequency, $s(t)$ is a transmitted baseband signal, a_i , $\varphi_i(t, \mathbf{p}_t, \mathbf{p}_r, f)$, and τ_i are the time domain path coefficient, phase, and propagation delay, respectively, of the i th component. The phase is defined as

$$\varphi_i(t, \mathbf{p}_t, \mathbf{p}_r, f) = 2\pi [v_i t + (\mathbf{p}_t \cdot \mathbf{d}_{ti} + \mathbf{p}_r \cdot \mathbf{d}_{ri}) \lambda_c^{-1} - f \tau_i], \quad (2)$$

where v_i is the Doppler frequency and \mathbf{d}_{ti} and \mathbf{d}_{ri} are the unit vectors determining the departure and arrival directions, respectively, of the i th multipath component, and λ_c is the wavelength of the center carrier.

The received lowpass signal can be rewritten as

$$r(t, \mathbf{p}_t, \mathbf{p}_r, f) \approx \sum_{k=1}^K s(t - \bar{\tau}_k) \sum_i a_{ki} e^{j\varphi_{ki}(t, \mathbf{p}_t, \mathbf{p}_r, f)}, \quad (3)$$

where $\bar{\tau}_k$ denotes the mean delay of the k th cluster with the set of delays $\boldsymbol{\tau}_k = [\min_i \tau_i + (k-1)/W, \min_i \tau_i + k/W]$, where W is the bandwidth of a baseband signal on a subcarrier. Now, a_{ki} and $\varphi_{ki}(t, \mathbf{p}_t, \mathbf{p}_r, f)$ are the path coefficient and phase, respectively, of the i th unresolvable multipath component in the k th resolvable path. The summation of unresolvable multipath components in (3) is the channel coefficient for the k th resolvable path, denoted as $c_k(t, \mathbf{p}_t, \mathbf{p}_r, f)$. This coefficient is recast as

$$c_k(t, \mathbf{p}_t, \mathbf{p}_r, f) = a_{k0} e^{j\varphi_{k0}(t, \mathbf{p}_t, \mathbf{p}_r, f)} + \sum_{i>0} a_{ki} e^{j\varphi_{ki}(t, \mathbf{p}_t, \mathbf{p}_r, f)}, \quad (4)$$

where the two terms represent the parts of the channel coefficient that are, respectively, due to the LOS or dominant scattered path, and due to the other scattered paths in the k th resolvable path. These terms are denoted, respectively, as $c_{0k}(t, \mathbf{p}_t, \mathbf{p}_r, f)$ and

$c_{sk}(t, \mathbf{p}_t, \mathbf{p}_r, f)$. When the scattered paths can be viewed as a continuum, $c_{sk}(t, \mathbf{p}_t, \mathbf{p}_r, f)$ can be expressed as

$$c_{sk}(t, \mathbf{p}_t, \mathbf{p}_r, f) = \int_{\boldsymbol{\tau}_k} \iiint a(\nu, \mathbf{d}_t, \mathbf{d}_r, \tau) e^{j\varphi(t, \mathbf{p}_t, \mathbf{p}_r, f)} d\nu d\mathbf{d}_t d\mathbf{d}_r d\tau, \quad (5)$$

where $a(\nu, \mathbf{d}_t, \mathbf{d}_r, \tau)$ is the spread function of the channel (Fleury 2000). Assuming uncorrelated scattering (US) and $i \gg 1$, it follows from the central limit theorem that c_{sk} approaches a zero-mean complex Gaussian random variable. When c_{sk} is added up with c_{0k} , the resulting coefficient $c_k = \alpha_k e^{j\beta_k}$ has a Rice distributed envelope α_k and a phase β_k uniformly distributed over $[0, 2\pi)$.

The cross-correlation between the channel coefficients of the resolvable paths is assumed to be zero (Turkmani *et al.* 1991). The autocorrelation of the coefficients $c_k(t, \mathbf{p}_t, \mathbf{p}_r, f)$ can be partitioned according to the US assumption into a sum of the autocorrelation functions for $c_{0k}(t, \mathbf{p}_t, \mathbf{p}_r, f)$ and $c_{sk}(t, \mathbf{p}_t, \mathbf{p}_r, f)$. The autocorrelation of $c_{0k}(t, \mathbf{p}_t, \mathbf{p}_r, f)$ becomes

$$R_{0k}(\Delta t, \Delta \mathbf{p}_t, \Delta \mathbf{p}_r, \Delta f) = \mu_k^2 e^{j\varphi_{k0}(\Delta t, \Delta \mathbf{p}_t, \Delta \mathbf{p}_r, \Delta f)}, \quad (6)$$

where $\Delta(\cdot)$ is a difference in the argument and μ_k^2 is the power of $c_{0k}(t, \mathbf{p}_t, \mathbf{p}_r, f)$. The autocorrelation of $c_{sk}(t, \mathbf{p}_t, \mathbf{p}_r, f)$ can be written as

$$R_{sk}(\Delta t, \Delta \mathbf{p}_t, \Delta \mathbf{p}_r, \Delta f) = \int_{\boldsymbol{\tau}_k} \iiint p(\nu, \mathbf{d}_t, \mathbf{d}_r, \tau) e^{j\varphi(\Delta t, \Delta \mathbf{p}_t, \Delta \mathbf{p}_r, \Delta f)} d\nu d\mathbf{d}_t d\mathbf{d}_r d\tau, \quad (7)$$

where $p(\nu, \mathbf{d}_t, \mathbf{d}_r, \tau)$ is the power spectrum of the channel (Fleury 2000). Now, the power spectrum can be partitioned as $p_k(\nu, \mathbf{d}_t, \mathbf{d}_r, \tau) = p(\nu, \mathbf{d}_t, \mathbf{d}_r, \tau)|_{\tau \in \boldsymbol{\tau}_k}$. Then, the average power of $c_{sk}(t, \mathbf{p}_t, \mathbf{p}_r, f)$ is defined as $\sigma_k^2 = \iiint p_k(\nu, \mathbf{d}_t, \mathbf{d}_r, \tau) d\nu d\mathbf{d}_t d\mathbf{d}_r d\tau$.

If it can be assumed that

$$p_k(\nu, \mathbf{d}_t, \mathbf{d}_r, \tau) = p_k(\nu) p_k(\mathbf{d}_t, \mathbf{d}_r, \tau), \quad (8)$$

where $p_k(\nu)$ is the Doppler power spectrum, $R_{sk}(\Delta t, \Delta \mathbf{p}_t, \Delta \mathbf{p}_r, \Delta f)$ is the product of the temporal and spatio-spectral correlations, $R_{sk}(\Delta t)$ and $R_{sk}(\Delta \mathbf{p}_t, \Delta \mathbf{p}_r, \Delta f)$, respectively. This assumption holds true, strictly speaking, only on the condition that the Doppler frequency of an unresolvable multipath component is independent of the component's departure and arrival directions and propagation delay. The independence of the Doppler frequency from the departure and arrival directions is best fulfilled when the scatterers are moving in different directions, whereas that from the propagation delay is best

fulfilled when multiple scatterers in the same direction have different distances from the mobile.

Again, if it can be assumed that

$$p_k(\mathbf{d}_t, \mathbf{d}_r, \tau) = p_k(\mathbf{d}_t, \mathbf{d}_r) p_k(\tau), \quad (9)$$

where $p_k(\tau)$ is the delay power spectrum, $R_{sk}(\Delta\mathbf{p}_t, \Delta\mathbf{p}_r, \Delta f)$ is the product of the spatial and spectral correlations $R_{sk}(\Delta\mathbf{p}_t, \Delta\mathbf{p}_r)$ and $R_{sk}(\Delta f)$, respectively. This assumption holds true only on the condition that the delay of an unresolvable multipath component is independent of the departure and arrival directions. This condition has been reported to occur in obstructed or non-LOS links (Chong *et al.* 2003).

Once again, if it can be assumed that

$$p_k(\mathbf{d}_t, \mathbf{d}_r) = p_k(\mathbf{d}_t) p_k(\mathbf{d}_r), \quad (10)$$

where $p_k(\mathbf{d}_t)$ and $p_k(\mathbf{d}_r)$ are the direction power spectra for the transmitting and receiving end, respectively, the joint spatial correlation is obtained as a product of the respective spatial correlation functions $R_{sk}(\Delta\mathbf{p}_t)$ and $R_{sk}(\Delta\mathbf{p}_r)$. This assumption holds true only on the condition that the departure and arrival directions of an unresolvable multipath component are independent. This assumption has been shown to give good approximations for 2×2 MIMO channels with non-LOS propagation, but to be more mismatched in channels with larger MIMO dimensions or a LOS component (McNamara *et al.* 2002, Özcelik *et al.* 2003).

4.1.2 Structure of a fading simulator

The presented realization of a small-scale fading simulator relies on the assumption (8). This assumption firstly makes it possible to simulate fading channel coefficients with a separable, commonly known temporal correlation and with the desired spatio-spectral correlation. Secondly, it enables a continuous flow of simulated channel coefficients in time, and thirdly, results in a computationally less complex simulator. The number of sequences to be generated is $KLMN$, where K , L , M and N are the number of resolvable paths, subcarriers, and transmit and receive antennas, respectively. The K sets of LMN sequences give the tap values of the well-known tapped delay-line model.

Note that when an OFDM system is modeled in the time domain, the channel can be simulated as for a single-carrier system by employing a number of taps in a tapped delay line. In the frequency-domain modeling of an OFDM system, the channel can be

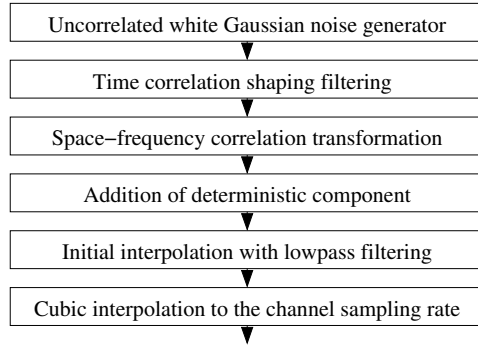


Fig. 7. Structure of the small-scale fading simulator.

simulated as for a multicarrier system, and with only a single tap if the delay spread is shorter than the guard interval. The proposed channel simulator can be used in both the time-domain and frequency-domain approaches.

The broad outline of the simulator structure is presented in Fig. 7. The noise generator outputs $KLMN$ uncorrelated zero-mean complex white Gaussian noise sequences that are fed to parallel time correlation shaping filters. After that, the mutually uncorrelated output sequences with the desired temporal correlation are fed into a space-frequency correlation transformation performed for the K sets of LMN samples to obtain the desired spatio-spectral correlation. Then the resulting Gaussian variables, representing the part of channel coefficients that is due to the scattered multipath components, are added up with complex deterministic variables, representing the part due to a LOS or dominant scattered component. Finally, the sequences are interpolated to get to the desired channel sampling rate. A more detailed description of the above mentioned parts of the simulator and their realization is given in the following.

The desired temporal correlation for the Gaussian part of the channel coefficients is generated by applying appropriate filtering to complex white Gaussian noise. The frequency response of the filter approximates the square root of the desired Doppler power spectrum that is related to the temporal correlation via the Fourier transform. Time correlation shaping filtering is performed by a low order IIR filter to reduce the computational complexity. Two filters with either the classical Jakes' or flat spectra were included. The filter coefficients for the classical spectrum were those given by Stephenne & Champagne (2000). For compatibility, the filter for the flat spectrum was designed by using the same sampling rate of three times the maximum Doppler frequency and the same filter order of four as Stephenne & Champagne (2000) used.

where σ_k^2 is the average power of the Gaussian component in the k th path and $\rho_{klmn}^{kl'm'n'}$ is the complex spatio-spectral correlation coefficient between $c_{sklmn}^{(i)}$ and $c_{sk'l'm'n'}^{(i)}$. The power σ_k^2 in (14) is given by $\sigma_k^2 = P_k/(1 + K_k)$, where P_k and $K_k = \mu_k^2/\sigma_k^2$ are the total power and Rice K -factor, respectively, in the k th path. The power P_k is given by $P_k = \mu_k^2 + \sigma_k^2$. If the assumption (9) holds, $\mathbf{\Sigma}_{p_t p_r f_k}$ is the Kronecker product of the spectral and spatial covariance matrices $\mathbf{\Sigma}_{f_k} \in \mathbb{C}^{L \times L}$ and $\mathbf{\Sigma}_{p_t p_r k} \in \mathbb{C}^{MN \times MN}$, respectively. Furthermore, if the assumption (10) holds, $\mathbf{\Sigma}_{p_t p_r k}$ is obtained from the Kronecker product of the spatial covariance matrices for the transmitter and receiver end, $\mathbf{\Sigma}_{p_r k} \in \mathbb{C}^{M \times M}$ and $\mathbf{\Sigma}_{p_t k} \in \mathbb{C}^{N \times N}$, respectively.

The addition of the Gaussian and deterministic components of the channel coefficients can be expressed as $\mathbf{c}^{(i)} = \mathbf{c}_0^{(i)} + \mathbf{c}_s^{(i)}$, where $\mathbf{c}_0^{(i)} = [\mathbf{c}_{01}^{(i)T} \quad \mathbf{c}_{02}^{(i)T} \quad \cdots \quad \mathbf{c}_{0K}^{(i)T}]^T$ contains the vectors of deterministic components for the K paths. Vector $\mathbf{c}_{0k}^{(i)} \in \mathbb{C}^{LMN}$ for the k th path can be given as

$$\mathbf{c}_{0k}^{(i)} = \mu_k \mathbf{a}_{f_k} \otimes \mathbf{a}_{p_t k} \otimes \mathbf{a}_{p_r k} e^{j(\vartheta_k i + \xi_k)}, \quad (15)$$

where μ_k is the magnitude, vectors \mathbf{a}_{f_k} , $\mathbf{a}_{p_t k}$, and $\mathbf{a}_{p_r k}$ determine the phase shift over subcarriers and transmit and receive antennas, respectively, ϑ_k is the phase shift over a sampling interval, and ξ_k is a random initial phase uniformly distributed over $[0, 2\pi)$, in the k th path. The magnitude μ_k is given by $\mu_k = [K_k P_k / (1 + K_k)]^{1/2}$.

After the addition of the deterministic component, the channel coefficients are interpolated to get to the desired channel sampling frequency. Typically, the channel sampling frequency is much higher than the sampling frequency of a time correlation shaping filter, which results in a large interpolation factor. The classical interpolation with zero-padding and lowpass filtering is computationally intensive when the interpolation factor is large. A computationally simpler method such as the cubic interpolation can be used with a high precision if the signal being interpolated has a sampling frequency much higher than the Nyquist frequency. Therefore, the interpolation process can be decomposed into two parts (Stephenné & Champagne 2000). The classical interpolation is employed initially to achieve a higher sampling rate which is then further increased to the desired value by the cubic interpolation. The filter for the classical interpolation was a 28-order linear phase FIR filter using ten nonzero samples and the interpolation factor of three. The cubic interpolation, including also decimation, was done in blocks of 6 output samples of the interpolation filter and over the midmost 3 sample intervals.

4.1.3 Performance of the simulator

The critical operations in the simulator are the time correlation shaping filtering and the subsequent interpolation. The non-ideal filter responses and cubic interpolation may result in a distorted envelope distribution and inaccurate temporal correlation. The space-frequency correlation transformation and the addition of the deterministic part, on the other hand, can be done very accurately. They are not noticeably distorted by the subsequent interpolation either. For the sake of comparison with the results reported by Young & Beaulieu (2000), the results herein were obtained with 2^{20} channel coefficients and, if not otherwise stated, with the normalized maximum Doppler shift $v_D T_s = 0.05$, which results in a cubic interpolation factor of $I_c = 20/9$.

In order to provide comparable, quantitative quality measures for the time correlation generation, the mean power margin G_{mean} and the maximum power margin G_{max} defined by Young & Beaulieu (2000) are given in the upper half of Table 1. As the agreement between the theory and simulations improves, these measures approach 0 dB in logarithmic scale. The power margins are somewhat better for the flat than for the classical Doppler power spectrum due to the more straightforward design of the respective time correlation shaping filter. The power margins also decrease gradually for

Table 1. Comparison of methods for generating correlated fading.

Method	Doppler spectrum	G_{mean} [dB]	G_{max} [dB]	FLOPs/coeff.
IIR & Interpolation				
$K = -\infty$ dB	Classical	0.094	0.11	298
	Flat	0.029	0.033	298
$K = 0$ dB	Classical	0.048	0.053	300
	Flat	0.015	0.017	300
$K = 10$ dB	Classical	0.0088	0.0094	300
	Flat	0.0025	0.0031	300
IDFT				
2^{10} samples	Classical	1.7	2.3	80
2^{20} samples	Classical	0.0036	0.0040	160
FIR				
length-127	Classical	0.86	0.93	500
length-1023	Classical	0.086	0.093	4000
SOS				
16 sinusoids	Classical	18.0	22.0	300
256 sinusoids	Classical	0.25	0.29	4000

larger Rice K -factors, since larger portion of the coefficients is modeling the constant envelope LOS or dominant scattered path whose phase is changing deterministically.

The lower part of Table 1 presents the power margins obtained with the IDFT method with two different numbers of samples, with a direct FIR filtering with two filter lengths, and with the SOS method with two different numbers of sinusoids. The values for the IDFT method were obtained by averaging over several sequences, and for the other two methods, they were quoted from those reported by Young & Beaulieu (2000). The power margins obtained with the considered IIR filtering and subsequent two part interpolation should be more than enough for all practical purposes and are remarkably better than the ones obtained for the SOS or direct FIR filtering approaches with a similar computational complexity. The accuracy of the IDFT method was found to be approximately equally good for sequences of length 2^{15} but inferior for sequences shorter than that. The accuracy of the other methods, on the other hand, is invariable with respect to the sequence length.

The spatio-spectral correlation of simulated fading matches the desired one very well when a small enough drop tolerance is used in incomplete Cholesky factorization of (13). As the drop tolerance decreases, the incomplete Cholesky factorization approaches the complete one and, therefore, results in better accuracy, which then becomes limited by the number of samples. However, the robustness of the factorization towards badly conditioned covariance matrices lessens with the drop tolerance. The same order of accuracy as with the time-correlation generation is obtained already with a drop tolerance of the order of $2 \cdot 10^{-2}$.

The number of floating-point operations (FLOPs) to generate a sequence of $S > 1$ temporally correlated Rayleigh fading channel coefficients is $1802 \lceil 3v_D T_s (S - 1) \rceil + 28S$, where 1802 is the number of FLOPs used at each sampling interval of a time correlation shaping filter, regardless of the number of generated coefficients, and 28 is the number of FLOPs per coefficient used by the cubic interpolation. The computational complexity of both the time correlation generation method proposed in this thesis and the IDFT method is several orders of magnitude smaller than in the SOS or direct FIR filtering methods with a similar accuracy, as can be seen from the last column of Table 1 which shows the number of FLOPs per channel coefficient. For $S = 2^{15}$ and $v_D T_s = 0.05$, for which the proposed method and the IDFT method were found to be approximately equally accurate, the proposed method is less complex for $v_D T_s < 0.017$ and more accurate for $v_D T_s < 0.05$. Since the number of FLOPs in the IDFT method is $8S \log_2(S)$, the number of FLOPs per coefficient slightly decreases for shorter sequences, but at the cost of

accuracy. The proposed method, on the other hand, maintains its accuracy without a significant increase in the complexity down to sequence lengths of few tens of samples.

In addition to the FLOPs used in the generation of temporal correlation, the complete Cholesky factorization based space-frequency correlation transformation and the addition of a deterministic component use $4K[(LMN)^2 + LMN]$ and $8KLMN$ FLOPs, respectively, once in approximately every $\lceil 1/3v_D T_s \rceil$ channel coefficients. When the incomplete Cholesky factorization is used instead of the complete one, the number of FLOPs per channel coefficient decreases because the number of zero elements in the lower triangular matrix increases with the drop tolerance.

4.2 Performance analysis of multirate MC-CDMA

The performance analysis of multirate MC-CDMA over Rayleigh-fading channels with a delay power spectrum exceeding the guard interval was published as a whole in Article III. Shortly before it, some additional numerical results were presented in Article II. The sectioning of the following summary of Articles II and III follows that of the original articles. The system model is presented in Section 4.2.1, an overview of the performance analysis is given Section 4.2.2, and the numerical results are summarized in Section 4.2.3.

4.2.1 System model

The unified system model enables the modeling of both the multicode and VSF multirate schemes and also a hybrid of those two schemes, although realizations of the hybrid are not considered in this section. In addition, the same model enables the modeling of both synchronous and asynchronous transmission over both downlink and uplink channels. The model comprises H active rate groups, the h th of which has a symbol rate R_h and K_h active users. In the hybrid of the multicode and VSF schemes, each user in the h th rate group employs Q_h overlapping multicode streams, each of which are composed of P_h parallel VSF streams. Therefore, the overall symbol rate in the h th group is $R_h = Q_h P_h$. The spreading factor and, therefore, the number of subcarriers used for one stream in the h th rate group is $G_h = L/P_h$, where L is the total number of available subcarriers. Note that in a plain multicode scheme $R_h = Q_h$, $P_h = 1$, and $G_h = L$, and in a plain VSF scheme $R_h = P_h$, $Q_h = 1$, and $G_h = L/P_h$.

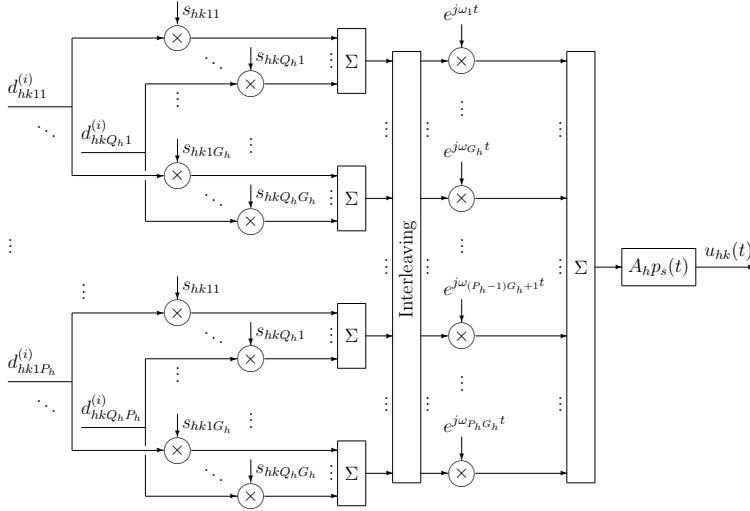


Fig. 8. Transmitter for a hybrid of the multicode and VSF multirate schemes.

The block diagram of a hybrid multicode and VSF multirate transmitter for one user is illustrated in Fig. 8. The transmitted baseband signal of the k th user in the h th rate group at time t can be expressed as

$$u_{hk}(t) = \sum_{i=-\infty}^{\infty} A_h \sum_{q=1}^{Q_h} \sum_{p=1}^{P_h} d_{hkqp}^{(i)} \sum_{g=1}^{G_h} s_{hkgq} p_s(t - iT_s) e^{j\omega_l(t - iT_s)}, \quad (16)$$

where $A_h = \sqrt{E_s/T_s G_h}$ is the amplitude in the h th group, in which E_s is the symbol energy, $d_{hkqp}^{(i)}$ and s_{hkgq} are, respectively, the i th data symbol of the p th VSF substream and the g th chip of the q th multicode stream of the k th user in the h th group, $p_s(t)$ is a rectangular symbol waveform of length T_s including a useful symbol span T_u and a guard interval T_g , and $\omega_l = 2\pi(l-1)/T_u$ is the angular frequency of the l th subcarrier. The subcarrier index l depends on whether interleaving is used or not and is defined as

$$l \equiv l(h, p, g) = \begin{cases} (p-1)G_h + g, & \text{noninterleaved,} \\ p + (g-1)P_h, & \text{interleaved.} \end{cases} \quad (17)$$

After propagation over a multipath channel, the received lowpass signal is given as

$$r(t) = \sum_{i=-\infty}^{\infty} \sum_{h=1}^H A_h \sum_{k=1}^{K_h} \sum_{q=1}^{Q_h} \sum_{p=1}^{P_h} d_{hkqp}^{(i)} \sum_{g=1}^{G_h} s_{hkgq} \sum_n c_{hkn}^{(i)} p_s(t - iT_s - \tau_{hkn}) e^{j\omega_l(t - iT_s - \tau_{hkn})} + n(t), \quad (18)$$

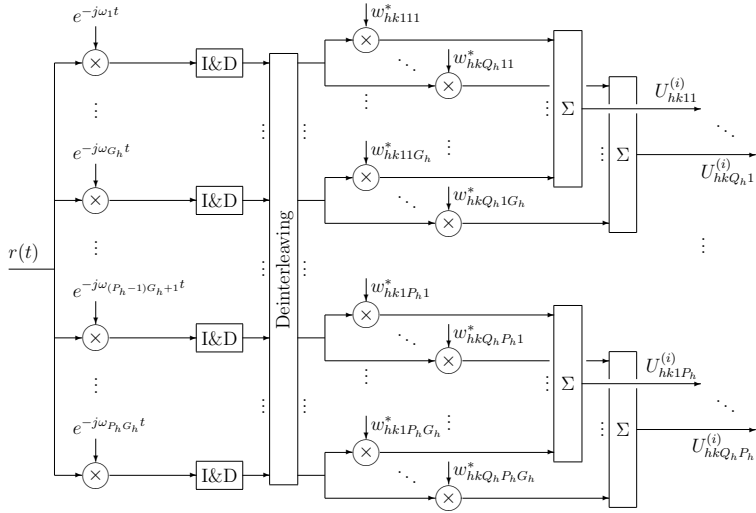


Fig. 9. Receiver for a hybrid of the multicode and VSF multirate schemes.

where $c_{hkn}^{(i)}$ and τ_{hkn} are the complex path coefficient and delay of the n th multipath component of the k th user in the h th rate group, and $n(t)$ is complex zero-mean white Gaussian noise with power spectral density N_0 . Following the US assumption, the complex path coefficients are assumed to be independent for different n . In an uplink, users are assumed to experience independent but identically distributed channels. The delay τ_{hkn} is defined as $\tau_{hkn} = \tau_{hk} + \tau_n$, where τ_{hk} and τ_n are the relative user and path delay, respectively. The user delays τ_{hk} are assumed to be zero for synchronous transmission and independent and uniformly distributed over $[0, T_s)$ for asynchronous transmission. The path delays τ_n are defined as $0 \leq \tau_n < \tau_{n+1} < T_s$. It follows that $\tau_{hkn} \in [0, T_s)$ for synchronous transmission and $\tau_{hkn} \in [0, 2T_s)$ for asynchronous transmission. The channel is assumed to vary in time so slowly that it can be considered to be quasi-static over adjacent symbol intervals, that is, $c_{hkn}^{(i)} \approx c_{hkn}^{(i-1)}$. It is also assumed that the number n of multipath components is large throughout the considered delay range.

The block diagram of the receiver for one user is illustrated in Fig. 9. After the integrate-and-dump (I&D) operation, the output of the OFDM demodulator for the l th subcarrier of the k th user in the h th rate group at the i th symbol interval can be expressed as

$$y_{hkl}^{(i)} = \int_{iT_s + \hat{\tau}_{hk}}^{(i+1)T_s - T_g + \hat{\tau}_{hk}} r(t) e^{-j\hat{\omega}_l(t - iT_s - \hat{\tau}_{hk})} dt, \quad (19)$$

where $\hat{\tau}_{hk}$ and $\hat{\omega}_l$ are the estimated user delay and subcarrier frequency, respectively. It is assumed that the time and frequency synchronization is perfect, that is, $\hat{\tau}_{hk} = \tau_{hk}$ and $\hat{\omega}_l = \omega_l$. Without the loss of generality, the delay of the user of interest is set to zero. The decision metric is then obtained as a weighted sum of G_h demodulated subcarrier components and is given by

$$U_{hkqp}^{(i)} = \sum_{g=1}^{G_h} w_{hkqpg}^* y_{hkl}^{(i)}, \quad (20)$$

where w_{hkqpg} is a combining weight and $(\cdot)^*$ denotes the complex conjugate. Note that combining includes also despreading.

After substituting (18) into (19) and performing the integration, the decision metric $U_{hkqp}^{(i)}$ can be decomposed as

$$U_{hkqp}^{(i)} = D_{hkqp}^{(i)} + I_{hkqp}^{(i)} + N_{hkqp}^{(i)}, \quad (21)$$

where $D_{hkqp}^{(i)}$, $I_{hkqp}^{(i)}$ and $N_{hkqp}^{(i)}$ are due to the desired signal, interference, and noise, respectively. The desired signal term $D_{hkqp}^{(i)}$ can be written as

$$D_{hkqp}^{(i)} = \sqrt{\frac{E_s T_u}{T_s}} d_{hkqp}^{(i)} \sum_{g=1}^{G_h} w_{hkqpg}^* c_{hkl} s_{hkqg}, \quad (22)$$

where c_{hkl} is the effective frequency domain channel coefficient for the l th subcarrier of the k th user in the h th rate group. The effective channel coefficient is given by

$$c_{hkl} = c_{hkl}^{[0, T_g]} + c_{hkl}^{(T_g, T_s)_2}, \quad (23)$$

where $c_{hkl}^{[0, T_g]}$ and $c_{hkl}^{(T_g, T_s)_2}$ represent the effective channel coefficients terms that are composed of the multipath components in the delay ranges from 0 to T_g and from T_g to T_s , respectively. It follows from the US assumption and the central limit theorem that the channel coefficients are spectrally correlated zero-mean complex Gaussian random variables with a Rayleigh distributed envelope and a uniformly distributed phase. The interference term $I_{hkqp}^{(i)}$ can be decompressed as

$$I_{hkqp}^{(i)} = \sum_{g=1}^{G_h} w_{hkqpg}^* \sum_{h'=1}^H \sum_{k'=1}^{K_{h'}} \sum_{q'=1}^{Q_{h'}} \sum_{p'=1}^{P_{h'}} \sum_{g'=1}^{G_{h'}} I_{h'k'q'p'g'}^{(i)}, \quad (24)$$

where $I_{h'k'q'p'g'}^{(i)}$ is the mutual interference from the g' th chip of the p' th VSF substream of the q' th multicode stream of the k' th user in the h' th group to the g th chip of the

p th VSF substream of the q th multicode stream of the k th user in the h th group at the i th symbol interval. The mutual interference $I_{hkqp}^{(i)}$ can be categorized as either $w'k'q'p'g'$ intercarrier interference (ICI) that is the interference from the same or another stream on another subcarrier, intercode interference that is the interference from another stream on the same subcarrier, or ISI that is the interference from the preceding symbol of the same stream on the same subcarrier. The noise term $N_{hkqp}^{(i)}$ is an independent complex zero-mean Gaussian random variable with variance

$$\sigma_N^2 = N_0 \sum_{g=1}^{G_h} |w_{hkqp} g|^2. \quad (25)$$

4.2.2 Performance analysis

After the combining of demodulated subcarrier components, the instantaneous SINR of a received symbol can be expressed as

$$\gamma_{hkqp} = \mathbb{E}_{\{d_{hkqp}^{(i)}\}, n(t)} \left(\frac{|D_{hkqp}^{(i)}|^2}{|I_{hkqp}^{(i)} + N_{hkqp}^{(i)}|^2} \right), \quad (26)$$

where $\mathbb{E}_{\{d_{hkqp}^{(i)}\}, n(t)}(\cdot)$ denotes the expectation over noise and the set of transmitted symbols $\{d_{hkqp}^{(i)}\}$, $h = 1, \dots, H$, $k = 1, \dots, K_h$, $q = 1, \dots, Q_h$, $p = 1, \dots, P_h$, $i = -\infty, \dots, \infty$. After substitution of (22), (24), and (25), and assuming that the transmitted symbols are independent and have zero mean and unit variance, the SINR given in (26) can be rewritten in matrix notation as

$$\gamma_{hkqp} = \frac{|\mathbf{w}_{hkqp}^H \text{diag}[\mathbf{C}_{hk}^{(0)}]_{\mathbf{I}, \mathbf{I}} \mathbf{s}_{hkq}|^2}{\mathbf{w}_{hkqp}^H [\mathbf{R}_{Ihkqp} + \frac{T_s N_0}{T_u E_s} \mathbf{I}] \mathbf{w}_{hkqp}}, \quad (27)$$

where $\mathbf{w}_{hkqp} = [w_{hkqp1}, \dots, w_{hkqpG_h}]^T$ is a vector containing the combining weights for the subcarriers used, $\mathbf{C}_{hk}^{(0)}$ is a channel coupling matrix, $\text{diag}(\cdot)$ is a diagonal matrix with the same diagonal elements as the matrix in the argument, $[\cdot]_{\mathbf{i}, \mathbf{j}}$ is a submatrix of the matrix in the argument and is composed of the rows and columns indexed, respectively, in vectors \mathbf{i} and \mathbf{j} , $\mathbf{I} \equiv \mathbf{I}_{hp} = [l(h, p, 1), \dots, l(h, p, G_h)]$ is the vector of indices of the used subcarriers, $\mathbf{s}_{hkq} = [s_{hkq1}, \dots, s_{hkqG_h}]^T / \sqrt{G_h}$ is the vector containing the chips, \mathbf{R}_{Ihkqp}

denotes an interference covariance matrix, \mathbf{I} is the identity matrix, and $(\cdot)^T$ and $(\cdot)^H$ denote the transpose and the complex conjugate transpose, respectively.

By employing the central limit theorem based Gaussian approximation for the interference, the SINR γ_{hkqp} in (27) which is conditioned on fading, user delays, spreading sequences, and combining weights, can be used in known error probability expressions for an AWGN channel. The error probability in an AWGN channel P_{AWGN} is then averaged over the SINR distribution $p(\gamma_{hkqp})$ to get the error probability in a fading channel, that is,

$$P_{\text{fading}} = \int_0^{\infty} P_{\text{AWGN}}(\gamma_{hkqp}) p(\gamma_{hkqp}) d\gamma_{hkqp}. \quad (28)$$

For rectangular QAM, which is commonly used in OFDM systems and into which category also the modulation formats considered in this study fall, P_{AWGN} is given by Cho & Yoon (2002, eqn. 22). Due to the difficulty in obtaining the distribution function $p(\gamma_{hkqp})$, this study resorts to Monte Carlo integration in averaging the error rate performance over fading, user delays, and a given set of spreading sequences.

The elements of channel coupling matrices, which embody both the effective channel coefficients and the coupling of intercarrier, intercode and intersymbol interference, are composed of frequency domain channel coefficient terms derived for multipath delay ranges from 0 to T_g , from T_g to T_s , from T_s to $T_s + T_g$, and from $T_s + T_g$ to $2T_s$. The channel coefficient terms, which are spectrally correlated within the delay ranges, can be generated for Monte Carlo integration by using a correlation transformation similar to that presented in the summary of Articles I and IV in Section 4.1. The operation exploits the factorization of the spectral covariance matrix of the channel coefficient terms. The covariance matrix was derived assuming an exponentially decaying delay power spectrum that was truncated to T_s .

4.2.3 Numerical results

The number of subcarriers was 32 and the subcarrier combining schemes considered were MRC, EGC, ORC, MMSECC, MMSEUC, and OC. If not otherwise stated, spreading was done by Walsh-Hadamard OVFSF sequences and modulation was BPSK. The length of the guard interval was 20% of the useful symbol part, that is, $T_g/T_u = 1/5$, from which it follows that $T_g/T_s = 1/6$, that is, approximately 17%. Note that the analysis does not rely on the absolute but on the relative values of T_s , T_u , T_g , and σ_d .

In Article III, the bit error probability (BEP) P_b as a function of the multipath rms delay spread normalized with the guard interval σ_d/T_g was evaluated for the different combining schemes in conjunction with the multicode scheme and the VSF scheme both with and without interleaving over a downlink and both a synchronous and asynchronous uplink. The SNR per bit, E_b/N_0 was 20 dB. The system was fully loaded and had 8 users with $R = 1$, that is, with a single stream, and 3 users with $R = 8$, that is, with 8 streams. Therefore, all the $8 \cdot 1 + 3 \cdot 8 = 32$ available spreading sequences of length 32 were used in the multicode scheme. In the VSF scheme, 3 out of the 4 available length-4 sequences and all the 8 length-32 offspring sequences of the 4th length-4 sequence were used. In Article II, a similar evaluation was done with OC and rates $R = 1, 2, 4, 8, 16$ over a downlink. A simple modulation format, full or close to full system load, high SNR and rates of wide range were chosen in order to emphasize the differences that the multirate and combining schemes have in their ability to cope with the interuser and interstream interference that are inherent in multirate MC-CDMA systems. If not otherwise stated, the following discussions are based on the above mentioned evaluations.

When the delay spread is very low, the BEP is the same for the both multirate schemes and all the transmission rates and combining schemes in both a downlink and synchronous uplink channel. In this situation, fading is frequency nonselective and, consequently, there is no spectral diversity to be exploited in combining. But neither is there interference, neither between the users and streams due to the frequency selectivity of the channel, nor between the carriers and adjacent symbols due to significant multipath components exceeding the guard interval. Therefore, the performance is dictated by the AWGN level, and the differences in the capability of the multirate and combining schemes to utilize channel diversity or mitigate interference have no effect. The frequency nonselectivity of the channel sustains the orthogonality between the users also in the case of a synchronous uplink, even though the users experience independent fading. However, the differences in the performance of the combining schemes arise already at normalized delay spread values of the order of 10^{-4} , whereas in a downlink the differences do not arise until σ_d/T_g is almost one order larger. In an asynchronous uplink, the performance is degraded in comparison with the synchronous counterpart. This is due to the interference that is caused by the loss of orthogonality between the users regardless of the delay spread. Moreover, the BEPs of the different rates differ even at low delay spreads. This is because the users no longer share the same channel and, consequently, the lower rate users perform worse as they experience more multiuser

interference which is more difficult to combat than the interference between the streams of a higher rate user.

Due to an increasing part of the delay power spectrum exceeding the guard interval, ISI turns the BEP to rise at around σ_d/T_g of 0.2 to 0.3. Therefore, with the given system parameters the guard interval should be at least 4 times the rms delay spread in the case of an exponentially decaying delay power spectrum in order to insure that the ISI does not limit the performance.

In Article II, the BEP was also evaluated as a function of E_b/N_0 for the multicode scheme with rates $R = 1, 8$ and for both Walsh-Hadamard and orthogonal Gold spreading sequences over a downlink and both a synchronous and asynchronous uplink. MMSEUC, $\sigma_d/T_g = 0.2$, and 3 users of the both rates were applied. The performance in a synchronous uplink is clearly degraded in comparison with a downlink. Still, it is significantly better than in an asynchronous uplink where the performance is limited by severe intercarrier interference. Orthogonal Gold sequences were found to result in notably better BEP than Walsh-Hadamard sequences, especially in an uplink.

Comparison of multirate schemes

The multicode multirate scheme results in identical BEP for the different rates in a downlink. This is expected since all the streams are transmitted with equal power on all subcarriers and undergo the same fading. In an uplink, however, there are some differences. In a synchronous uplink, the BEPs for the different rates are the same at low delay spreads but deviate slightly for the advantage of the higher rate streams as the delay spread increases. The reason for this was already pointed out above in context with an asynchronous uplink.

The VSF multirate scheme differs fundamentally from the multicode scheme in that it results in different BEPs for the different rates even in a downlink. In general, in both a downlink and uplink and whether or not interleaving is used, the BEP is lower for low-rate streams than for high-rate streams when the more advanced MMSECC, MMSEUC, or OC combining schemes are used. For the simpler MRC, EGC, and ORC schemes, the situation is the opposite. The advanced combining schemes, especially MMSEUC and OC, can utilize diversity and suppress interference the better the smaller the rate, that is, the wider in frequency the streams are spread. The simpler combining schemes, on the other hand, suffer more from the increased interference than benefit from

the additional spectral diversity when the number of subcarriers per stream increases inversely proportionally to the rate.

The comparison of the BEPs for the multicode and VSF schemes in a downlink reveals that the multicode scheme is performing, depending on the rate and combining scheme, either considerably better than or approximately as well as the VSF scheme with or without interleaving. Considerably better performance with the multicode scheme is obtained for the high-rate streams by using MMSECC, MMSEUC or OC which can utilize the increased spectral diversity. The multicode scheme is also better for the rate-1 streams when EGC or MMSECC is used, although the streams use all the subcarriers in the both multirate schemes. These combining schemes seem to be vulnerable to the concentration of the power of the high-rate streams on fewer subcarriers which is inherent to the VSF scheme. In Article III, the VSF scheme was found to provide noticeably better performance only for the rate-8 streams and only with MRC and when no interleaving was used. Of the considered combining schemes, MRC copes with interference worst and, consequently, the smaller the number of subcarriers assigned for a stream, the less interference is collected. In Article II where OC was used, the VSF scheme performed better only with rate 1 and without interleaving.

Interleaving in conjunction with the VSF scheme improves the performance of only the higher rate streams and only when MMSECC, MMSEUC, or OC is used. The lower rate streams with the aforementioned combining schemes and the streams of the both rates with the other combining schemes have in fact worse performance when interleaving is used. Without interleaving, the channel is piecewise frequency nonselective over the subcarriers assigned for a higher rate stream and, consequently, the higher rate stream remains orthogonal to the lower rate streams to some extent. Only the higher rate streams with MMSECC, MMSEUC, and OC benefit from interleaving as they benefit more from the additional diversity than suffer from the loss of orthogonality.

In a synchronous uplink, the multicode scheme and the VSF scheme with or without interleaving are performing almost equally well for the rate 1 in conjunction with all the combining schemes. For the rate 8, however, the multicode scheme is better with MMSEUC and OC, which was the case also in a downlink channel. With the rest of the combining schemes, the VSF scheme without interleaving is better. The loss of orthogonality between the users, which arises with the delay spread, is accelerated in an uplink by the independency of their fading channels. The higher rate streams suffer from this the least when the VSF scheme without interleaving is used in conjunction with the less advanced combining schemes. In that case, the higher rate streams benefit from

the piecewise frequency nonselectivity of the channel which the interleaving would remove and which the multicode scheme does not provide in the first place. Opposite to a downlink, the loss of piecewise frequency nonselectivity in interleaving deteriorates the performance of the higher rate streams in the VSF scheme also when MMSECC, MMSEUC, and OC are used.

The above statements about the relative performance of the multirate schemes in a synchronous uplink also hold true for the asynchronous case. Moreover, the loss of orthogonality between the users due to their asynchronicity raises a difference in the performance of the rate-8 streams in favor of the multicode scheme already in frequency-nonselective channels when MMSEUC and OC schemes are used. These combining schemes can utilize the additional diversity against interference that the multicode scheme can provide over the VSF scheme at the higher rates.

Comparison of combining schemes

The MMSEUC and OC subcarrier combining schemes, which determine the combining weights jointly for all subcarriers being combined, are the best at exploiting the increasing diversity while not enhancing noise or giving rise to interference. Indeed, they perform better as the delay spread increases. This holds true especially for a downlink but also for an uplink. These two schemes have practically an equal performance up to the normalized rms delay spread of approximately 0.2. Beyond that point, ISI increases to the extent that the performance of both of the schemes weakens dramatically. OC suffers slightly less from ISI as it bases the computation of combining weights on the interference covariance matrix only and not on the whole received signal as MMSEUC does. This advantage of OC on high delay spreads, however, may not be sufficient in the tradeoff for its higher computational complexity.

Also MMSECC benefits greatly from frequency selectivity, but only in a downlink where it is able to restore the orthogonality between the users. In conjunction with the multicode multirate scheme, MMSECC is actually performing as well as MMSEUC and OC in a fully loaded system, except for the highest delay spreads where it suffers from ISI more than the other two. This, together with a lower computational complexity in comparison with MMSEUC and OC, makes MMSECC an attractive choice for a downlink. In partially loaded systems, however, MMSECC performs worse than MMSEUC, which was shown already by H elard *et al.* (2000) and confirmed in Article II where also the BEP as a function of the number of streams in the multicode scheme was

evaluated. Moreover, MMSECC needs information on the other active streams in the system and also on the noise level, which are not required by the simpler combining schemes that are discussed in the following.

Even EGC benefits slightly from frequency selectivity in a downlink, especially in conjunction with the multicode scheme with which it performs better than or as well as ORC regardless of the delay spread, but also in conjunction with rate 1 in the VSF scheme without interleaving in which case it performs better than or as well as ORC at σ_d/T_g below $7 \cdot 10^{-2}$. MRC, on the other hand, is clearly performing worse than EGC and ORC in a downlink since it pronouncedly distorts the orthogonality of the users and streams. In Article II, where the BEP was considered as a function of the number of streams in the multicode scheme, EGC was also found to perform better than MRC and ORC except for the single stream case in which MRC achieves the optimum performance. Therefore, EGC compromises fairly successfully the diversity utilization and interference rejection properties of MRC and ORC, respectively.

In a downlink, the performance of ORC degrades more rapidly than that of EGC at high delay spreads where ISI arises. Up to that point, ORC is able to combat interuser and interstream interference by the channel inversion. However, ORC suffers from the noise enhancement as a channel becomes frequency selective, that is, noise on deeply faded subcarriers is greatly amplified in the channel inversion. The performance degradation due to the noise enhancement is interestingly at its highest at medium delay spreads and eases off as the delay spread further increases. This can be explained by the fact that as the selectivity of the fading becomes high enough, deep fades suppress fewer subcarriers when they occur and, respectively, severe noise amplification takes place on fewer subcarriers in one combining act. Since ORC prevents the intercode interference between the streams in a downlink, it results in invariable performance over the system load, as was shown in Article II. In both a synchronous and asynchronous uplink, ORC performs worse than both EGC and MRC as the delay spread increases. This is because the orthogonality between the users can not be restored when they experience independent frequency-selective fading. Instead, the interference on deeply faded subcarriers is greatly amplified.

Comparison of modulation schemes

The usage of higher order modulation schemes does not change what was stated above about the performance differences of the multirate schemes, although the BEP gradually

increases with the modulation order. At very low delay spreads in a downlink and synchronous uplink, where there is no interference present yet, QPSK expectedly results in the same performance as BPSK and performs clearly better than 16-QAM. As the delay spread increases, the performance with the higher order modulations degrades gradually earlier than with BPSK because of the greater sensitivity to the arising interference.

The greater interference sensitivity of QPSK and 16-QAM also emphasizes the differences that the combining schemes have in their ability to combat interference. Therefore, in conjunction with the higher order modulations, opposite to the case of BPSK, EGC performs much worse than ORC also with the multicode scheme in a downlink. Otherwise, the relative order of the combining schemes does not change as the performance is gradually degraded with QPSK and 16-QAM.

4.3 OFDM-UWB systems enhanced with MC-CDMA

The performance analysis of multirate MC-CDMA when applied to frequency-domain code-division multiplexed OFDM-based UWB systems was presented in the original articles separately for scenarios with either a single or multiple SOPs. The case of a single piconet, in which CDM is used only to enhance the obtained frequency diversity while maintaining the transmission rate, was published in Article VI that is summarized below in Section 4.3.1. The case of multiple SOPs, in which CDM is also used to provide multiple-access, was published in Article V that is summarized in Section 4.3.2.

4.3.1 A single piconet

The system model was modified from that of Article III and is indeed now a hybrid of the VSF and multicode techniques. Therefore, it enables the modeling of a continuum of schemes from a plain nonspread OFDM scheme to a maximally spread multicode scheme via medium-spread combinations of the VSF and multicode transmissions. The overall symbol rate R is a product of the numbers of multicode and VSF streams and it should be equal to the number of subcarriers L in order to maintain equal, maximal rate for different schemes. The combining schemes considered are ORC and MMSECC. For the numerical results, the number of subcarriers was limited to 32 for simplicity, the modulation was QPSK, and the length of the guard interval was 20% of the symbol interval, that is, $T_g/T_s = 0.2$, which is close to the $T_g/T_s = 0.22$ of

a standardized UWB-OFDM (Ecma International 2005). If not otherwise stated, the spreading sequences were Walsh-Hadamard sequences and the SNR per bit, E_b/N_0 was 15 dB.

The BEP as a function of the rms delay spread normalized with the guard interval, σ_d/T_g , was derived for the different possible spreading factors G and for both non-interleaved and interleaved cases. At very low σ_d/T_g , where the fading is frequency nonselective, the performance is the same regardless of the combining scheme, spreading factor, or whether or not interleaving is used, as stated in Section 4.2.3. The differences in the performance of the different schemes become apparent when the frequency selectivity of a channel increases with σ_d/T_g .

The channel inversion of ORC ensures that the orthogonality between the multicode streams is maintained and, consequently, intercode interference does not ruin the performance. However, the channel inversion prevents the utilization of frequency diversity that increases with the spreading factor. The increased frequency selectivity, quite on the contrary, results in a severer noise enhancement and, therefore, in a performance degradation which arises already before $\sigma_d/T_g = 0.01$ for a spreading factor of $G = 32$. For smaller spreading factors, this performance degradation arises earlier with than without interleaving.

The ability of MMSECC to utilize the increasing frequency diversity, without suffering excessively from intercarrier interference, results in a significant performance enhancement when larger spreading factors are used. In the case of the smallest spreading factors with interleaving, however, the noise enhancement overrides the benefit of diversity at the considered SNR level. The interleaving, nevertheless, improves the performance obtained with the spreading factors of 8 and 16 already at fairly low delay spreads. The performance of MMSECC with the spreading factors of 8 and above is at its best around $\sigma_d/T_g = 0.2$. With $T_g/T_s = 0.2$ and $T_s = 312.5$ ns defined by Ecma International (2005), the above rms delay spread corresponds to $\sigma_d = 12.5$ ns that is common for NLOS indoor channels (Batra *et al.* 2004). As the delay spread further increases and a greater portion of the delay power spectrum exceeds the guard interval, ISI causes the BEP of both MMSECC and ORC to rise. This occurs slightly later for larger spreading factors as they have diversity against interference.

The BEP as a function of E_b/N_0 for the different spreading factors and MMSECC with and without interleaving at $\sigma_d/T_g = 0.2$ was also presented. As with any other scheme that is providing diversity, the higher the SNR, the more gain frequency-domain spreading gives. Moreover, increasing the diversity order, which is the spreading factor

herein, improves the performance at higher SNR levels, although the improvement gradually lessens at each step. Naturally, interleaving does not improve the experienced frequency selectivity with the spreading factors of 1 and 32, but is advantageous with $G = 4, 8,$ and 16 at higher SNR levels. With $G = 2,$ however, the deterioration due to the noise enhancement overwhelms the potential diversity benefit and, eventually, interleaving worsens the performance even at higher SNR levels. At low SNR, interleaving degrades the performance also with $G = 4.$ Altogether, even the lowest possible spreading factor of $G = 2$ results in performance improvement over the plain OFDM with $G = 1$ when the SNR increases sufficiently.

The multicode transmission also provides a flexible way to control the transmission rate. The number of employed multicode streams may be reduced in order to lessen the intercode interference and, therefore, trade rate for error rate performance. To illustrate this, the BEP as a function of the number of multicode streams with $G = 32$ and MMSECC was derived. In addition to Walsh-Hadamard spreading sequences, also orthogonal Gold sequences were considered. Decrease in the number of active streams improves the error rate performance, although a more significant improvement would be most likely obtained by using all streams and a channel code with a respective decrease in the rate. The orthogonal Gold sequences interestingly give a somewhat better performance than the Walsh-Hadamard sequences when there are only a few streams. For larger numbers of streams, however, the performance of these two sequence sets is very similar.

4.3.2 Multiple simultaneously operating piconets

The system model differs from the above single-SOP model in that it accommodates a continuum of schemes from a plain nonspread single-SOP OFDM scheme to a maximally spread multi-SOP, multicode scheme via medium-spread VSF transmissions. The number of active SOPs is denoted by K and they are assumed to be time-synchronized and of equal received power. For simplicity, all SOPs are assumed to have the same number of multicode and VSF streams, denoted by Q and $P,$ respectively, and therefore the same rate $R = QP.$ The system load with orthogonal spreading sequences is assumed to be maximal, that is, QPK equals the number of subcarriers $L.$ The combining schemes considered are MMSECC and MMSEUC. For the numerical results, similarly to the single-SOP case, 32 subcarriers, QPSK modulation, Walsh-Hadamard spreading sequences, a guard interval of 20% of the symbol interval and an E_b/N_0 of 15 dB were

used. The BEP as a function of the rms delay spread normalized with the guard interval, σ_d/T_g , was derived for the different numbers of SOPs with either the multicode scheme or the VSF scheme either with or without interleaving. In the VSF scheme, the spreading factor G was minimal for the accommodation of all SOPs, that is, $G = K$, whereas in the multicode scheme the spreading was maximal, that is, $G = L$.

Although MMSECC and MMSEUC perform similarly with only a single SOP, the performance of MMSECC starts to degrade in a multi-SOP environment immediately when the subcarriers that are employed by a data stream become frequency selective and, consequently, the orthogonality between the SOPs deteriorates. In the VSF scheme without interleaving, the smaller the G , the longer the subcarriers remain piecewise frequency nonselective. With interleaving, as well as with the multicode scheme, the loss of orthogonality between the SOPs starts already before $\sigma_d/T_g = 10^{-3}$, regardless of K . Moreover, the performance with the multicode or interleaved VSF scheme with only two SOPs is nearly as bad as with larger numbers of SOPs at larger delay spreads. Consequently, MMSECC can not provide an acceptable performance in a multi-SOP environment, except maybe with the noninterleaved VSF scheme and very limited number of SOPs.

The performance of MMSEUC does not degrade as a channel becomes frequency selective. The combining weights, which are jointly determined for all the subcarriers of a data stream, can suppress the interference from other SOPs. In the VSF scheme, neither interleaving, the number of SOPs, nor the normalized delay spread σ_d/T_g when below 0.2 appreciably affect the performance of MMSEUC. In the multicode scheme, on the other hand, MMSEUC and also MMSECC can utilize all the frequency selectivity as diversity when there is only a single SOP and consequently no interference from other SOPs to be mitigated. This can significantly improve the performance over that obtained in the VSF scheme. However, after more than two SOPs, the interference mitigation trades off the diversity utilization in MMSEUC. Consequently, the performance with more than 2 SOPs is invariant with respect to K and dictated by an AWGN level. With MMSECC, on the other hand, already one other SOP ruins the performance, as was discussed above. When the delay spread increases above $\sigma_d/T_g = 0.2$, ISI causes the BEP of MMSEUC to rise rapidly.

5 Conclusion

This thesis consisted of three main areas based on the characterization and simulation of small-scale fading multicarrier MIMO channels, on the performance analysis of multirate MC-CDMA systems over delay dispersive channels, and on the application of the analysis on OFDM-based UWB systems enhanced with frequency-domain code-division multiplexing is summarized below in Section 5.1. Possible future extensions to the conducted research are considered subsequently in Section 5.2.

5.1 Summary and discussion

Firstly, an extensive review of the literature on small-scale fading mobile radio channels and their simulation was presented. Drawing on the existing literature, a statistical characterization of a small-scale fading mobile radio channel and a conforming fading channel simulator for the simulation of MIMO multicarrier systems were derived. The channel was presented as a well-known tapped delay line model with time-, space-, and frequency-selective taps representing channel coefficients of resolvable multipath clusters. These resolvable paths were modeled as the sum of a LOS or dominant scattered path and a number of unresolvable scattered paths and, therefore, were Rice fading. The unresolvable scattered paths were modeled based on the channel spread function, that is, the joint spread in Doppler frequency, in direction at both a transmitter and receiver, and in delay. In the special case where the channel spread was separable in the aforementioned factors, the model unified the well-known independent characteristics of fading in time, space, at both the mobile and base station, and frequency. In the simulator, the small-scale fading channel coefficients were composed of a complex valued deterministic part and a zero-mean Gaussian part and, consequently, the coefficients had a Rice distributed envelope. The Gaussian parts had desired temporal, spatial, and spectral correlation characteristics, whereas the deterministic parts had a constant magnitude and a phase varying over time, space, and frequency.

The presented simulator has a low computational complexity and an excellent accuracy in the generation of a time-, space-, and frequency-selective Rice fading channel with well-defined characteristics. In contrast with the sum-of-sinusoids and direct FIR filtering based fading simulators, the accuracy of the presented simulator is

superb. In contrast with the IDFT-based simulators, on the other hand, the accuracy of the presented simulator is insensitive to the length of the simulated fading sequence and is maintained without a significant increase in complexity down to the sequence lengths of few tens of samples. Consequently, the method considered in this paper can be regarded as the most suitable when it is desirable that the channel coefficients can be generated as they are needed, and especially when the length of the sequence is not known in advance or is either very short or long. The fading simulator has found extensive use in performance evaluations of various multiantenna and multicarrier systems that have been conducted by research colleagues in both academia and industry.

Secondly, a review was given on spread-spectrum communications with an emphasis on MC-CDMA with frequency-domain spreading that is considered as a promising air interface candidate especially for a downlink channel of future multi-user communication systems. Since the efficient support of various multimedia services in future systems requires a multirate capability, the performance of MC-CDMA with the multicode and VSF multirate schemes over Rayleigh fading frequency-selective channels was analyzed. The VSF scheme was considered both with and without interleaving. The analysis contained a synchronous downlink and both a synchronous and asynchronous uplink. The delay power spectrum of a channel was assumed to be exponentially decaying with a given rms delay spread and not truncated to the length of a guard interval as is commonly carried out in the literature. Therefore, ISI was also taken into account.

The results show that the multicode multirate scheme can offer a better error rate performance than the VSF scheme. Moreover, the multicode scheme enables similar performance for different rates, opposite to the VSF scheme in which the performance of different rates varies greatly. It was also shown that besides the more advanced and complex OC and MMSEUC combining methods, also the simpler MMSECC gives a good performance in a downlink, even in a fully loaded system. In an uplink, however, only OC and MMSEUC give reasonably good, nearly equal performances. As expected, the performance in an asynchronous uplink is greatly degraded in comparison with the synchronous counterpart. The orthogonal Gold spreading sequences were shown to result in a slightly better performance than the Walsh-Hadamard sequences in the multicode scheme. With the considered system parameters, the guard interval should be approximately five times the rms delay spread of an exponentially decaying delay power spectrum in order to secure that ISI does not limit the performance.

Thirdly, the performance analysis of multirate MC-CDMA was applied to OFDM-based UWB systems enhanced with frequency-domain CDM. The results for a single

piconet case show that frequency-domain spreading can significantly improve the performance when sufficient spreading factors and a suitable combining method such as MMSECC is used. MMSECC was shown to be able to resist intercode interference while exploiting frequency diversity that is available in a typical UWB radio channel already with a spreading factor of as low as 8. As expected, larger spreading factors and interleaving provided further performance improvements. The ability of the multicode scheme to trade transmission rate for an improved error rate performance was also illustrated.

In the case of multiple simultaneously operating synchronous piconets, it was shown that frequency-domain CDMA can be employed to accommodate multiple SOPs while maintaining an acceptable performance when a suitable combining method such as MMSEUC is used. Both the VSF and multicode schemes were shown to result in a similar performance when there were several SOPs, whereas in the case of only a few SOPs, the greater frequency diversity provided by the multicode scheme resulted in a better performance with MMSEUC. In the VSF scheme, interleaving does not have an effect on the performance of MMSEUC, but with the simpler MMSECC subcarrier combining scheme, the performance is actually degraded.

5.2 Future work

The presented small-scale fading channel model and the complying fading simulator could be fairly easily extended to also include polarization selectivity, the importance of which is increasing now that MIMO techniques are being exploited in wireless terminals with very restricted space for diversity antennas. The factorization of covariance matrices for the space-frequency correlation transformation, which is done currently by incomplete Cholesky factorization, could be perfected for the cases of large matrices with highly correlated elements. This would further improve the numerical stability in situations such as a large number of closely spaced subcarriers in a nearly frequency-nonselective channel. The modeling of the temporal correlation of the taps of the delay line could be modified to enable the different taps to have Doppler power spectra of different shapes, as is proposed by some measurement-based characterizations. Furthermore, the spatio-spectral correlation could be derived directly from a measured multipath cluster with joint delay and direction dispersion. A more challenging task would be the revision of the simulator structure to enable the modeling of joint temporal and spatio-spectral correlation.

The performance analysis of MC-CDMA could be detailed to take into account a number of imperfections in a realistic receive process that have been disregarded in order to simplify and conceptualize the analysis. However, abandoning some of these idealizations, such as the the assumption of quasi-static fading between adjacent OFDM symbols, would require extensive changes to the system model and yield increasingly complicated derivations. On the other hand, the fading between adjacent OFDM symbol intervals, or even within one symbol, can not be considered as quasi-static when the mobile is moving very fast and the symbol interval is relatively long. In this situation, intercarrier interference would arise. A somewhat easier extension would be to incorporate the effects of imperfect channel estimations, whereas the modeling of frequency and time synchronization errors would be again more cumbersome. Adaptive implementations of MMSEUC and OC, which avoid the computationally complex matrix inversion of the ideal direct forms of the combining weight derivations of these two schemes, would be another step towards practical systems. Besides these two per user combining schemes, zero-forcing per user combining needs to be considered. The use of complementary spreading sequences and their effect on the performance would also be worth investigating.

The inclusion of the above mentioned imperfections to the analysis would reduce the benefit of frequency diversity and, therefore, most likely also the advantage of the multicode multirate transmission over the VSF scheme and that of MMSEUC and OC over the simpler combining schemes. Also the use of the Gaussian approximation for the interference, although conditioned on the channel state and spreading sequences, seems to give, based on preliminary simulations, slightly optimistic results compared to the simulated interference distributions that have slightly more pronounced tails. However, neither this nor the other above mentioned imperfections are expected to be significant enough to change the conclusions of this thesis. But then again, inclusion of spatial and temporal diversity to the system model through MIMO techniques and channel coding, respectively, would most likely improve the performance of the VSF scheme more than that of the multicode scheme. This is because the overall diversity gain of the latter over the former diminishes with additional diversity sources. The above and a number of other issues need to be investigated before MC-CDMA, in one form or another, will be adopted into an air interface for future UWB and cellular systems, beyond MB-OFDM and 3GPP LTE, respectively.

References

- Abdi A, Barger HA & Kaveh M (2000a) Signal modeling in wireless fading channels using spherically invariant processes. *Proc. IEEE International Conference on Acoustics, Speech, and Signal Processing*, Istanbul, Turkey, 5: 2997–3000.
- Abdi A, Barger JA & Kaveh M (2002) A parametric model for the distribution of the angle of arrival and the associated correlation function and power spectrum at the mobile station. *IEEE Transactions on Vehicular Technology* 51(3): 425–434.
- Abdi A, Hashemi H & Nader-Esfahani S (2000b) On the PDF of the sum of random vectors. *IEEE Transactions on Communications* 48(1): 7–12.
- Abdi A & Kaveh M (2002) A space-time correlation model for multielement antenna systems in mobile fading channels. *IEEE Journal on Selected Areas in Communications* 20(3): 550–560.
- Abeta S, Atarashi H, Sawahashi M & Adachi F (2000) Coherent multicarrier/DS-SS and MC-SS for broadband packet wireless access. *Proc. IEEE Vehicular Technology Conference*, Tokyo, Japan, 3: 1918–1922.
- Adachi F, Feeney MT, Williamson AG & Parsons JD (1986) Crosscorrelation between the envelopes of 900 MHz signals received at a mobile radio base station site. *IEE Proceedings Part F. Radar and Signal Processing* 133(6): 506–512.
- Adachi F, Sawahashi M & Okawa K (1997) Tree-structured generation of orthogonal spreading codes with different lengths for forward link of DS-SS mobile radio. *Electronics Letters* 33(1): 27–28.
- Akhavan-Bahabdi M & Shiva M (2005) Double orthogonal codes for increasing capacity in MC-SS systems. *Proc. IFIP International Conference on Wireless and Optical Communications Networks*, Dubai, United Arab Emirates, 468–471.
- Andersen JB & Kovacs IZ (2002) Power distributions revisited. Technical Report TD(02) 004, COST 273, Guildford, UK.
- Andrews JG & Meng THY (2004) Performance of multicarrier SS with successive interference cancellation in a multipath fading channel. *IEEE Transactions on Communications* 52(5): 811–822.
- Aranguren WL & Langseth RE (1973) Baseband performance of a pilot diversity system with simulated Rayleigh fading signals and co-channel interference. *IEEE Transactions on Communications* 21(11): 1248–1257.
- Arnold HW & Bodtmann WF (1983) A hybrid multichannel hardware simulator for frequency-selective mobile radio paths. *IEEE Transactions on Communications* 31(3): 370–377.
- Arredondo GA, Chriss WH & Walker EH (1973) A multipath fading simulator for mobile radio. *IEEE Transactions on Vehicular Technology* 22(4): 241–244.
- Atarashi H, Maeda N, Abeta S & Sawahashi M (2002) Broadband packet wireless access based on VSF-OFDM and MC/SS-SS. *Proc. IEEE International Symposium on Personal, Indoor and Mobile Radio Communications*, Lisbon, Portugal, 3: 992–997.
- Aulin T (1979) A modified model for the fading signal at a mobile radio channel. *IEEE Transactions on Vehicular Technology* 28(3): 182–203.
- Aulin T (1981) Characteristics of a digital mobile radio channel. *IEEE Transactions on Vehicular Technology* 30(2): 45–53.

- Baddour KE & Beaulieu NC (2004) Accurate simulation of multiple cross-correlated Rician fading channels. *IEEE Transactions on Communications* 52(11): 1980–1987.
- Baddour KE & Beaulieu NC (2005) Autoregressive modeling for fading channel simulation. *IEEE Transactions on Wireless Communications* 4(4): 1650–1662.
- Baier A, Fiebig UC, Granzow W, Koch W, Teder P & Thielecke J (1994) Design study for a CDMA-based third-generation mobile radio system. *IEEE Journal on Selected Areas in Communications* 12(4): 733–743.
- Bar-Ness Y, Linnartz JP & Liu X (1994) Synchronous multi-user multi-carrier CDMA communication system with decorrelating interference canceler. *Proc. IEEE International Symposium on Personal, Indoor and Mobile Radio Communications*, Hague, Netherlands, 1: 184–188.
- Barrett TW (2001) History of ultra wideband communications and radar: Part I, UWB communications. *Microwave Journal* 44(1): 22–56.
- Batra A, Balakrishnan J, Aiello GR, Foerster JR & Dabak A (2004) Design of a multiband OFDM system for realistic UWB channel environments. *IEEE Transactions on Microwave Theory and Techniques* 52(9): 2123–2138.
- Beauchamp KG (1975) *Walsh Functions and Their Applications*. Academic Press, London.
- Beaulieu NC & Merani ML (2000) Efficient simulation of correlated diversity channels. *Proc. IEEE Wireless Communications and Networking Conference*, Chicago, USA, 1: 207–210.
- Bellanger MG & Daguët JL (1974) TDM-FDM transmultiplexer: Digital polyphase and FFT. *IEEE Transactions on Communications* 22(9): 1199–1205.
- Bello PA (1963) Characterization of randomly time-variant linear channels. *IEEE Transactions on Communications Systems* 11(4): 360–393.
- Bello PA (1965) Selective fading limitations of the Kathryn modem and some system design considerations. *IEEE Transactions on Communication Technology* 13(3): 320–333.
- Berens F, Dimitrov E, Kaiser T, Anttonen A, Krause A & Weir A (2007) The PULSER II view towards very high data rate OFDM based UWB systems. *Proc. IST Mobile and Wireless Communications Summit*, Budapest, Hungary.
- Bertoni HL (ed) (1988) Coverage prediction for mobile radio systems operating in the 800/900 MHz frequency range. *IEEE Transactions on Vehicular Technology* 37(1): 3–72.
- Biglieri E, Caire G & Taricco G (2000) CDMA system design through asymptotic analysis. *IEEE Transactions on Communications* 48(11): 1882–1896.
- Bingham JAC (1990) Multicarrier modulation for data transmission: An idea whose time has come. *IEEE Communications Magazine* 28(5): 5–14.
- Braun WR & Dersch U (1991) A physical mobile radio channel model. *IEEE Transactions on Vehicular Technology* 40(2): 472–482.
- Bray WJ, Lillcrap HG & Owen FC (1947) The fading machine, and its use for the investigation of the effects of frequency-selective fading. *Journal of Institution of Electrical Engineers, Part IIIA* 94(12): 283–297.
- Bultitude RJC & Bedal GK (1989) Propagation characteristics on microcellular urban mobile radio channels at 910 MHz. *IEEE Journal on Selected Areas in Communications* 7(1): 31–39.
- Busgang JJ, Getchell EH, Goldberg B & Mahoney PF (1976) Stored channel simulation of tactical VHF radio links. *IEEE Transactions on Communications* 24(2): 154–163.
- Byers GJ & Takawira F (2004) Spatially and temporally correlated MIMO channels: Modeling and capacity analysis. *IEEE Transactions on Vehicular Technology* 53(3): 634–643.
- Cacciapuoti AS, Gelli G & Verde F (2007) FIR zero-forcing multiuser detection and code designs for downlink MC-CDMA. *IEEE Transactions on Signal Processing* 55(10): 4737–4751.

- Caples EL, Massad KE & Minor TR (1980) A UHF channel simulator for digital mobile radio. *IEEE Transactions on Vehicular Technology* 29(2): 281–289.
- Casas E & Leung C (1990) A simple digital fading simulator for mobile radio. *IEEE Transactions on Vehicular Technology* 39(3): 205–212.
- Chang RW (1966) Synthesis of band-limited orthogonal signals for multichannel data transmission. *Bell System Technical Journal* 45(12): 1775–1796.
- Chang RW & Gibby RA (1968) A theoretical study of performance of an orthogonal multiplexing data transmission scheme. *IEEE Transactions on Communication Technology* 16(4): 529–540.
- Chapin EW & Roberts WK (1966) A radio propagation and fading simulator using radio-frequency acoustic waves in a liquid. *Proceedings of the IEEE* 54(8): 1072.
- Chen HH, Yeh JF & Suehiro N (2001) A multicarrier CDMA architecture based on orthogonal complementary codes for new generations of wideband wireless communications. *IEEE Communications Magazine* 39(10): 126–135.
- Chen TA, Fitz MP, Kuo WY, Zoltowski MD & Grimm JH (2000) A space-time model for frequency nonselective rayleigh fading channels with applications to space-time modems. *IEEE Journal on Selected Areas in Communications* 18(7): 1175–1190.
- Chen Y & Dubey VK (2005) Parabolic distribution of scatterers for street-dominated mobile environments. *IEEE Transactions on Vehicular Technology* 54(1): 1–8.
- Chizhik D, Foschini GJ, Gans MJ & Valenzuela RA (2002) Keyholes, correlations, and capacities of multielement transmit and receive antennas. *IEEE Transactions on Wireless Communications* 1(2): 361–368.
- Chizhik D, Ling J, Wolniansky PW, Valenzuela RA, Costa N & Huber K (2003) Multiple-input-multiple-output measurements and modeling in Manhattan. *IEEE Journal on Selected Areas in Communications* 21(3): 321–331.
- Cho K & Yoon D (2002) On the general BER expression of one- and two-dimensional amplitude modulations. *IEEE Transactions on Communications* 50(7): 1074–1080.
- Choi BJ & Hanzo L (2003) Crest factors of complementary-sequence-based multicode MC-CDMA signals. *IEEE Transactions on Wireless Communications* 2(6): 1114–1119.
- Choi BJ, Kuan EL & Hanzo L (1999) Crest-factor study of MC-CDMA and OFDM. *Proc. IEEE Vehicular Technology Conference, Amsterdam, Netherlands*, 1: 233–237.
- Choi BJ, Tellambura C & Hanzo L (2002) Crest factors of Shapiro-Rudin sequence based multi-code MC-CDMA signals. *Proc. IEEE Vehicular Technology Conference, Birmingham, USA*, 3: 1472–1476.
- Chong CC, Tan CM, Laurenson DI, McLaughlin S, Beach MA & Nix AR (2003) A new statistical wideband spatio-temporal channel model for 5-GHz band WLAN systems. *IEEE Journal on Selected Areas in Communications* 21(2): 139–150.
- Chouly A, Brajal A & Jourdan S (1993) Orthogonal multicarrier techniques applied to direct sequence spread spectrum CDMA systems. *Proc. IEEE Global Telecommunication Conference, Houston, USA*, 3: 1723–1728.
- Clarke RH (1968) A statistical theory of mobile-radio reception. *Bell System Technical Journal* 47(6): 957–1000.
- Clarke RH & Khoo WL (1997) 3-D mobile radio channel statistics. *IEEE Transactions on Vehicular Technology* 46(3): 798–799.
- Cohn M & Lempel A (1977) On fast m-sequence transforms. *IEEE Transactions on Information Theory* 23(1): 135–137.

- Correia LM (ed) (2001) *Wireless Flexible Personalised Communications*. COST 259 final report. John Wiley & Sons, Chichester, UK.
- Correia LM (ed) (2006) *Mobile Broadband Multimedia Networks*. COST 273 final report. Academic Press, Oxford, UK.
- Cosovic I, Schnell M & Springer A (2005) Combined equalization for uplink MC-CDMA in Rayleigh fading channels. *IEEE Transactions on Communications* 53(10): 1609–1614.
- Coulson AJ, Williamson AG & Vaughan RG (1998a) Improved fading distribution for mobile radio. *IEE Proceedings Communications* 145(3): 197–202.
- Coulson AJ, Williamson AG & Vaughan RG (1998b) A statistical basis for lognormal shadowing effects in multipath fading channels. *IEEE Transactions on Communications* 46(4): 494–502.
- Cox DC (1971) Doppler spectrum measurements at 910 MHz over a suburban mobile radio path. *Proceedings of the IEEE* 59(6): 1017–1018.
- Cox DC (1972) Delay Doppler characteristics of multipath propagation at 910 MHz in a suburban mobile radio environment. *IEEE Transactions on Antennas and Propagation* 20(5): 625–635.
- Cox DC, Murray RR, Arnold HW, Norris AW & Wazowicz MF (1986) Cross-polarization coupling measured for 800 MHz radio transmission in and around houses and large buildings. *IEEE Transactions on Antennas and Propagation* 34(1): 83–87.
- Crespo PM & Jiménez J (1995) Computer simulation of radio channels using a harmonic decomposition technique. *IEEE Transactions on Vehicular Technology* 44(3): 414–419.
- Czink N, Yin X, Özcelik H, Herdin M, Bonek E & Fleury BH (2007) Cluster characterization in a MIMO indoor propagation environment. *IEEE Transactions on Wireless Communications* 6(4): 1465–1475.
- Damosso E & Correia LM (eds) (1999) *Digital Mobile Radio Towards Future Generation Systems*. COST 231 final report. Office for Official Publications of the European Communities, Luxembourg.
- DaSilva V & Sousa ES (1993) Performance of orthogonal CDMA codes for quasi-synchronous communication systems. *Proc. IEEE International Conference on Universal Personal Communications*, Ottawa, Canada, 2: 995–999.
- DaSilva V & Sousa ES (1994) Multicarrier orthogonal CDMA signals for quasi-synchronous communication systems. *IEEE Journal on Selected Areas in Communications* 12(5): 842–852.
- Dent P, Bottomley GE & Croft T (1993) Jakes fading model revisited. *Electronics Letters* 29(13): 1162–1163.
- Doelz ML, Heald ET & Martin DL (1957) Binary data transmission techniques for linear systems. *Proceedings of the IRE* 45(5): 656–661.
- Doi K, Matsumura T, Mizutani K & Kohno R (2003) Ultra wideband ranging system using improved chirp waveform. *Proc. IEEE Radio and Wireless Conference*, Boston, USA, 207–210.
- Doi N, Yano T & Kobayashi N (1994) DS/CDMA prototype system transmitting low bit-rate voice and high bit-rate ISDN signals. *Proc. IEEE Vehicular Technology Conference*, Stockholm, Sweden, 1: 51–55.
- Donelan H & O'Farrel T (1999) Method for generating sets of orthogonal sequences. *Electronics Letters* 35(18): 1537–1538.
- Dowla F & Nekoogar F (2003) Multiple access in ultra-wideband communications using multiple pulses and the use of least squares filters. *Proc. IEEE Radio and Wireless Conference*, Boston, USA, 211–214.

- Duan Z, Valkama M & Renfors M (2005) Turbo multiuser detection for LDPC coded MC-CDMA systems. Proc. IEEE International Symposium on Personal, Indoor and Mobile Radio Communications, Berlin, Germany, 1: 262–265.
- Ecma International (2005) High rate ultra wideband PHY and MAC standard. ECMA-368.
- Eggers PCF, Toftgård J & Oprea AM (1993) Antenna systems for base station diversity in urban small and micro cells. IEEE Journal on Selected Areas in Communications 11(7): 1046–1057.
- Egli JJ (1957) Radio propagation above 40 mc over irregular terrain. Proceedings of the IRE 45(10): 1383–1391.
- Ertel RB & Reed JH (1999) Angle and time of arrival statistics for circular and elliptical scattering models. IEEE Journal on Selected Areas in Communications 17(11): 1829–1840.
- Failli M (ed) (1989) Digital Land Mobile Radio Communications. COST 207 final report. Office for Official Publications of the European Communities, Luxembourg.
- Fan M, Hoffmann C & Siu KY (2003) Error-rate analysis for multirate DS-SS transmission schemes. IEEE Transactions on Communications 51(11): 1897–1909.
- Fan P (2004) Spreading sequence design and theoretical limits for quasisynchronous CDMA systems. EURASIP Journal on Wireless Communications and Networking 2004(1): 19–31.
- Farkas P & Turcsany M (2004) On spreading efficiency of complementary codes. Proc. Joint IST Workshop on Mobile Future and the Symposium on Trends in Communications, Bratislava, Slovakia, 95–97.
- Fazel K (1993) Performance of CDMA/OFDM for mobile communication system. Proc. IEEE International Conference on Universal Personal Communications, Ottawa, Canada, 975–979.
- Fazel K & Papke L (1993) On the performance of convolutionally-coded CDMA/OFDM for mobile communication system. Proc. IEEE International Symposium on Personal, Indoor and Mobile Radio Communications, Yokohama, Japan, 468–472.
- Fechtel SA (1993) A novel approach to modeling and efficient simulation of frequency-selective fading radio channels. IEEE Journal on Selected Areas in Communications 11(3): 422–431.
- Fitting RC (1967) Wideband troposcatter radio channel simulator. IEEE Transactions on Communication Technology 15(4): 565–570.
- Fleury BH (2000) First- and second-order characterization of direction dispersion and space selectivity in the radio channel. IEEE Transactions on Information Theory 46(6): 2027–2044.
- Foerster JR (2002) The performance of a direct-sequence spread ultra-wideband system in the presence of multipath, narrowband interference, and multiuser interference. Proc. IEEE Conference on Ultra Wideband Systems and Technologies, Baltimore, USA, 87–91.
- Franco GA & Lachs G (1961) An orthogonal coding technique for communications. Proc. IRE International Convention, New York, USA, 9: 126–133.
- Freudberg R (1965) A laboratory simulator for frequency selective fading. Proc. IEEE Communications Convention, Boulder, USA, 609–614.
- Fu H & Mark JW (2003) Uplink performance of asynchronous multicode multicarrier CDMA systems. Proc. IEEE International Symposium on Personal, Indoor and Mobile Radio Communications, Beijing, China, 3: 2343–2347.
- Fuhl J, Rossi JP & Bonek E (1997) High-resolution 3-d direction-of-arrival determination for urban mobile radio. IEEE Transactions on Antennas and Propagation 45(4): 672–682.
- Ganesh R & Pahlavan K (1991) Statistical modelling and computer simulation of indoor radio channel. IEE Proceedings Part I. Communications, Speech and Vision 138(3): 153–161.
- Gans MJ (1972) A power-spectral theory of propagation in the mobile-radio environment. IEEE Transactions on Vehicular Technology 21(1): 27–38.

- Gerakoulis D & Ghassemzadeh S (2000) Extended orthogonal code designs with applications in CDMA. *Proc. IEEE International Symposium on Spread Spectrum Techniques and Applications*, Parsippany, USA, 2: 657–661.
- Gerakoulis D & Salmi P (2002) An interference suppressing OFDM system for ultra wide bandwidth radio channels. *Proc. IEEE Conference on Ultra Wideband Systems and Technologies*, Baltimore, USA, 259–264.
- Geramita AV (1979) *Orthogonal Designs: Quadratic Forms and Hadamard Matrices*. Dekker, New York.
- Gerrits JFM, Kouwenhoven MHL, Meer PR van der, Farserotu JR & Long JR (2005) Principles and limitations of ultra-wideband FM communications systems. *EURASIP Journal on Applied Signal Processing* 2005(3): 382–396.
- Gesbert D, Bölcskei H, Gore DA & Paulraj AJ (2002) Outdoor MIMO wireless channels: Models and performance prediction. *IEEE Transactions on Communications* 50(12): 1926–1934.
- Giannakis GB, Wang Z, Scaglione A & Barbarossa S (2000) AMOUR — Generalized multicarrier transceivers for blind CDMA regardless of multipath. *IEEE Transactions on Communications* 48(12): 2064–2076.
- Gilbert EN (1965) Energy reception for mobile radio. *Bell System Technical Journal* 44(8): 1779–1803.
- Glazunov AA, Asplund H & Berg JE (1999) Statistical analysis of measured short-term impulse response functions of 1.88 GHz radio channels in Stockholm with corresponding channel model. *Proc. IEEE Vehicular Technology Conference*, Amsterdam, Netherlands, 1: 107–111.
- Golay MJE (1961) Complementary series. *IRE Transactions on Information Theory* 7(2): 82–87.
- Gold R (1967) Optimal binary sequences for spread spectrum multiplexing. *IEEE Transactions on Information Theory* 13(4): 619–621.
- Goldberg B, Heyd RL & Pochmerski D (1965) Stored ionosphere. *Proc. IEEE Communications Convention*, Boulder, USA, 619–622.
- Gong P, Xue P, Lee JS & Kim DK (2006) Performance enhancement of an MB-OFDM based UWB system in multiple SOPs environments. *Proc. International Symposium on Wireless Pervasive Computing*, Phuket, Thailand, 1–4.
- Gu Z, Xie S, Rahardja S, Sze ET & Xin Y (2005) Performance comparison of spreading sequences in synchronous mc-cdma systems. *Proc. IEEE International Conference on Information, Communications and Signal Processing*, Bangkok, Thailand, 633–637.
- Gui X & Ng TS (1999) Performance of asynchronous orthogonal multicarrier CDMA system in frequency selective fading channel. *IEEE Transactions on Communications* 47(7): 1084–1091.
- Guo Z & Letaief KB (2001) Performance of VSG-CDMA and MC-CDMA in multirate systems. *Proc. IEEE Vehicular Technology Conference*, Rhodes, Greece, 501–505.
- Haas R & Belfiore JC (1994) Multiple carrier transmission with time-frequency well-localized impulses. *Proc. IEEE Symposium on Communications and Vehicular Technology in the Benelux*, Louvain-la-Neuve, Belgium, 187–193.
- Hämäläinen M (2006) Singleband UWB systems. Analysis and measurements of coexistence with selected existing radio systems. Ph.D. thesis, University of Oulu, Oulu.
- Han SH (2005) An overview of peak-to-average power ratio reduction techniques for multicarrier transmission. *IEEE Transactions on Wireless Communications* 12(2): 56–65.
- Hansen J (2003) An analytical calculation of power delay profile and delay spread with experimental verification. *IEEE Communications Letters* 7(6): 257–259.

- Hara S & Prasad R (1997) Overview of multicarrier CDMA. *IEEE Communications Magazine* 35(12): 126–133.
- Hara S & Prasad R (1999) Design and performance of multicarrier CDMA system in frequency-selective Rayleigh fading channels. *IEEE Transactions on Vehicular Technology* 48(5): 1584–1595.
- Harmuth HF (1960) On the transmission of information by orthogonal time functions. *Transactions of the AIEE Part I. Communication and Electronics* 79: 248–255.
- Hashemi H (1979) Simulation of the urban radio propagation channel. *IEEE Transactions on Vehicular Technology* 28(3): 213–225.
- Hassan-Ali M & Pahlavan K (1997) Site-specific wideband indoor channel modelling using ray-tracing software. *Electronics Letters* 33(23): 1983–1984.
- Hélar JF, Baudais JY & Citerne J (2000) Linear MMSE detection techniques for MC-CDMA. *Electronics Letters* 36(7): 665–666.
- Hiertz GR, Zang Y, Habetha J & Sirin H (2005) Multiband OFDM alliance — The next generation of wireless personal area networks. *Proc. IEEE Sarnoff Symposium on Advances in Wired and Wireless Communication, Princeton, USA*, 208–214.
- Hirosaki B (1980) An analysis of automatic equalizers for orthogonally multiplexed QAM systems. *IEEE Transactions on Communications* 28(1): 73–83.
- Hirosaki B (1981) An orthogonally multiplexed QAM system using the discrete Fourier transform. *IEEE Transactions on Communications* 29(7): 982–989.
- Howard SJ & Pahlavan K (1992) Autoregressive modeling of wide-band indoor radio propagation. *IEEE Transactions on Communications* 40(9): 1540–1552.
- Hoyt RS (1947) Probability functions for the modulus and angle of the normal complex variate. *Bell System Technical Journal* 26(2): 318–359.
- Hu X & Chew YH (2004) On the capacity of multicode and variable spreading gain multirate space-time block coded multicarrier CDMA systems over frequency selective Rayleigh fading channels. *Proc. IEEE Vehicular Technology Conference, Los Angeles, USA*, 1: 353–357.
- Hülsmeier C (1906) Wireless transmitting and receiving mechanism for electric waves. US patent 810.150.
- Ihalainen T, Stütz TH, Rinne M & Renfors M (2007) Channel equalization in filter bank based multicarrier modulation for wireless communications. *EURASIP Journal on Applied Signal Processing* 2007(49389): 1–18.
- Iltis RA (1997) Decorrelator detection for quasi-synchronous multicarrier CDMA. *Proc. IEEE Military Communications Conference, Monterey, USA*, 2: 862–866.
- Jakes WC (1974) *Microwave Mobile Communications*. John Wiley & Sons, New York.
- Johansson AL (1999) Group-wise successive interference cancellation in multirate CDMA systems. *Proc. IEEE Vehicular Technology Conference, Houston, USA*, 2: 1435–1439.
- Kailath T (1963) Time-variant communication channels. *IEEE Transactions on Information Theory* 9(4): 233–237.
- Kaiser S & Fazel K (1997) A flexible spread-spectrum multi-carrier multiple-access system for multi-media applications. *Proc. IEEE International Symposium on Personal, Indoor and Mobile Radio Communications, Helsinki, Finland*, 1: 100–104.
- Kalkan M & Clarke RH (1997) Prediction of the space-frequency correlation function for base station diversity reception. *IEEE Transactions on Vehicular Technology* 46(1): 176–184.

- Kalliola K, Laitinen H, Vainikainen P, Toeltsch M, Laurila J & Bonek E (2003) 3-D double-directional radio channel characterization for urban macrocellular applications. *IEEE Transactions on Antennas and Propagation* 51(11): 3122–3133.
- Kalliola K, Sulonen K, Laitinen H, Kivekäs O, Krogerus J & Vainikainen P (2002) Angular power distribution and mean effective gain of mobile antenna in different propagation environments. *IEEE Transactions on Vehicular Technology* 51(5): 823–838.
- Kalofonos DN, Stojanovic M & Proakis JG (2003) Performance of adaptive MC-CDMA detectors in rapidly fading Rayleigh channels. *IEEE Transactions on Wireless Communications* 2(2): 229–239.
- Kermoal JP, Schumacher L, Pedersen KI, Mogensen PE & Frederiksen F (2002) A stochastic MIMO radio channel model with experimental validation. *IEEE Journal on Selected Areas in Communications* 20(6): 1211–1226.
- Kim ST, Yoo JH & Park HK (1999) A spatially and temporally correlated fading model for array antenna applications. *IEEE Transactions on Vehicular Technology* 48(6): 1899–1905.
- Kivinen J, Zhao X & Vainikainen P (2001) Empirical characterization of wideband indoor radio channel at 5.3 GHz. *IEEE Transactions on Antennas and Propagation* 49(8): 1192–1203.
- Klingenbrunn T & Mogensen P (1999) Modelling frequency correlation of fast fading in frequency hopping GSM link simulations. *Proc. IEEE Vehicular Technology Conference, Amsterdam, Netherlands*, 4: 2398–2402.
- Kolu J & Jämsä T (2002) A real-time simulator for MIMO radio channels. *Proc. International Symposium on Wireless Personal Multimedia Communications, Honolulu, USA*, 2: 568–572.
- Kondo S & Milstein LB (1993) On the use of multicarrier direct sequence spread spectrum systems. *Proc. IEEE Military Communications Conference, Boston, USA*, 1: 52–56.
- Kondo S & Milstein LB (1996) Performance of multicarrier DS CDMA systems. *IEEE Transactions on Communications* 44(2): 238–246.
- Kotowski P & Dannehl K (1940) Method of transmitting secret messages. US patent 2.211.132.
- Kozono S, Tsuruhara T & Sakamoto M (1984) Base station polarization diversity reception for mobile radio. *IEEE Transactions on Vehicular Technology* 33(4): 301–306.
- Krulic R (1963) Design of a fading simulator. *Proc. IRE National Communications Symposium, Utica, USA*.
- Kuchar A, Rossi JP & Bonek E (2000) Directional macro-cell channel characterization from urban measurements. *IEEE Transactions on Antennas and Propagation* 48(2): 137–146.
- Kunnari E (2000) Space-time coded transmit diversity techniques for wideband CDMA systems. Master's thesis, University of Oulu, Oulu, Finland.
- Kunnari E (2002) Space-time coding combined with phase sweeping transmit diversity. *Proc. IEEE Global Telecommunication Conference, Taipei, Taiwan*, 2: 1920–1924.
- Kunnari E (2003a) Modeling and simulation of Rice fading with temporal, spatial and spectral correlation — Part I: Characterization of fading. *Proc. URSI National Convention on Radio Science & Finnish Wireless Communication Workshop, Oulu, Finland*, 102–105.
- Kunnari E (2003b) Modeling and simulation of Rice fading with temporal, spatial and spectral correlation — Part II: Structure of fading simulator. *Proc. URSI National Convention on Radio Science & Finnish Wireless Communication Workshop, Oulu, Finland*, 106–109.
- Kunnari E & Tujkovic D (2001a) Convolutionally coded multi-antenna transmission in WCDMA over frequency-selective Rayleigh fading channel. *Proc. IEEE Vehicular Technology Conference, Rhodes, Greece*, 1: 127–131.

- Kunnari E & Tujkovic D (2001b) Performance evaluation of space-time codes in wideband CDMA over frequency-selective Rayleigh fading downlink channel. Proc. IEEE International Conference on Communications, Helsinki, Finland, 10: 3046–3050.
- Lacy RE (1947) Two multichannel microwave relay equipments for the United States Army communication network. Proceedings of the IRE 35(1): 65–70.
- Laurila J, Kalliola K, Toeltsch M, Hugel K, Vainikainen P & Bonek E (2002) Wide-band 3-D characterization of mobile radio channels in urban environments. IEEE Transactions on Antennas and Propagation 50(2): 233–243.
- Le Floch B, Alard M & Berrou C (1995) Coded orthogonal frequency division multiplex. Proceedings of the IEEE 83(6): 982–996.
- Lee WCY (1969) An extended correlation function of two random variables applied to mobile radio transmission. Bell System Technical Journal 48(10): 3423–3440.
- Lee WCY (1970) Level crossing rates of an equal-gain predetection diversity combiner. IEEE Transactions on Communication Technology 18(4): 417–426.
- Lee WCY (1971) Antenna spacing requirement for a mobile radio base-station diversity. Bell System Technical Journal 50(6): 1859–1876.
- Lee WCY (1973) Effects on correlation between two mobile radio base-station antennas. IEEE Transactions on Communications 21(11): 1214–1224.
- Lee WCY & Brandt RH (1973) The elevation angle of mobile radio signal arrival. IEEE Transactions on Communications 21(11): 1194–1197.
- Lee WCY & Yeh YS (1972) Polarization diversity system for mobile radio. IEEE Transactions on Communications 20(5): 912–923.
- Lestable T, Husson L, Antoine J & Wautier A (2002) Performance of adaptive MC-CDMA in HiperLAN/2++. Proc. IEEE Vehicular Technology Conference, Vancouver, Canada, 2: 1091–1095.
- Li Z & Latva-aho M (2002) BER performance evaluation for MC-CDMA systems in Nakagami-m fading. Electronics Letters 38(24): 1516–1518.
- Li Z & Latva-aho M (2005) Error probability of interleaved MC-CDMA systems with MRC receiver and correlated Nakagami-m fading channels. IEEE Transactions on Communications 53(6): 919–923.
- Li Z & Latva-aho M (2006) Nonblind and semiblind space-frequency multiuser detection for multirate MC-CDMA systems. IEEE Transactions on Signal Processing 54(11): 4393–4404.
- Liberti JC & Rappaport TS (1996) A geometrically based model for line-of-sight multipath radio channels. Proc. IEEE Vehicular Technology Conference, Atlanta, USA, 2: 844–848.
- Lim KS & Lee JH (2001) Performance of multirate transmission schemes for a multicarrier DS/CDMA system. Proc. IEEE Vehicular Technology Conference, Atlantic City, USA, 2: 767–771.
- Linnartz JPMG (2001) Performance analysis of synchronous MC-CDMA in mobile Rayleigh channel with both delay and Doppler spreads. IEEE Transactions on Vehicular Technology 50(6): 1375–1387.
- Liu R, Chester EG & Sharif BS (2004) Performance of asynchronous multicarrier CDMA multiuser receiver over frequency selective multipath fading channels. Electronics Letters 40(1): 48–49.
- Lo T & Litva J (1992) Angles of arrival of indoor multipath. Electronics Letters 28(18): 1687–1689.

- Lok TM, Wong TF & Lehnert JS (1999) Blind adaptive signal reception for MC-CDMA systems in Rayleigh fading channels. *IEEE Transactions on Communications* 47(3): 464–471.
- Matsumoto A, Miyoshi K, Uesugi M & Kato O (2002) A study on time domain spreading for OFCDM. *Proc. International Symposium on Wireless Personal Multimedia Communications, Honolulu, USA, 2*: 725–728.
- McNamara DP, Beach MA & Fletcher PN (2002) Spatial correlation in indoor MIMO channels. *Proc. IEEE International Symposium on Personal, Indoor and Mobile Radio Communications, Lisboa, Portugal, 1*: 290–294.
- McTiffin MJ, Hulbert AP, Ketsoglou TJ, Heimsch W & Crisp G (1994) Mobile access to an ATM network using a CDMA air interface. *IEEE Journal on Selected Areas in Communications* 12(5): 900–908.
- Mitra U (1999) Comparison of maximum-likelihood-based detection for two multirate access schemes for CDMA signals. *IEEE Transactions on Communications* 47(1): 64–77.
- Morgan BJT (1984) *Elements of Simulation*. Chapman & Hall, London.
- Mourad AM, Guéguen A & Pyndiah R (2004) MAI analysis for forward link mono-dimensionally spread OFDM systems. *Proc. IEEE Vehicular Technology Conference, Milan, Italy, 3*: 1528–1533.
- Mucchi L, Tesi R, Tujkovic D & Kunnari E (2002) Space-time coded transmit diversity in multi-satellite UMTS. *Proc. International Symposium on Wireless Personal Multimedia Communications, Honolulu, USA, 2*: 696–700.
- Müller T, Rohling H & Grünheid R (1995) Comparison of different detection algorithms for OFDM-CDMA in broadband Rayleigh fading. *Proc. IEEE Vehicular Technology Conference, Chicago, USA, 2*: 835–838.
- Muquet B, Wang Z, Giannakis GB, de Courville M & Duhamel P (2002) Cyclic prefixing or zero padding for wireless multicarrier transmissions. *IEEE Transactions on Communications* 50(12): 2136–2148.
- Nakagami M (1960) The m -distribution — A general formula of intensity distribution of rapid fading. In: Hoffman WG (ed) *Statistical Methods in Radio Wave Propagation*, 3–36. Pergamon Press, Oxford.
- Narasimhan R & Cox DC (1999) A generalized Doppler power spectrum for wireless environments. *IEEE Communications Letters* 3(6): 164–165.
- Nasri A, Schober R & Lampe L (2007) Analysis of narrowband communication systems impaired by MB-OFDM UWB interference. *IEEE Transactions on Wireless Communications* 6(11): 4090–4100.
- Natarajan B, Wu Z, Nassar CR & Shattil S (2004) Large set of CI spreading codes for high-capacity MC-CDMA. *IEEE Transactions on Communications* 52(11): 1862–1866.
- Nee R van & Prasad R (2000) *OFDM Wireless Multimedia Communications*. Artech House, London.
- Nguyen TT & Lampe L (2006) On partial transmit sequences to reduce PAR in OFDM systems. *Proc. IEEE Global Telecommunication Conference, San Francisco, USA*.
- Nguyen TT & Lampe L (2007) On trellis shaping for PAR reduction in OFDM systems. *IEEE Transactions on Communications* 55(9): 1678–1682.
- Nikookar H & Hashemi H (2000) Phase modeling of indoor radio propagation channels. *IEEE Transactions on Vehicular Technology* 49(2): 594–606.

- Nobilet S, Helard JF & Mottier D (2001) Spreading sequences selection for uplink and downlink MC-CDMA systems. Proc. International Workshop on Multi-Carrier Spread-Spectrum, Oberpfaffenhofen, Germany, 123–130.
- Nørklit O & Andersen JB (1998) Diffuse channel model and experimental results for array antennas in mobile environments. *IEEE Transactions on Antennas and Propagation* 46(6): 834–840.
- Ossanna JF Jr (1964) A model for mobile radio fading due to building reflections: Theoretical and experimental fading waveform power spectra. *Bell System Technical Journal* 43(6): 2935–2971.
- Ottosson T & Svensson A (1995) Multi-rate schemes in DS/CDMA systems. Proc. IEEE Vehicular Technology Conference, Chicago, USA, 2: 1006–1010.
- Özcelik H, Herdin M, Weichselberger W, Wallace J & Bonek E (2003) Deficiencies of 'Kronecker' MIMO radio channel model. *Electronics Letters* 39(16): 1209–1210.
- Pajusco P (2003) Double characterisations of power angular spectrum in macro-cell environments. *Electronics Letters* 39(22): 1965–1966.
- Panday N & Natarajan B (2007) Impact of error weight distribution in MB-OFDM based UWB system with spreading. Proc. International Symposium on Wireless Pervasive Computing, San Juan, Puerto Rico, 115–119.
- Park YB, Kim CS, Cho KK, Lee CJ, Lee HK, Kim JM & Kwak KS (2004) Performance of UWB DS-CDMA/OFDM/MC-CDMA system. Proc. IEEE International Midwest Symposium on Circuits and Systems, Hiroshima, Japan, 1: 37–40.
- Parsons JD (1992) *The Mobile Radio Propagation Channel*. Pentech Press, London.
- Parsons JD & Turkmani AMD (1991) Characterisation of mobile radio signals: Model description. *IEE Proceedings Part I. Communications, Speech and Vision* 138(6): 549–556.
- Pätzold M, García R & Laue F (2000) Design of high-speed simulation models for mobile fading channels by using table look-up techniques. *IEEE Transactions on Vehicular Technology* 49(4): 1178–1190.
- Pätzold M, Killat U, Laue F & Li Y (1998) On the statistical properties of deterministic simulation models for mobile fading channels. *IEEE Transactions on Vehicular Technology* 47(1): 254–269.
- Pedersen KI, Andersen JB, Kermoal JP & Mogensen PE (2000a) A stochastic multiple-input-multiple-output radio channel model for evaluation of space-time coding algorithms. Proc. IEEE Vehicular Technology Conference, Boston, USA, 2: 893–897.
- Pedersen KI, Mogensen PE & Fleury BH (1997) Power azimuth spectrum in outdoor environments. *Electronics Letters* 33(18): 1583–1584.
- Pedersen KI, Mogensen PE & Fleury BH (1998) Spatial channel characteristics in outdoor environments and their impact on BS antenna system performance. Proc. IEEE Vehicular Technology Conference, Ottawa, Canada, 2: 719–723.
- Pedersen KI, Mogensen PE & Fleury BH (2000b) A stochastic model of the temporal and azimuthal dispersion seen at the base station in outdoor propagation environments. *IEEE Transactions on Vehicular Technology* 49(2): 437–447.
- Peng X, Png KB & Chin F (2006) Performance improvement of chip interleaved scheme for MB-OFDM system for 480 Mbps. Proc. IEEE Vehicular Technology Conference, Melbourne, Australia, 3: 1161–1165.
- Pickholtz RL, Milstein LB & Schilling DL (1991) Spread spectrum for mobile communications. *IEEE Transactions on Vehicular Technology* 40(2): 313–322.

- Pickholtz RL, Schilling DL & Milstein LB (1982) Theory of spread-spectrum communications — A tutorial. *IEEE Transactions on Communications* 30(5): 855–884.
- Pierce JA (1946) An introduction to Loran. *Proceedings of the IRE* 34(5): 216–234.
- Pierce JR & Hopper AL (1952) Nonsynchronous time division with holding and with random sampling. *Proceedings of the IRE* 40(9): 1079–1088.
- Pop MF & Beaulieu NC (2001) Limitations of sum-of-sinusoids fading channel simulators. *IEEE Transactions on Communications* 49(4): 699–708.
- Popescu DC & Yaddanapudi P (2006) A simulation study of interference suppressing OFDM for UWB systems with multiple users. *Proc. IEEE Radio and Wireless Symposium, San Diego, USA*, 359–362.
- Popović BM (1997) Efficient despanders for multi-code CDMA systems. *Proc. IEEE International Conference on Universal Personal Communications, San Diego, USA*, 2: 516–520.
- Popović BM (1999) Spreading sequences for multicarrier CDMA systems. *IEEE Transactions on Communications* 47(6): 918–926.
- Porter GC (1968) Error distribution and diversity performance of a frequency-differential PSK HF modem. *IEEE Transactions on Communication Technology* 16(4): 567–575.
- Powers EN & Zimmerman MS (1968) TADIM — A digital implementation of a multichannel data modem. *Proc. IEEE International Conference on Communications, Philadelphia, USA*, 706–711.
- Price R (1983) Further notes and anecdotes on spread-spectrum origins. *IEEE Transactions on Communications* 31(1): 85–97.
- Price R & Green PE (1958) A communication technique for multipath channels. *Proceedings of the IRE* 46(3): 555–570.
- Proakis JG (1995) *Digital Communications*. McGraw-Hill, New York, third edition.
- Qu S & Yeap T (1999) A three-dimensional scattering model for fading channels in land mobile environment. *IEEE Transactions on Vehicular Technology* 48(3): 765–781.
- Ramachandran I, Nakache YP, Orlik P, Molisch AF & Zhang J (2004) Symbol spreading for ultrawideband systems based on multiband OFDM. *Proc. IEEE International Symposium on Personal, Indoor and Mobile Radio Communications, Barcelona, Spain*, 2: 1204–1209.
- Rappaport TS, Seidel SY & Takamizawa K (1991) Statistical channel impulse response models for factory and open plan building radio communication system design. *IEEE Transactions on Communications* 39(5): 794–807.
- Rayleigh JWS (1880) On the resultant of a large number of vibrations of the same pitch and of arbitrary phase. *Philosophical Magazine, Series V* 10(60): 73–78.
- Renfors M, Xing H, Viholainen A & Rinne J (1999) On channel equalization in filter bank based multicarrier wireless access systems. *Proc. IEEE Vehicular Technology Conference, Amsterdam, Netherlands*, 1: 228–232.
- Rhee SB & Zysman GI (1974) Results of suburban base station spatial diversity measurements in the UHF band. *IEEE Transactions on Communications* 22(10): 1630–1636.
- Rice SO (1944) Mathematical analysis of random noise. *Bell System Technical Journal* 23(3): 282–332.
- Rice SO (1945) Mathematical analysis of random noise (concluded). *Bell System Technical Journal* 24(1): 46–156.
- Rice SO (1948) Statistical properties of a sine wave plus random noise. *Bell System Technical Journal* 27(1): 109–157.

- Ross GF (1973) Transmission and reception system for generating and receiving base-band duration pulse signals without distortion for short base-band pulse communication system. US patent 3.728.632.
- Rowitch DN & Milstein LB (1999a) Convolutionally coded multicarrier DS-CDMA systems in a multipath fading channel — Part I: Performance analysis. *IEEE Transactions on Communications* 47(10): 1570–1582.
- Rowitch DN & Milstein LB (1999b) Convolutionally coded multicarrier DS-CDMA systems in a multipath fading channel — Part II: Narrow-band interference suppression. *IEEE Transactions on Communications* 47(11): 1729–1736.
- Rustako AJ Jr (1967) Evaluation of a mobile radio multiple channel diversity receiver using pre-detection combining. *IEEE Transactions on Vehicular Technology* 16(1): 46–57.
- Saleh AAM & Valenzuela RA (1987) A statistical model for indoor multipath propagation. *IEEE Journal on Selected Areas in Communications* 5(2): 128–137.
- Salo J, El-Sallabi HM & Vainikainen P (2006) Statistical analysis of the multiple scattering radio channel. *IEEE Transactions on Antennas and Propagation* 54(11): 3114–3124.
- Saltzberg BR (1967) Performance of an efficient parallel data transmission system. *IEEE Transactions on Communication Technology* 15(6): 805–811.
- Salz J & Winters JH (1994) Effect of fading correlation on adaptive arrays in digital mobile radio. *IEEE Transactions on Vehicular Technology* 43(4): 1049–1057.
- Sayeed AM (2002) Deconstructing multiantenna fading channels. *IEEE Transactions on Signal Processing* 50(10): 2563–2579.
- Schilling DL, Nelson EA & Clarke KK (1967) Discriminator response to an FM signal in a fading channel. *IEEE Transactions on Communication Technology* 15(2): 252–263.
- Schmid HF (1970) A prediction model for multipath propagation of pulse signals at VHF and UHF over irregular terrain. *IEEE Transactions on Antennas and Propagation* 18(2): 253–258.
- Schniter P (2004) Low-complexity equalization of OFDM in doubly selective channels. *IEEE Transactions on Signal Processing* 52(4): 1002–1011.
- Scholtz RA (1982) The origins of spread-spectrum communications. *IEEE Transactions on Communications* 30(5): 822–854.
- Scholtz RA (1983) Notes on spread-spectrum history. *IEEE Transactions on Communications* 31(1): 82–84.
- Scholtz RA (1993) Multiple access with time-hopping impulse modulation. *Proc. IEEE Military Communications Conference, Boston, USA, 2: 447–450.*
- Schwartz JW, Aein JM & Kaiser J (1966) Modulation techniques for multiple access to a hard-limiting satellite repeater. *Proceedings of the IEEE* 54(5): 763–777.
- Shafi M, Zhang M, Moustakas AL, Smith PJ, Molisch AF, Tufvesson F & Simon SH (2006) Polarized MIMO channels in 3-D: Models, measurements and mutual information. *IEEE Journal on Selected Areas in Communications* 24(3): 514–527.
- Shepherd NH (1977) Radio wave loss deviation and shadow loss at 900 MHz. *IEEE Transactions on Vehicular Technology* 26(4): 309–313.
- Shi Q & Latva-aho M (2002a) Exact bit error rate calculations for synchronous MC-CDMA over a Rayleigh fading channel. *IEEE Communications Letters* 6(7): 276–278.
- Shi Q & Latva-aho M (2002b) An exact error floor for downlink MC-CDMA in correlated Rayleigh fading channels. *IEEE Communications Letters* 6(5): 196–198.
- Shi Q & Latva-aho M (2003a) Performance analysis of MC-CDMA in Rayleigh fading channels with correlated envelopes and phases. *IEE Proceedings Communications* 150(3): 214–220.

- Shi Q & Latva-aho M (2003b) Spreading sequences for asynchronous MC-CDMA revisited: Accurate bit error rate analysis. *IEEE Transactions on Communications* 51(1): 8–11.
- Shiu DS, Foschini GJ, Gans MJ & Kahn JM (2000) Fading correlation and its effects on the capacity of multielement antenna systems. *IEEE Transactions on Communications* 48(3): 502–513.
- Siohan P, Siclet C & Lacaille N (2002) Analysis and design of OFDM/OQAM systems based on filterbank theory. *IEEE Transactions on Signal Processing* 50(5): 1170–1183.
- Sklar B (1997) Rayleigh fading channels in mobile digital communication systems. Part I: Characterization. *IEEE Communications Magazine* 35(9): 136–146.
- Smida B, Despins CL & Delisle GY (2001) MC-CDMA performance evaluation over a multipath fading channel using the characteristic function method. *IEEE Transactions on Communications* 49(8): 1325–1328.
- Smith DB & Abhayapala TD (2003) Generalised space-time model for Rayleigh fading channels with non-isotropic scatterer distribution. *Electronics Letters* 39(21): 1541–1543.
- Smith JI (1975) A computer generated multipath fading simulation for mobile radio. *IEEE Transactions on Vehicular Technology* 24(3): 39–40.
- Snow C, Lampe L & Schober R (2007) Performance analysis and enhancement of multiband OFDM for UWB communications. *IEEE Transactions on Wireless Communications* 6(6): 2182–2192.
- Sourour EA & Nakagawa M (1996) Performance of orthogonal multicarrier CDMA in a multipath fading channel. *IEEE Transactions on Communications* 44(3): 356–367.
- Spencer QH, Jeffs BD, Jensen MA & Swindlehurst AL (2000) Modeling the statistical time and angle of arrival characteristics of an indoor multipath channel. *IEEE Journal on Selected Areas in Communications* 18(3): 347–360.
- Stein S (1987) Fading channel issues in system engineering. *IEEE Journal on Selected Areas in Communications* 5(2): 68–89.
- Steinbauer M, Molisch AF & Bonek E (2001) The double-directional radio channel. *IEEE Antennas and Propagation Magazine* 43(4): 51–63.
- Stephan A, Baudais JY & H elard JF (2007) Adaptive spread spectrum multicarrier multiple-access for UWB systems. *Proc. IEEE Vehicular Technology Conference, Dublin, Ireland*, 2926–2930.
- Stephane A & Champagne B (2000) Effective multi-path vector channel simulator for antenna array systems. *IEEE Transactions on Vehicular Technology* 49(6): 2370–2381.
- Stidham JR (1966) Experimental study of UHF mobile radio transmission using a directive antenna. *IEEE Transactions on Vehicular Technology* 15(2): 16–24.
- Suehiro N & Hatori M (1988) N-shift cross-orthogonal sequences. *IEEE Transactions on Information Theory* 34(1): 143–146.
- Suwa S, Atarashi H & Sawahashi M (2002) Performance comparison between MC/DS-CDMA and MC-CDMA for reverse link broadband packet wireless access. *Proc. IEEE Vehicular Technology Conference, Vancouver, Canada*, 4: 2076–2080.
- Suzuki H (1977) A statistical model for urban radio propagation. *IEEE Transactions on Communications* 25(7): 673–680.
- Swarts F & Ferreira HC (1993) Markov characterization of channels with soft decision outputs. *IEEE Transactions on Communications* 41(5): 678–682.
- Sylvester JJ (1867) Thoughts on orthogonal matrices, simultaneous sign-successions, and tessellated pavements in two or more colours, with application to Newton’s rule, ornamental tile-work, and the theory of numbers. *Philosophical Magazine, Series IV* 34: 461–475.

- Tachikawa SI (1992) Recent spreading codes for spread spectrum communication systems. *Electronics and Communications in Japan Part I. Communications* 75(6): 41–49.
- Tan M & Bar-Ness Y (2002) Performance comparison of the multi-code fixed spreading length (MFSL) scheme and the variable spreading length (VSL) scheme for multi-rate MC-CDMA. *Proc. IEEE International Symposium on Spread Spectrum Techniques and Applications, Prague, Czech*, 1: 108–112.
- Teal PD, Abhayapala TD & Kennedy RA (2002) Spatial correlation for general distributions of scatterers. *IEEE Signal Processing Letters* 9(10): 305–308.
- Tesla N (1903a) Method of signaling. US patent 723.188.
- Tesla N (1903b) Method of signaling. US patent 725.605.
- Toeltsch M, Laurila J, Kalliola K, Molisch AF, Vainikainen P & Bonek E (2002) Statistical characterization of urban spatial radio channels. *IEEE Journal on Selected Areas in Communications* 20(3): 539–549.
- Toscano A, Bilotti F & Vegni L (2003) Fast ray-tracing technique for electromagnetic field prediction in mobile communications. *IEEE Transactions on Magnetics* 39(3): 1238–1241.
- Tseng CC & Liu CL (1972) Complementary sets of sequences. *IEEE Transactions on Information Theory* 18(5): 644–652.
- Tseng SM & Bell MR (2000) Asynchronous multicarrier DS-CDMA using mutually orthogonal complementary sets of sequences. *IEEE Transactions on Communications* 48(1): 53–59.
- Turin GL, Clapp FD, Johnston TL, Fine SB & Lavry D (1972) A statistical model of urban multipath propagation. *IEEE Transactions on Vehicular Technology* 21(1): 1–9.
- Turkmani AMD, Demery DA & Parsons JD (1991) Measurement and modelling of wideband mobile radio channels at 900 MHz. *IEE Proceedings Part I. Communications, Speech and Vision* 138(5): 447–457.
- Turkmani AMD & Parsons JD (1991) Characterisation of mobile radio signals: Base station crosscorrelation. *IEE Proceedings Part I. Communications, Speech and Vision* 138(6): 557–565.
- Vahlin A & Holte N (1996) Optimal finite duration pulses for OFDM. *IEEE Transactions on Communications* 44(1): 10–14.
- Vandendorpe L (1993) Multitone direct sequence CDMA system in an indoor wireless environment. *Proc. IEEE Symposium on Communications and Vehicular Technology in the Benelux, Delft, Netherlands*, 4.1.1–4.1.8.
- Vandendorpe L (1995) Multitone spread spectrum multiple access communications system in a multipath Rician fading channel. *IEEE Transactions on Vehicular Technology* 44(2): 327–337.
- Vatalaro F & Forcella A (1997) Doppler spectrum in mobile-to-mobile communications in the presence of three-dimensional multipath scattering. *IEEE Transactions on Vehicular Technology* 46(1): 213–219.
- Vaughan RG (1990) Polarization diversity in mobile communications. *IEEE Transactions on Vehicular Technology* 39(3): 177–186.
- Verdin D & Tozer TC (1993) Generating a fading process for the simulation of land-mobile radio communications. *Electronics Letters* 29(23): 2011–2012.
- Verschoor A, Kegel A & Arnbak JC (1988) Hardware fading simulator for a number of narrowband channels with controllable mutual correlation. *Electronics Letters* 24(22): 1367–1369.
- Vetterli M (1987) A theory of multirate filter banks. *IEEE Transactions on Acoustics, Speech, and Signal Processing* 35(3): 356–372.

- Viholainen A, Alhava J, Helenius J, Rinne J & Renfors M (1999) Equalization in filter bank based multicarrier systems. Proc. IEEE International Conference on Electronics, Circuits and Systems, Paphos, Cyprus, 3: 1467–1470.
- Viholainen A, Saramäki T & Renfors M (1998) Cosine-modulated filter bank design for VDSL modems. Proc. IEEE International Symposium on Intelligent Signal Processing and Communication Systems, Melbourne, Australia, 143–147.
- Walsh JL (1923) A closed set of normal orthogonal functions. American Journal of Mathematics 45(1): 5–24.
- Wang HS & Moayeri N (1995) Finite-state Markov channel — A useful model for radio communication channels. IEEE Transactions on Vehicular Technology 44(1): 163–171.
- Wang J & Milstein LB (2004) Multicarrier CDMA overlay for ultra-wideband communications. IEEE Transactions on Communications 52(10): 1664–1669.
- Wang T, Proakis JG, Masry E & Zeidler JR (2006) Performance degradation of OFDM systems due to Doppler spreading. IEEE Transactions on Wireless Communications 5(6): 1422–1432.
- Wang T, Proakis JG & Zeidler JR (2007) Interference analysis of filtered multitone modulation over time-varying frequency-selective fading channels. IEEE Transactions on Communications 55(4): 717–727.
- Wang Z & Giannakis GB (2000) Wireless multicarrier communications – Where Fourier meets Shannon. IEEE Signal Processing Magazine 17(3): 29–48.
- Wang Z & Giannakis GB (2001) Block precoding for MUI/ISI-resilient generalized multicarrier CDMA with multirate capabilities. IEEE Transactions on Communications 49(11): 2016–2027.
- Weibull W (1951) A statistical distribution function of wide applicability. Journal of Applied Mechanics 18(3): 293–297.
- Weichselberger W, Herdin M, Özcelik H & Bonek E (2006) A stochastic MIMO channel model with joint correlation of both link ends. IEEE Transactions on Wireless Communications 5(1): 90–100.
- Weinstein SB & Ebert PM (1971) Data transmission by frequency-division multiplexing using the discrete Fourier transform. IEEE Transactions on Communication Technology 19(5): 628–634.
- Welch LR (1974) Lower bounds on the maximum cross correlation of signals. IEEE Transactions on Information Theory 20(3): 397–399.
- Weng T & Guangguo B (1987) Application of orthogonal complementary pair of sequences to CDMA-QAM communication system. Proc. International Conference on Communication Technology, Nanjing, China, 826–829.
- White WD (1950) Theoretical aspects of asynchronous multiplexing. Proceedings of the IRE 38(3): 270–275.
- Wiegand T & Fliege NJ (1996) Equalizers for transmultiplexers in orthogonal multiple carrier data transmission. Proc. European Signal Processing Conference, Trieste, Italy, 2: 1211–1214.
- Win MZ & Scholtz RA (2000) Ultra-wide bandwidth time-hopping spread-spectrum impulse radio for wireless multiple-access communications. IEEE Transactions on Communications 48(4): 679–691.
- Winters JH (1984) Optimum combining in digital mobile radio with cochannel interference. IEEE Journal on Selected Areas in Communications 2(4): 528–539.

- Witrisal K, Kim YH & Prasad R (1998) Frequency-domain simulation and analysis of the frequency-selective Ricean fading radio channel. Proc. IEEE International Symposium on Personal, Indoor and Mobile Radio Communications, Boston, USA, 3: 1131–1135.
- Xiao C, Wu J, Leong SY, Zheng YR & Letaief KB (2004) A discrete-time model for triply selective MIMO Rayleigh fading channels. IEEE Transactions on Wireless Communications 3(5): 1678–1688.
- Xiao C, Zheng YR & Beaulieu NC (2002) Second-order statistical properties of the WSS Jakes' fading channel simulator. IEEE Transactions on Communications 50(6): 888–891.
- Xiao C, Zheng YR & Beaulieu NC (2006) Novel sum-of-sinusoids simulation models for Rayleigh and Rician fading channels. IEEE Transactions on Wireless Communications 5(12): 3667–3679.
- Xie S & Rahardja S (2005) Performance evaluation for quaternary DS-SSMA communications with complex signature sequences over Rayleigh-fading channels. IEEE Transactions on Wireless Communications 4(1): 266–277.
- Xu H, Chizhik D, Huang H & Valenzuela R (2004) A generalized space-time multiple-input multiple-output (MIMO) channel model. IEEE Transactions on Wireless Communications 3(3): 966–975.
- Yacoub MD (2007) The α - μ distribution: A physical fading model for the Stacy distribution. IEEE Transactions on Vehicular Technology 56(1): 27–34.
- Yacoub MD, Fraidenaich G, Tercius HB & Martins FC (2005) The symmetrical η - κ distribution: A general fading distribution. IEEE Transactions on Broadcasting 51(4): 504–511.
- Yang L & Giannakis GB (2006) Crossband flexible UWB multiple access for high-rate multipiconet WPANs. IEEE Transactions on Communications 54(11): 2023–2032.
- Yee N & Linnartz JP (1993) Ber of multi-carrier CDMA in an indoor Rician fading channel. Proc. Asilomar Conference on Signals, Systems and Computers, Pacific Grove, USA, 1: 426–430.
- Yee N & Linnartz JP (1994a) Controlled equalization of multi-carrier CDMA in an indoor Rician fading channel. Proc. IEEE Vehicular Technology Conference, Stockholm, Sweden, 3: 1665–1669.
- Yee N & Linnartz JP (1994b) Wiener filtering of multi-carrier CDMA in Rayleigh fading channel. Proc. IEEE International Symposium on Personal, Indoor and Mobile Radio Communications, Hague, Netherlands, 4: 1344–1347.
- Yee N, Linnartz JP & Fettweis G (1993) Multi-carrier CDMA in indoor wireless radio networks. Proc. IEEE International Symposium on Personal, Indoor and Mobile Radio Communications, Yokohama, Japan, 1: 109–113.
- Yong SK & Thompson JS (2005) Three-dimensional spatial fading correlation models for compact MIMO receivers. IEEE Transactions on Wireless Communications 4(6): 2856–2869.
- You CW & Hong DS (2003) Multicarrier CDMA systems using time-domain and frequency-domain spreading codes. IEEE Transactions on Communications 51(1): 17–21.
- Young DJ & Beaulieu NC (2000) The generation of correlated Rayleigh random variates by inverse discrete Fourier transform. IEEE Transactions on Communications 48(7): 1114–1127.
- Young WR Jr (1952) Comparison of mobile radio transmission at 150, 450, 900, and 3700 mc. Bell System Technical Journal 31(6): 1068–1085.
- Young WR Jr & Lacy LY (1950) Echoes in transmission at 450 megacycles from land-to-car radio units. Proceedings of the IRE 38(3): 255–258.

- Yu K, Bengtsson M, Ottersten B, McNamara D, Karlsson P & Beach M (2004) Modeling of wide-band MIMO radio channels based on NLoS indoor measurements. *IEEE Transactions on Vehicular Technology* 53(3): 655–665.
- Zhang C, Lin X & Hatori M (2005a) Two dimensional combined complementary sequence and its application in multi-carrier CDMA. *IEICE Transactions on Communications* E88-B(2): 478–486.
- Zhang H, Fan HH & Lindsey AR (2005b) Receiver design for wavelet-based multicarrier CDMA communications. *IEEE Transactions on Vehicular Technology* 54(2): 615–628.
- Zhao X, Kivinen J, Vainikainen P & Skog K (2003) Characterization of Doppler spectra for mobile communications at 5.3 GHz. *IEEE Transactions on Vehicular Technology* 52(1): 14–23.
- Zheng YR & Xiao C (2002) Improved models for the generation of multiple uncorrelated Rayleigh fading waveforms. *IEEE Communications Letters* 6(6): 256–258.
- Zheng YR & Xiao C (2003) Simulation models with correct statistical properties for Rayleigh fading channels. *IEEE Transactions on Communications* 51(6): 920–928.
- Zhou Y, Wang J & Sawahashi M (2005) Downlink transmission of broadband OFCDM systems — Part I: Hybrid detection. *IEEE Transactions on Communications* 53(4): 718–729.
- Zhu J, Zhang H & Gu Y (2005) Principle and performance of variable rate multi-code CDMA method. *Proc. IEEE International Conference on Universal Personal Communications, Tokyo, Japan*, 256–259.
- Zimmerman MS & Kirsch AL (1967) The AN/GSC-10 (KATHRYN) variable rate data modem for HF radio. *IEEE Transactions on Communication Technology* 15(2): 197–204.
- Zong P, Wang K & Bar-Ness Y (2001) Partial sampling MMSE interference suppression in asynchronous multicarrier CDMA system. *IEEE Journal on Selected Areas in Communications* 19(8): 1605–1613.
- Zwick T, Fischer C, Didascalou D & Wiesbeck W (2000) A stochastic spatial channel model based on wave-propagation modeling. *IEEE Journal on Selected Areas in Communications* 18(1): 6–15.
- Zwick T, Fischer C & Wiesbeck W (2002) A stochastic multipath channel model including path directions for indoor environments. *IEEE Journal on Selected Areas in Communications* 20(6): 1178–1192.

Original articles

- I Kunnari E & Iinatti J (2005) A Rice fading MIMO multicarrier channel model. Proc. IEEE International Symposium on Personal, Indoor and Mobile Radio Communications, Berlin, Germany, 1: 527–531.
- II Kunnari E & Iinatti J (2005) Analysis of multirate MC-CDMA over multipath channels with delay spread exceeding the guard interval. Proc. IEEE Global Telecommunications Conference, St. Louis, USA, 6: 3221–3225.
- III Kunnari E & Iinatti J (2006) Performance analysis of multirate MC-CDMA in Rayleigh-fading channels with delay power spectrum exceeding the guard interval. IEEE Journal on Selected Areas in Communications 24(3): 542–553.
- IV Kunnari E & Iinatti J (2007) Stochastic modelling of Rice fading channels with temporal, spatial and spectral correlation. IET Communications 1(2): 215–224.
- V Kunnari E & Iinatti J (2007) Performance analysis of OFDM based UWB systems with a frequency-domain CDMA for multiple SOPs. Proc. IEEE Vehicular Technology Conference, Dublin, Ireland, 2651–2655.
- VI Kunnari E & Iinatti J (2007) Performance analysis of OFDM based UWB systems enhanced with frequency-domain spreading. Proc. IEEE International Conference on Communications, Glasgow, UK, 4873–4878.

Reprinted with permission from IEEE (I–III,V,VI) and IET (IV).

Original articles are not included in the electronic version of the dissertation.

Errata

- III, p. 544, eq. 7 Symbol $\hat{\tau}_k$ should be $\hat{\tau}_{hk}$.
- III, p. 545, eq. 17 Term $c_{hkl}^{(T_g, T_s)3shkqg}$ should be $c_{hkl}^{(T_g, T_s)3} shkqg$.
- III, p. 545, col. 2 Definition $p = 1, \dots, P$ should be $p = 1, \dots, P_h$.
- IV, p. 218, eq. 29 Term σ_a should be σ_a .
- V, p. 2653, col. 1 Definition $i = 1, 2$ should be $i = 1$.

282. Rahtu, Esa (2007) A multiscale framework for affine invariant pattern recognition and registration
283. Kröger, Virpi (2007) Poisoning of automotive exhaust gas catalyst components. The role of phosphorus in the poisoning phenomena
284. Codreanu, Marian (2007) Multidimensional adaptive radio links for broadband communications
285. Tiikkaja, Esa (2007) Koneäköä soveltavan kuituanalysaattorin ja virtauskenttäfraktionaattorin mittausten yhteydet kuumahierteen paperitekniisiin ominaisuuksiin. Kokeellinen tutkimus
286. Taparugssanagorn, Attaphongse (2007) Evaluation of MIMO radio channel characteristics from TDM-switched MIMO channel sounding
287. Elsilä, Ulla (2007) Knowledge discovery method for deriving conditional probabilities from large datasets
288. Perkkiö, Miia (2007) *Utilitas* restauroinnissa. Historiallisen rakennuksen käyttötarkoituksen muutos ja funktionaalinen integriteetti
289. Nissilä, Mauri (2008) Iterative receivers for digital communications via variational inference and estimation
290. Toivonen, Tuukka (2007) Efficient methods for video coding and processing
291. Lyöri, Veijo (2007) Structural monitoring with fibre-optic sensors using the pulsed time-of-flight method and other measurement techniques
292. Stoica, Lucian (2008) Non-coherent energy detection transceivers for Ultra Wideband Impulse radio systems
293. Koski, Anna (2008) Applicability of crude tall oil for wood protection
294. Gore, Amol (2008) Exploring the competitive advantage through ERP systems. From implementation to applications in agile networks
295. Kirillin, Mikhail (2008) Optical coherence tomography of strongly scattering media
296. Tölli, Antti (2008) Resource management in cooperative MIMO-OFDM cellular systems
297. Karkkila, Harri (2008) Consumer pre-purchase decision taxonomy
298. Rabbachin, Alberto (2008) Low complexity UWB receivers with ranging capabilities

Book orders:
OULU UNIVERSITY PRESS
P.O. Box 8200, FI-90014
University of Oulu, Finland

Distributed by
OULU UNIVERSITY LIBRARY
P.O. Box 7500, FI-90014
University of Oulu, Finland

S E R I E S E D I T O R S

A
SCIENTIAE RERUM NATURALIUM

Professor Mikko Siponen

B
HUMANIORA

Professor Harri Mantila

C
TECHNICA

Professor Hannu Heusala

D
MEDICA

Professor Olli Vuolteenaho

E
SCIENTIAE RERUM SOCIALIUM

Senior Researcher Eila Estola

E
SCRIPTA ACADEMICA

Information officer Tiina Pistokoski

G
OECONOMICA

Senior Lecturer Seppo Eriksson

EDITOR IN CHIEF

Professor Olli Vuolteenaho

EDITORIAL SECRETARY

Publications Editor Kirsti Nurkkala

ISBN 978-951-42-8808-1 (Paperback)

ISBN 978-951-42-8809-8 (PDF)

ISSN 0355-3213 (Print)

ISSN 1796-2226 (Online)

